Ricerca del bosone di Higgs e misura delle sue proprieta'

1. La ricerca a LEP
2. Sezioni d'urto di produzione ai collider adronici
3. Decadimenti del bosone di Higgs nel Modello Standard
4. La scoperta a LHC
5. Decadimenti in due bosoni
6. Misura di massa e larghezza
7. Determinazione di Spin Parita'
8. Decadimenti in fermioni
9. Determinazione degli accoppiamenti
10. Esempi di analisi per Higgs BSM
11. Prospettive

H→γγ (Backgrounds)

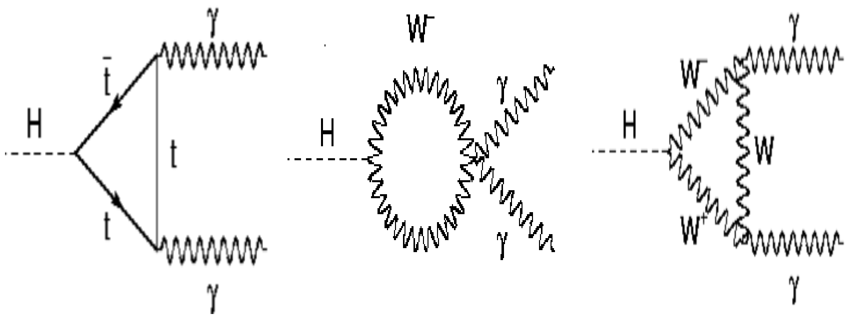

σ*Br= 20 * 2E-3 = 0.04 pb

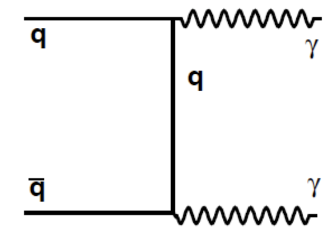

qqbar annihilation

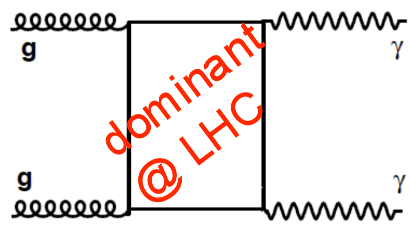

gluon-gluon {box}

σ≅ 0(10) pb

Fondo irriducibile

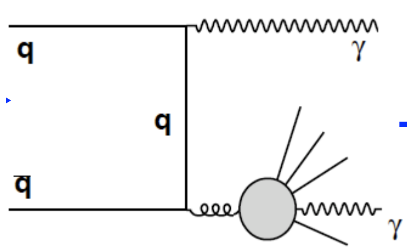

σ≅ 0(100) μb

Fondo riducibile

(dipende dalla capacita’ di discriminare fotoni da jet

- Essenziale una reiezione di $10^4 \div 10^5$ rispetto ai jet
- Ottimizzare la risoluzione in massa invariante γγ
  - Detector design, calibrazione, monitoring

H→γγ (Backgrounds)

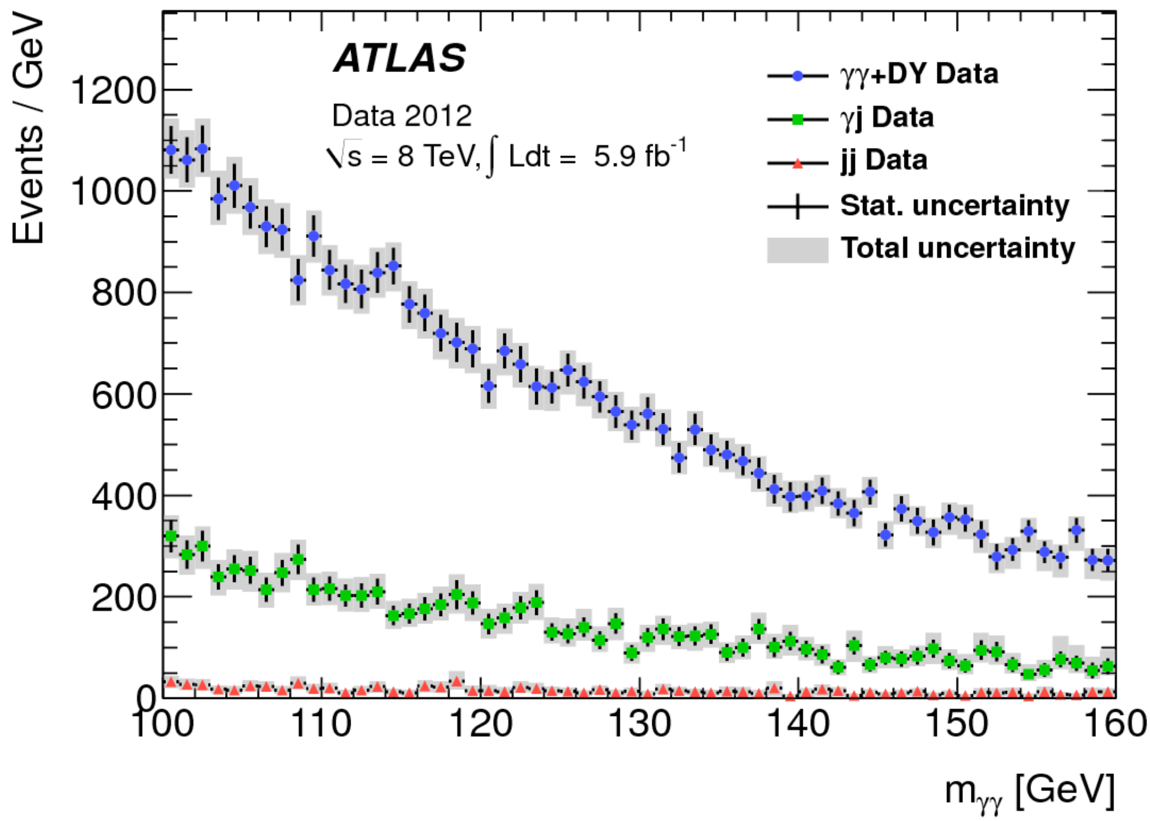

I fondi sono misurati indipendentemente, ma una misura della sez. D'urto e della distribuzione in massa invariante si ottiene "in-situ" dalle side-bands del segnale

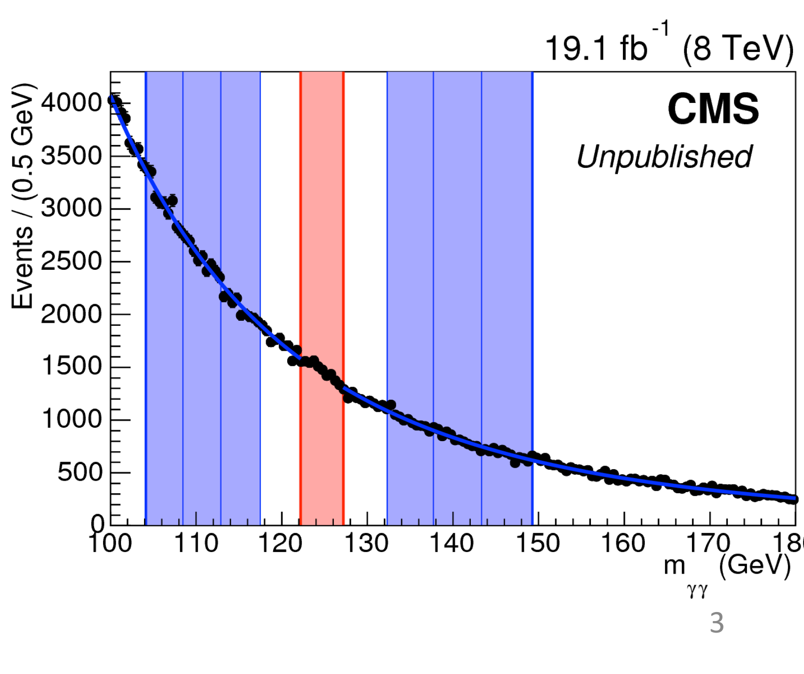

H→γγ(latest/CMS)

[EPJ C 74 (2014) 3076]

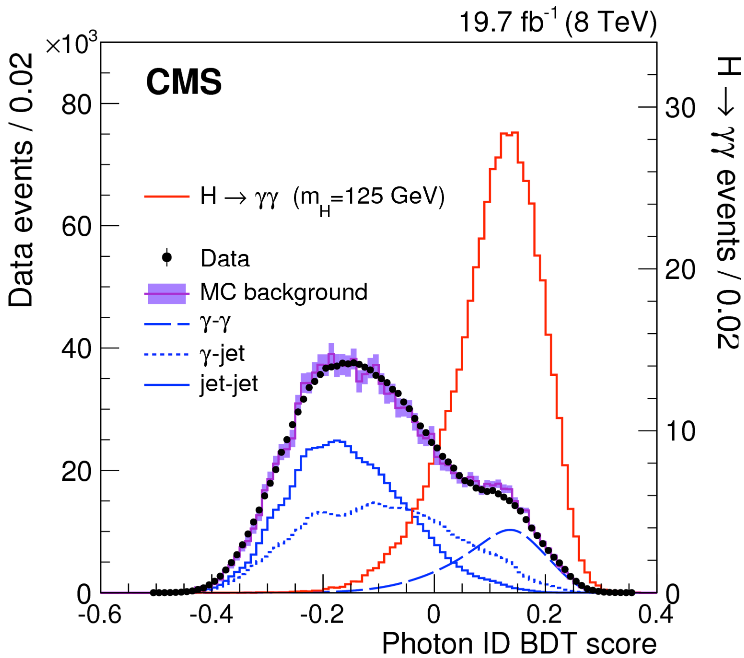

Isolation

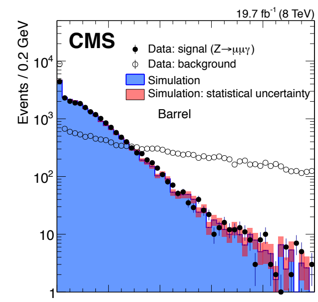

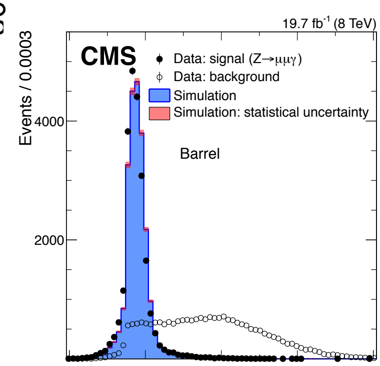

Shower shape

- Spinta al massimo la discriminazione tra fotoni e Jet/π^o ([CERN-PH-EP/ 2015-006 2015/02/11]
- Si utilizzano gli abbondanti campioni di Z→ee per calibrazioni e sistematiche

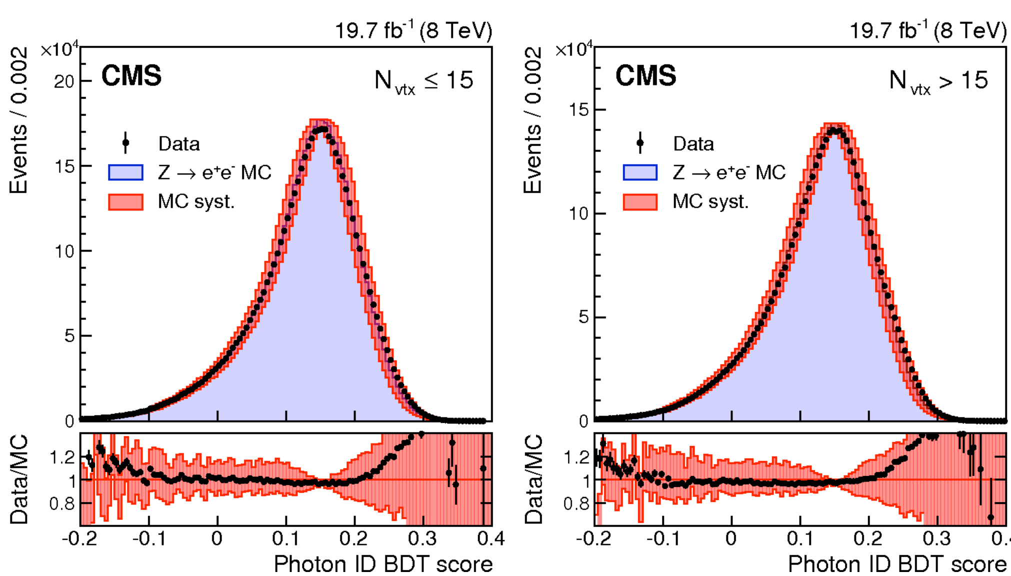

Calibrazione Calorimetro

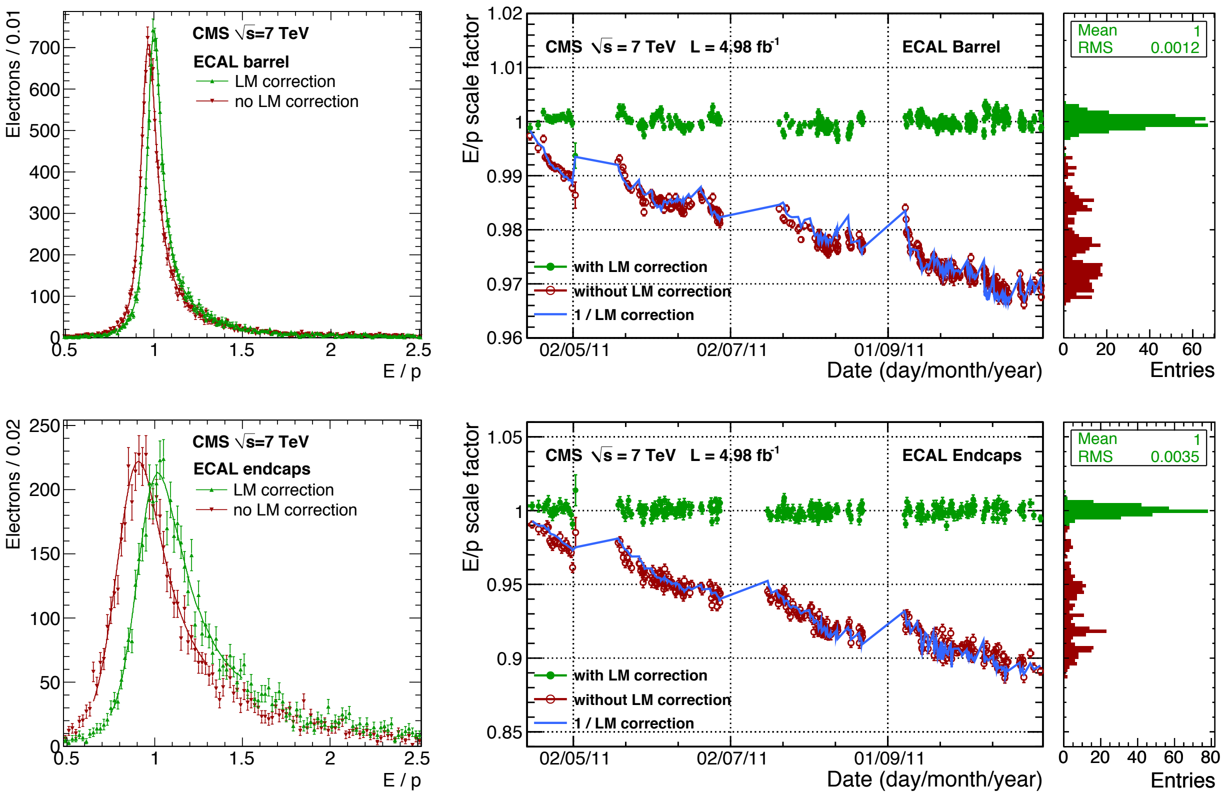

Figure 4: Relative energy response variation for EB (top) and EE (bottom) determined from the E/p analysis of electrons in W-boson decays. Left: examples of fits to the E/p distributions before (red) and after (green) LM corrections. Middle: Response stability during the 2011 pp data-taking period before (red open circles) and after (green points) response corrections; the blue line shows the inverse of the average LM corrections. Right: Distribution of the projected relative energy scales.

Diminuzione della risposta dovuta alla dose di radiazione integrata (recupera parzialmente con LHC fermo)

Z→ee peak

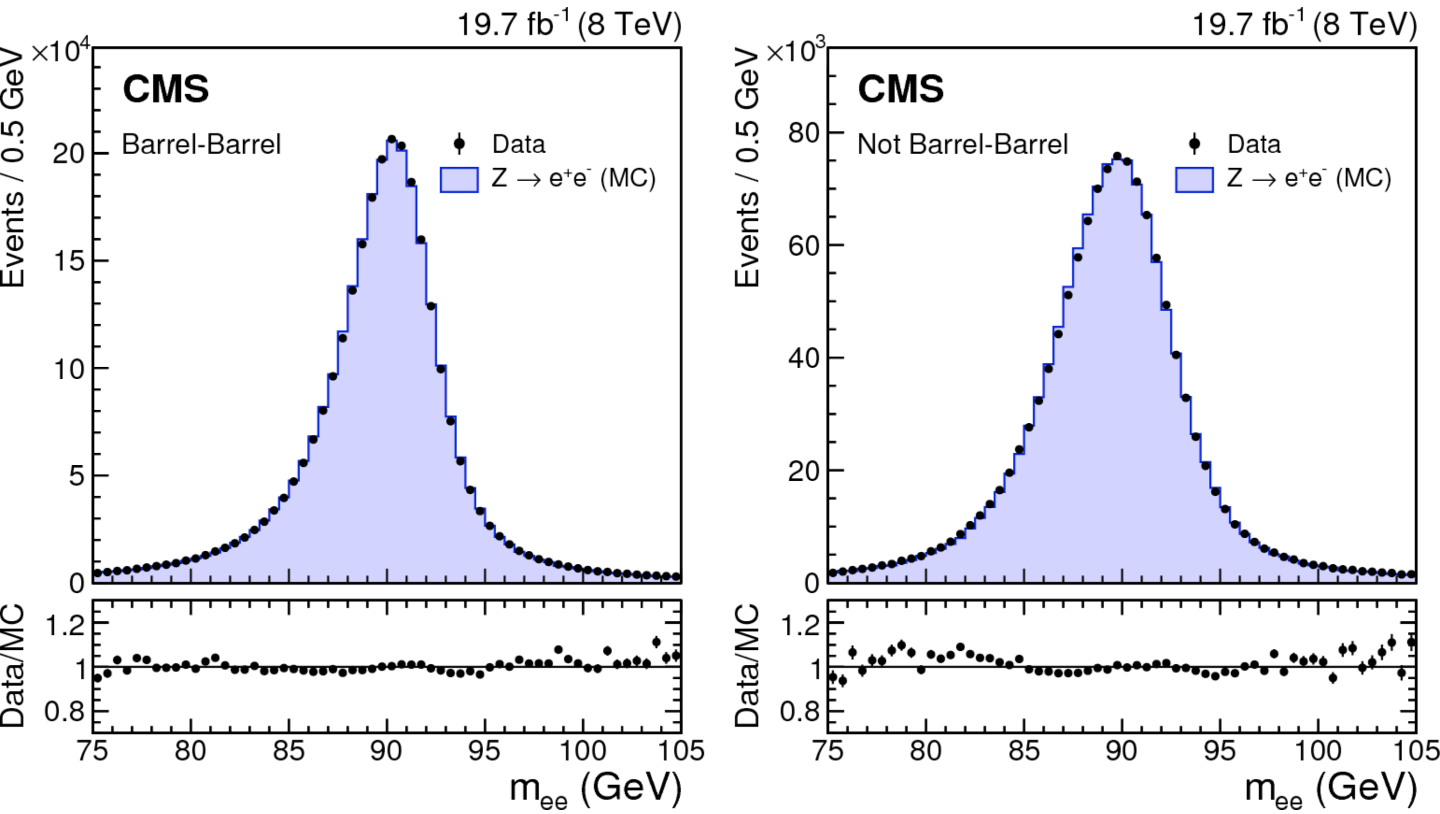

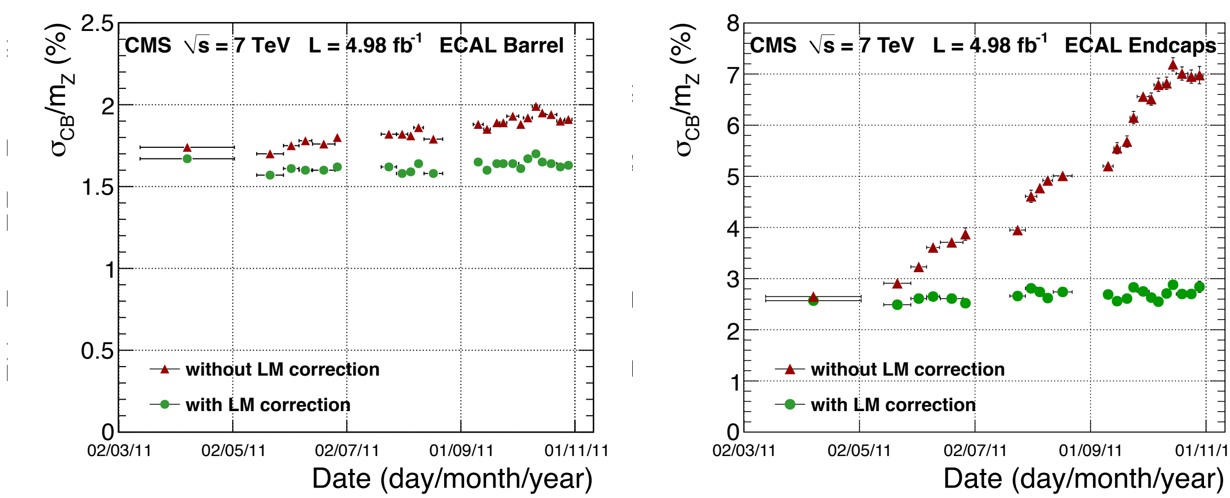

Figure 5: Mass resolution for the reconstructed Z-boson peak, from $Z \to e^+e^-$ decays, as a function of time for EB (left) and EE (right) before (red dots) and after (green dots) LM corrections are applied.

Vertex determination

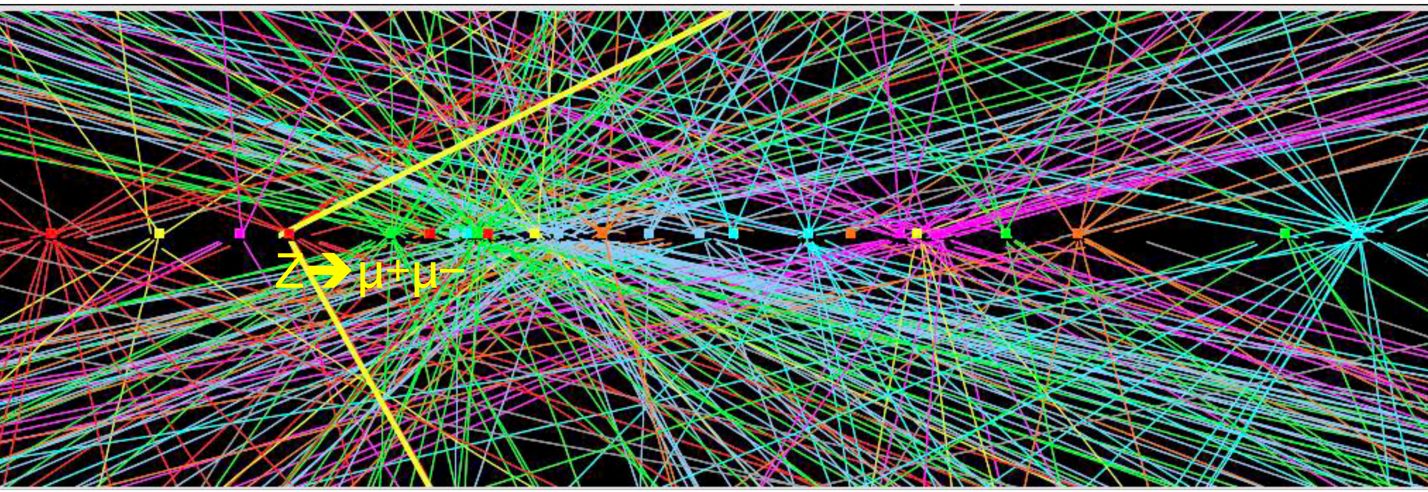

- Pile-up induce un numero di collissioni medio dipari a 21
- Normalmente il vertice primario della collisione viene identificato dalle tracce cariche dell'Higgs (tra le altre cose), ma nel caso di H→gg non e' possibile !
- Lo spred del fascio (5 cm di lunghezza di interazione) contribuirebbe in maniera significativa alla risoluzione
- Bisogna ricostruire il vertice giusto dal "resto dell'evento", in particolare prendendo il vertice che mostra piu' sbilanciamento del momento trasverso delle tracce che vi apparengono (che rinculano al nostro bosone di Higgs)

Impatto circa 1.4 GeV nella risoluzione su mγγ

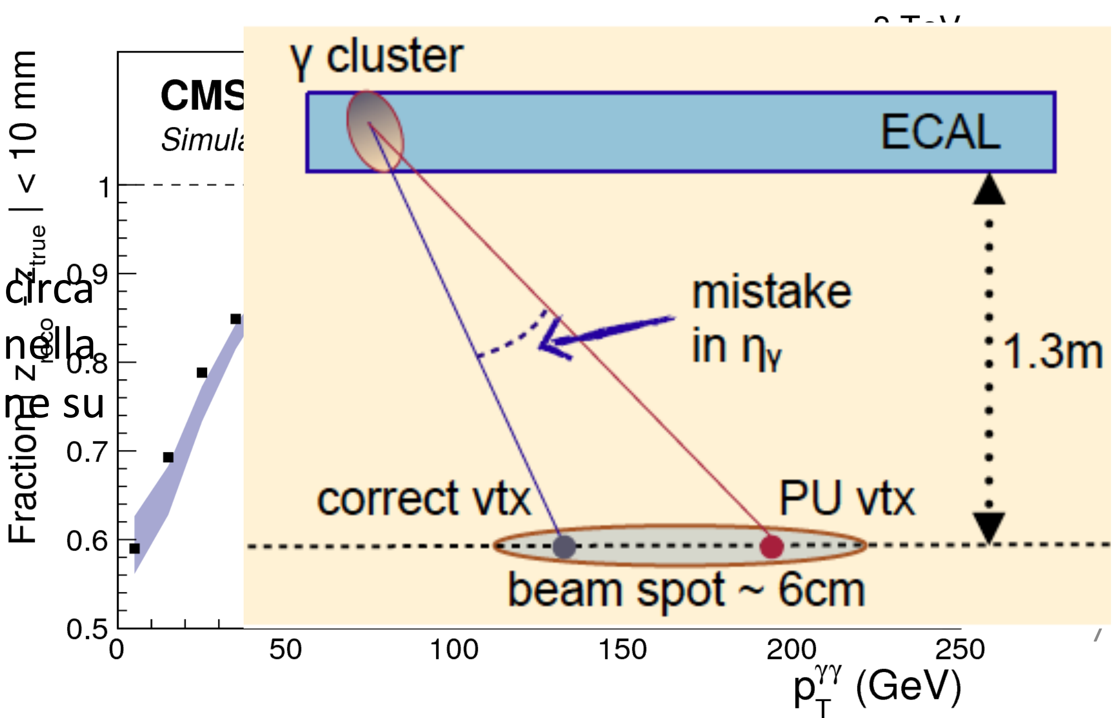

Vertex determination (ATLAS)

- $\sigma_z = 15\,\mathrm{mm}$ (6 mm using conversion)

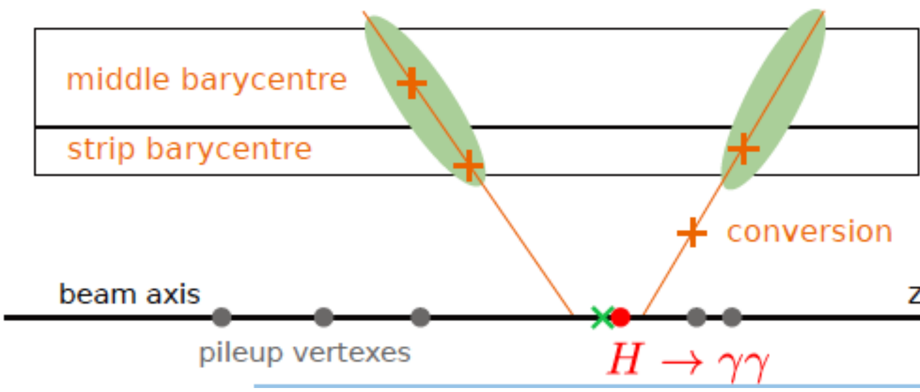

- Nel caso di ATLAS questa issue e' meno cruciale, perche' il calorimetro e' segmentato longitudinalmente
- La risoluzione e' dominata dal constant term del calorimetro in ogni caso
- Best resolution (Central - high p_{Tt}, σ_{68}=1.32 GeV) and worst resolution (Forward - low p_{Tt}, σ_{68}=1.86 GeV)
- Insensibile al pileup

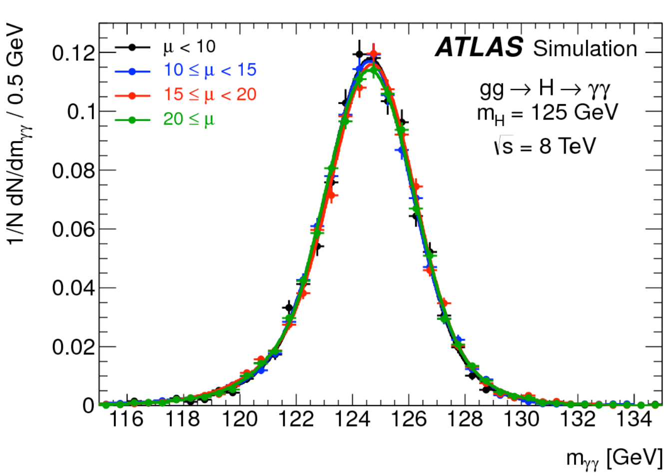

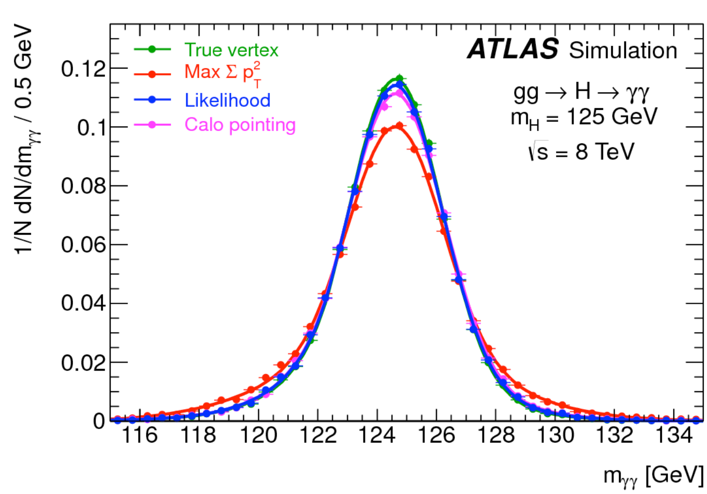

H→γγ(latest/CMS)

[EPJ C 74 (2014) 3076](EPJ C 74 (2014) 3076)

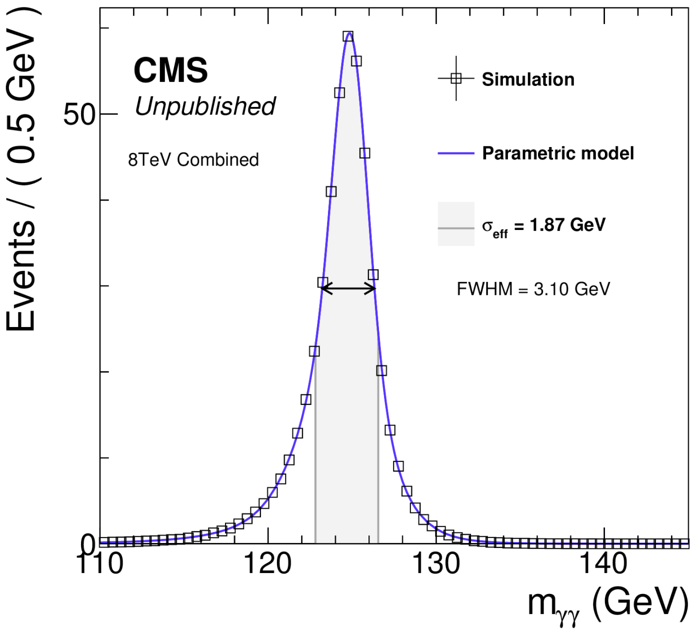

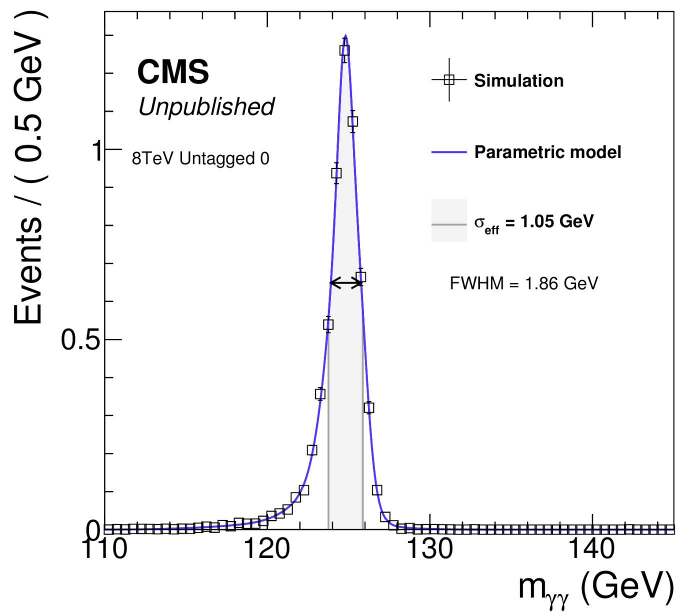

- La risoluzione media su tutto il sample e' quasi due volte peggio dei sotto-sample migliori
- Conviene dividere il sample in tanti sotto-sample separati per qualita' della misura del fotone e per meccanismo di produzione (ggF, VBF, VH etc.)

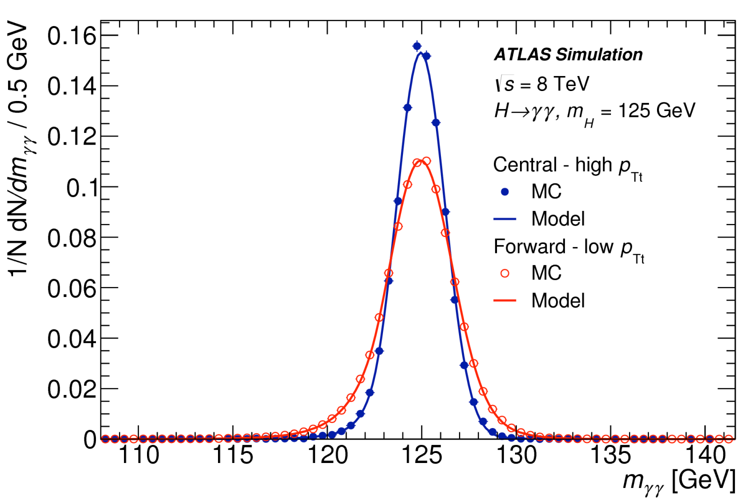

- Confronta con ATLAS best resolution (Central - high p_{Tt}, σ_{68}=1.32 GeV) and worst resolution (Forward - low p_{Tt}, σ_{68}=1.86 GeV)

H→γγ(latest/CMS)

EPJ C 74 (2014) 3076

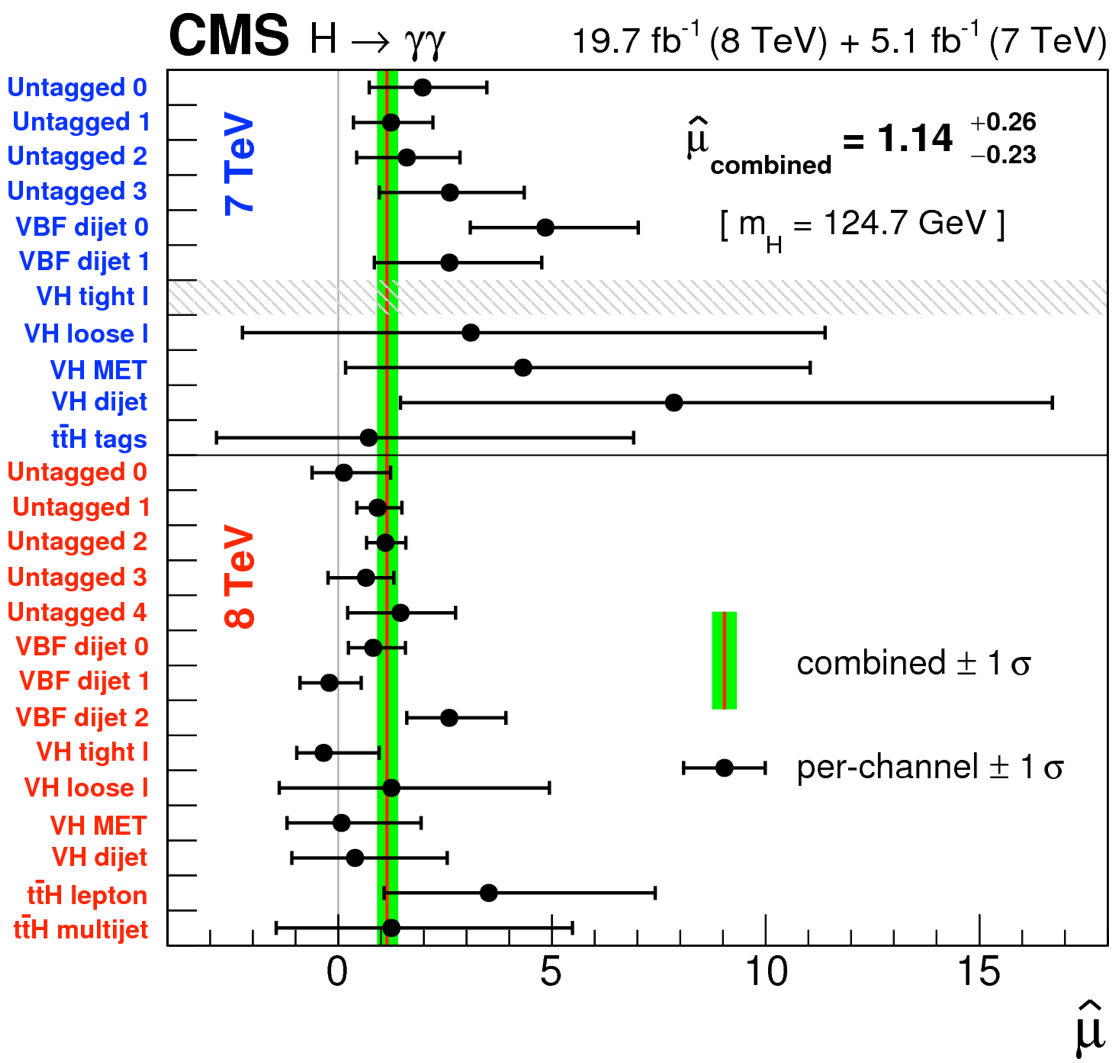

H→γγ(latest/CMS)

EPJ C 74 (2014) 3076

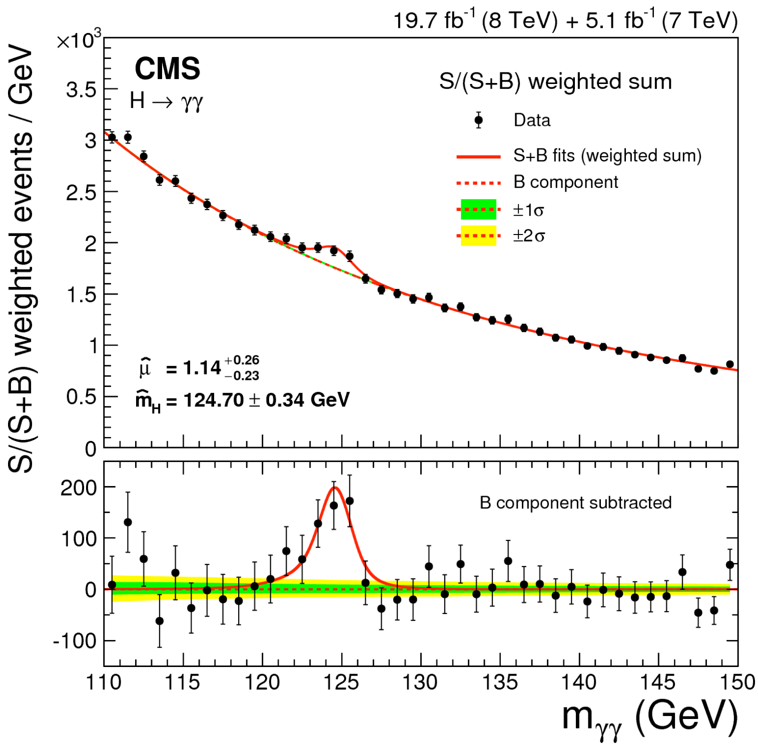

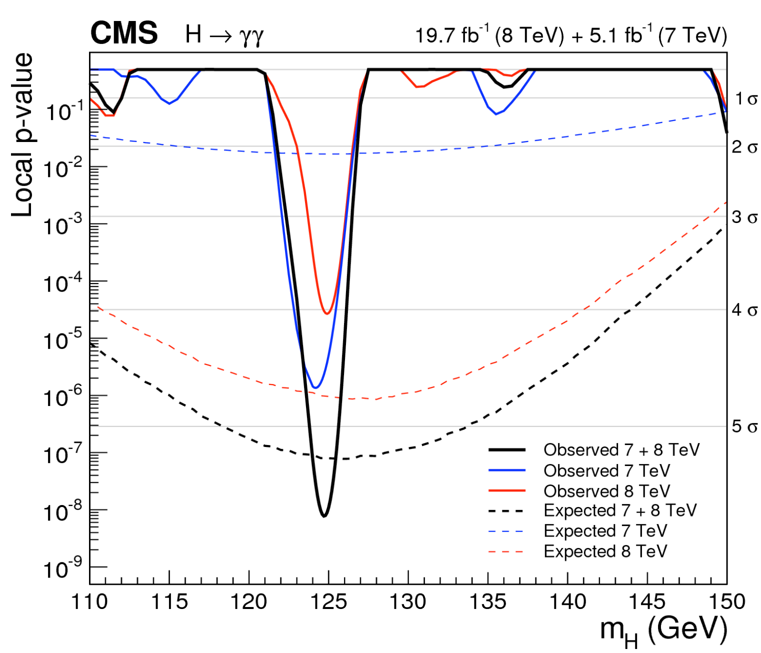

H→γγ(latest/CMS)

EPJ C 74 (2014) 3076

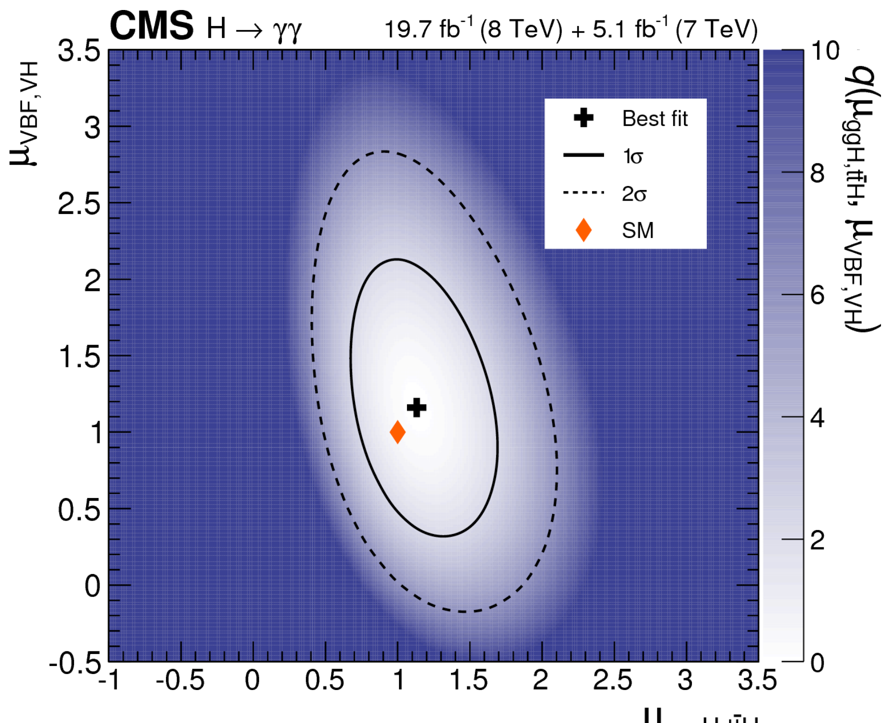

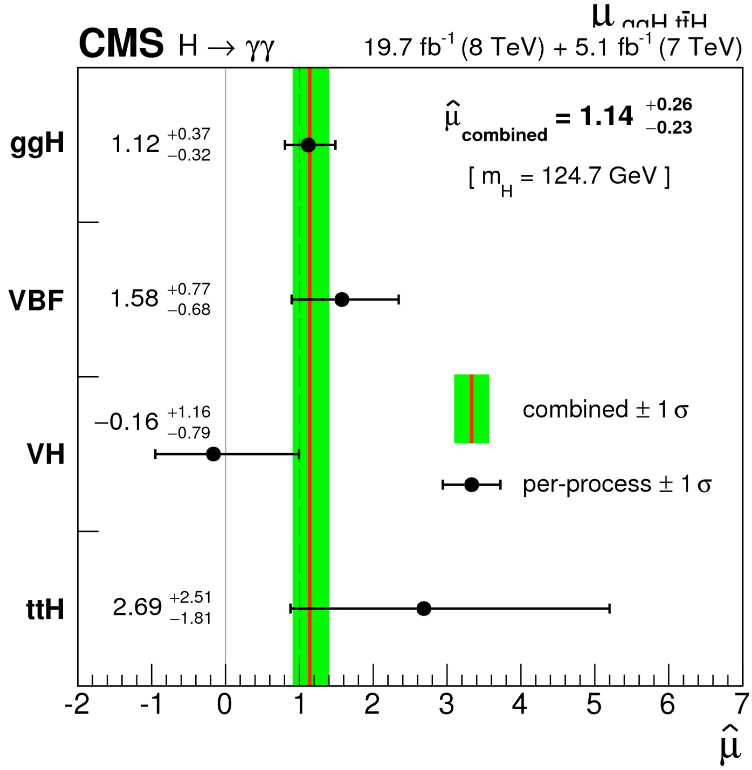

Combined Mass

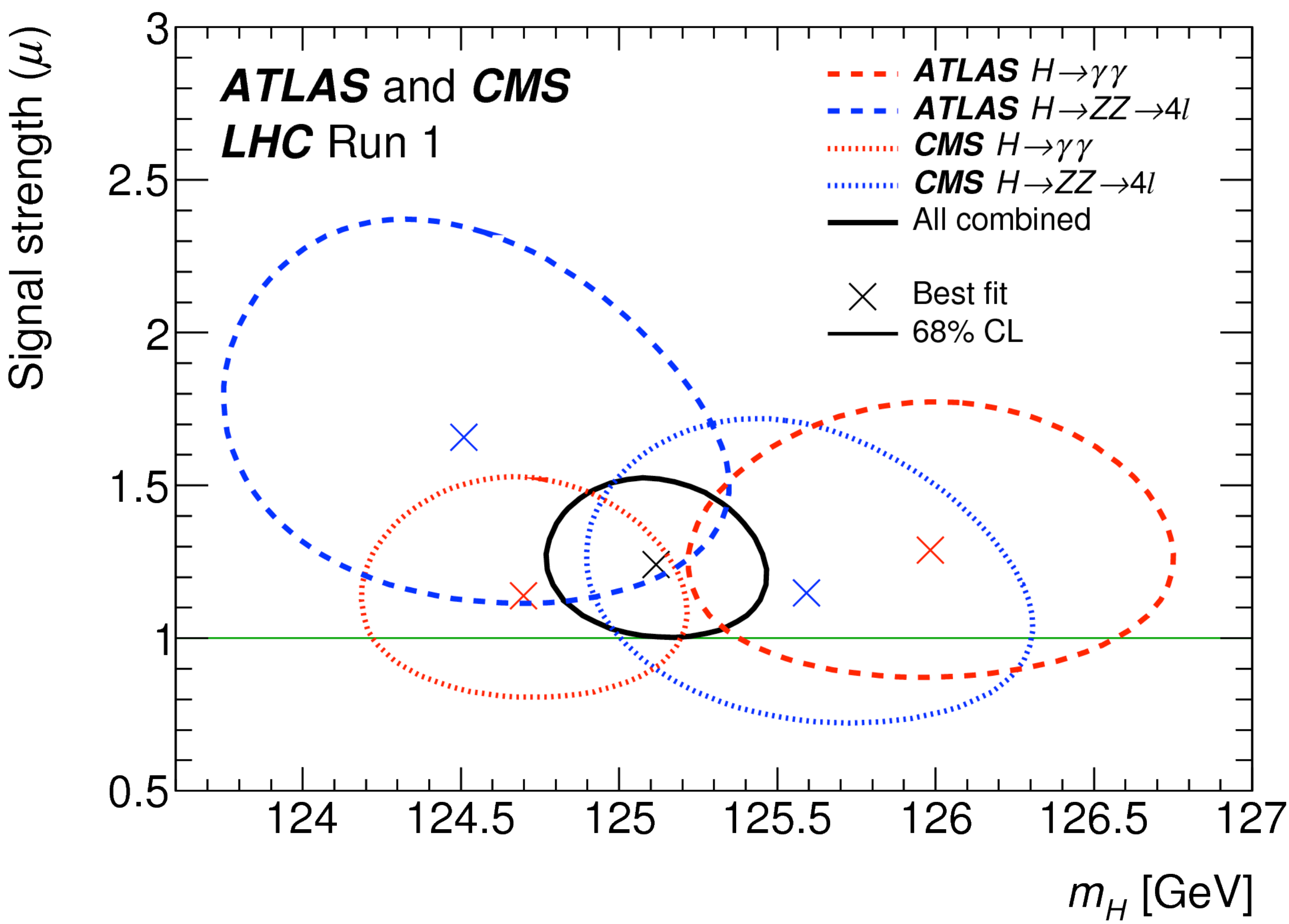

Combined Higgs Mass

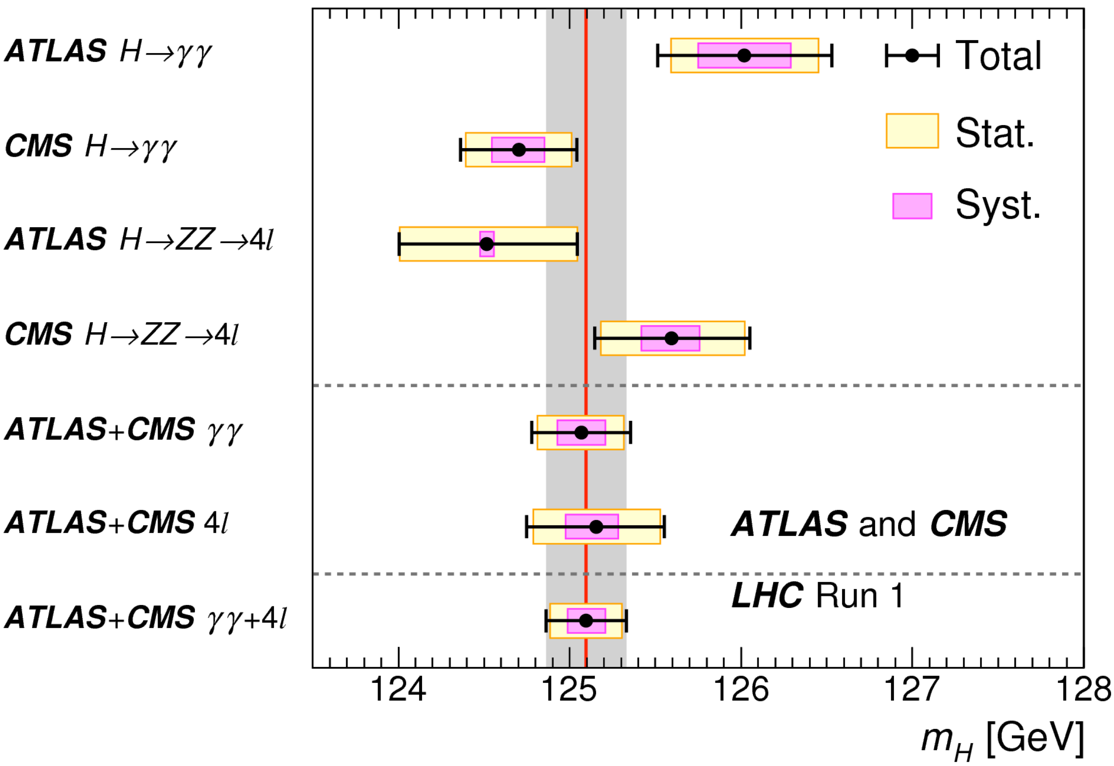

	Uncertainty in ATLAS results [GeV]: observed (expected)		Uncertainty in CMS results [GeV]: observed (expected)		Uncertainty in combined result [GeV]: observed (expected)	
	$H \to \gamma\gamma$	$H \to ZZ$llll	$H \to \gamma\gamma$	$H \to ZZ$llll	ATLAS	CMS
Scale uncertainties:						
ATLAS ECAL non-linearity / CMS photon non-linearity	0.14 (0.16)	–	0.10 (0.13)	–	0.02 (0.04)	0.05 (0.06)
Material in front of ECAL	0.15 (0.13)	–	0.07 (0.07)	–	0.03 (0.03)	0.04 (0.03)
ECAL longitudinal response	0.12 (0.13)	–	0.02 (0.01)	–	0.02 (0.03)	0.01 (0.01)
ECAL lateral shower shape	0.09 (0.08)	–	0.06 (0.06)	–	0.02 (0.02)	0.03 (0.03)
Photon energy resolution	0.03 (0.01)	–	0.01 (<0.01)	–	0.02 (<0.01)	<0.01 (<0.01)
ATLAS $H \to \gamma\gamma$ vertex & conversion reconstruction	0.05 (0.05)	–	–	–	0.01 (0.01)	–
$Z \to ee$ calibration	0.05 (0.04)	0.03 (0.02)	0.05 (0.05)	–	0.02 (0.01)	0.02 (0.02)
CMS electron energy scale & resolution	–	–	–	0.12 (0.09)	–	0.03 (0.02)
Muon momentum scale & resolution	–	0.03 (0.04)	–	0.11 (0.10)	<0.01 (0.01)	0.05 (0.02)
Other uncertainties:						
ATLAS $H \to \gamma\gamma$ background modeling	0.04 (0.03)	–	–	–	0.01 (0.01)	–
Integrated luminosity	0.01 (<0.01)	<0.01 (<0.01)	0.01 (<0.01)	<0.01 (<0.01)	0.01 (<0.01)	
Additional experimental systematic uncertainties	0.03 (<0.01)	<0.01 (<0.01)	0.02 (<0.01)	0.01 (<0.01)	0.01 (<0.01)	0.01 (<0.01)
Theory uncertainties	<0.01 (<0.01)	<0.01 (<0.01)	0.02 (<0.01)	<0.01 (<0.01)	0.01 (<0.01)	
Systematic uncertainty (sum in quadrature)	0.27 (0.27)	0.04 (0.04)	0.15 (0.17)	0.16 (0.13)	0.11 (0.10)	
Systematic uncertainty (nominal)	0.27 (0.27)	0.04 (0.05)	0.15 (0.17)	0.17 (0.14)	0.11 (0.10)	
Statistical uncertainty	0.43 (0.45)	0.52 (0.66)	0.31 (0.32)	0.42 (0.57)	0.21 (0.22)	
Total uncertainty	0.51 (0.52)	0.52 (0.66)	0.34 (0.36)	0.45 (0.59)	0.24 (0.24)	
Analysis weights	19% (22%)	18% (14%)	40% (46%)	23% (17%)	–	

Higgs Width

- Le misure di rate sono sensibili a $\sigma^*\Gamma_f/\Gamma_H$
- Non e' possibile ricavare gli accoppiamenti e la larghezza totale se non facendo assunzioni sull'assenza di decadimenti imprevisti dalMS

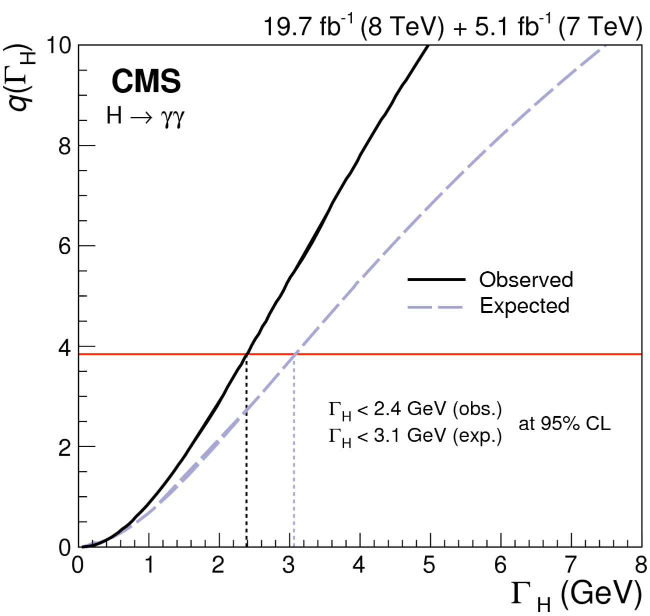

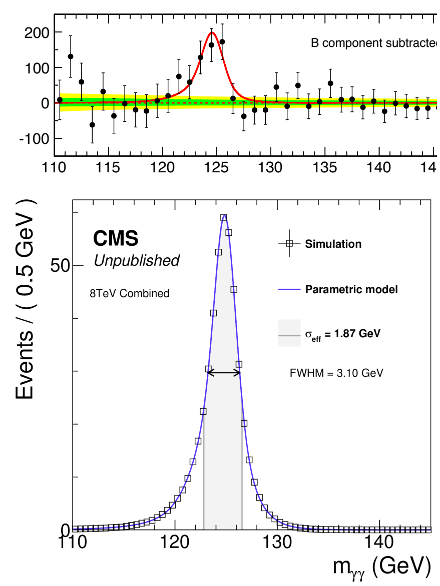

- Il picco osservato e' consistente con la larghezza predetta dalla simulazione assumendo Γ_H=0
- Possibile solo mettere un limite superiore 1000 volte piu' grande del valore atteso nel MS (Γ_H < 2.4 (3.1 expected) GeV at 95% CL.)

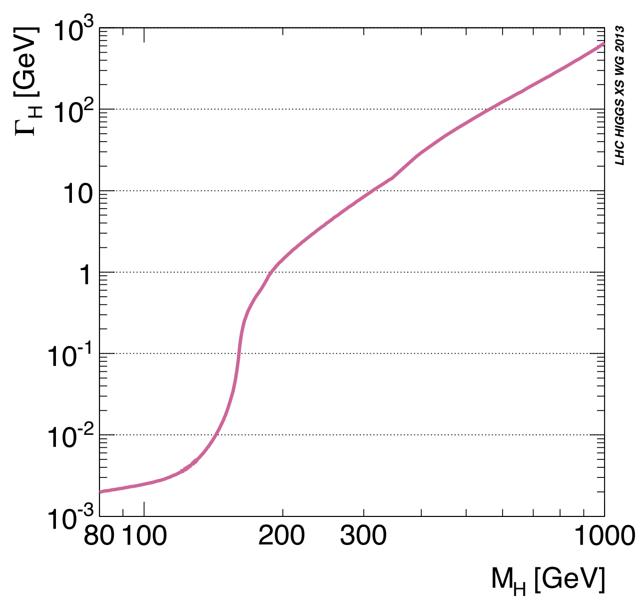

Higgs Width/Interference

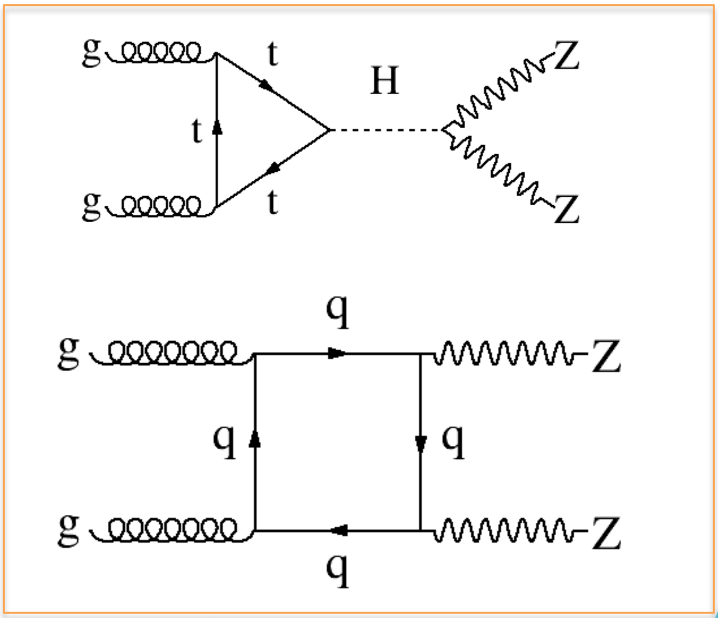

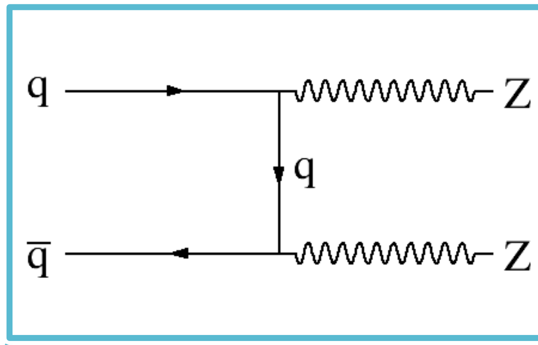

Non interferisce, trattato come fondo

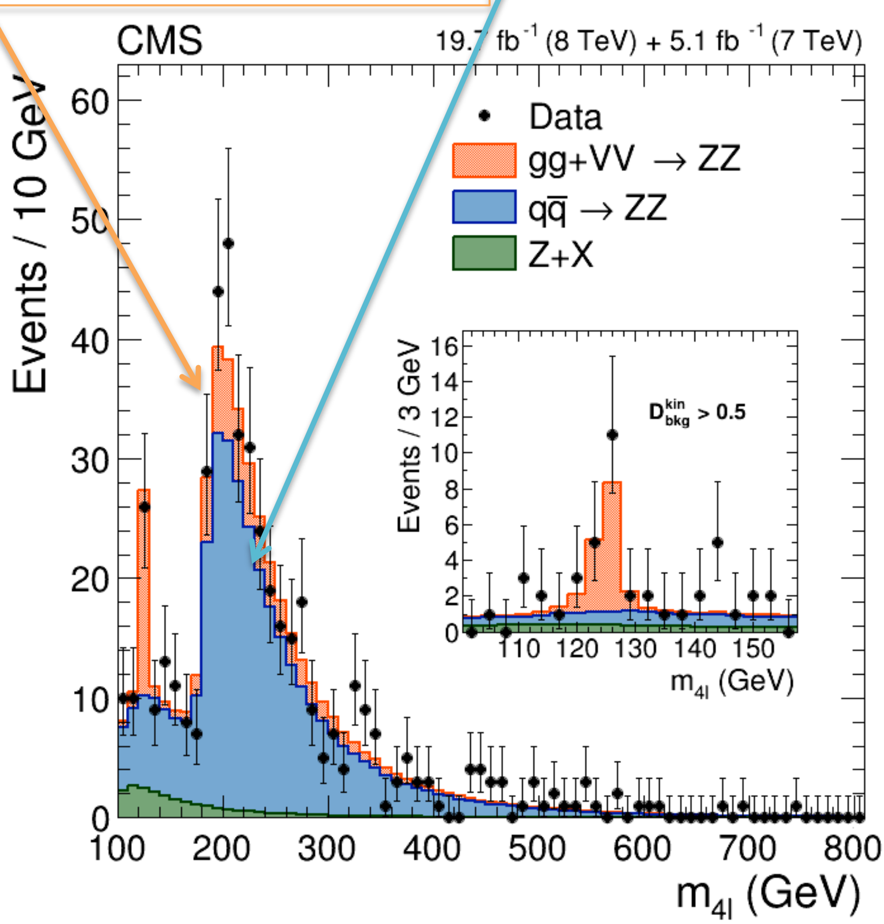

Higgs Width/Interference

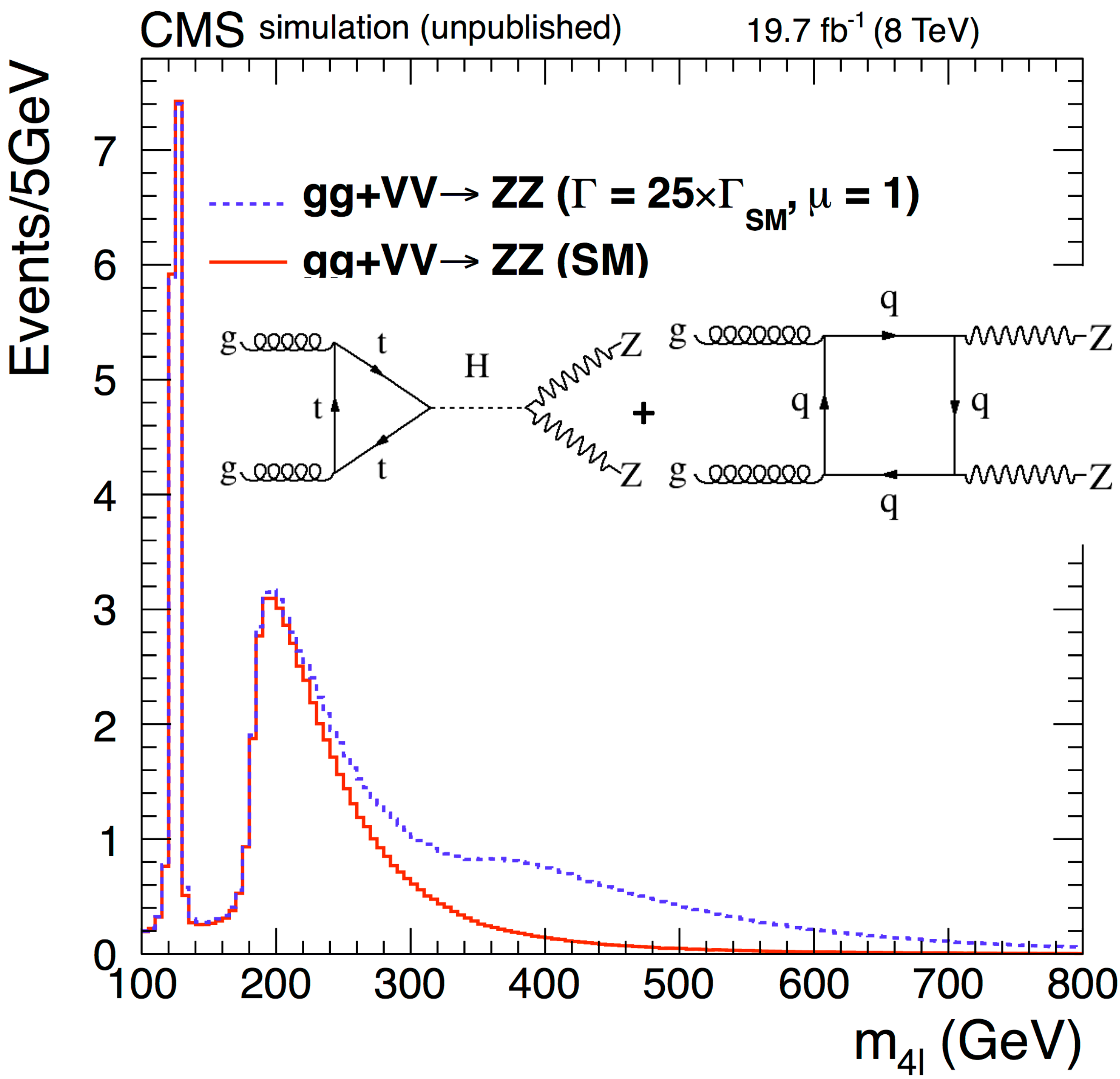

L'interferenza tra il grafico a box e quello che procede attraverso un bosone di Higgs altamente virtuale dipende dalla larghezza totale del bosone di Higgs.

Higgs Width/Interference

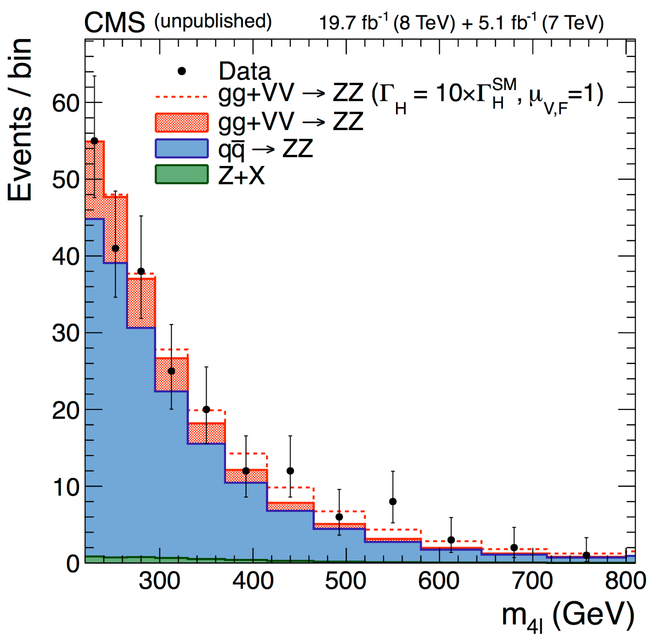

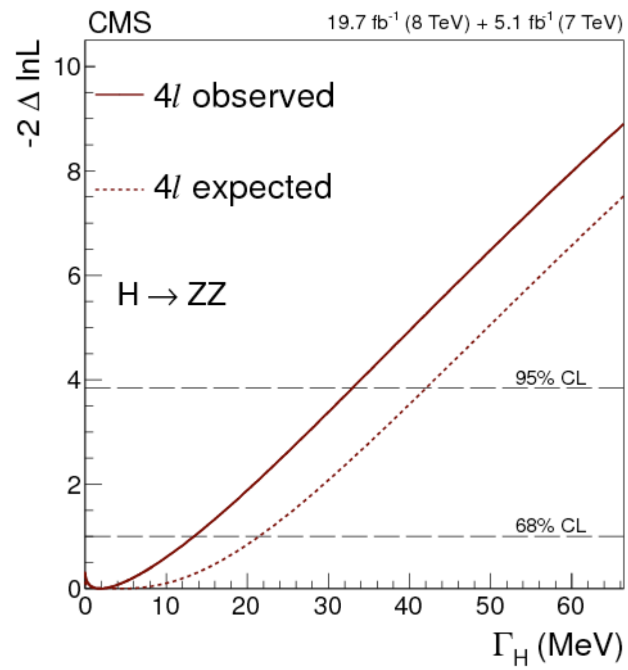

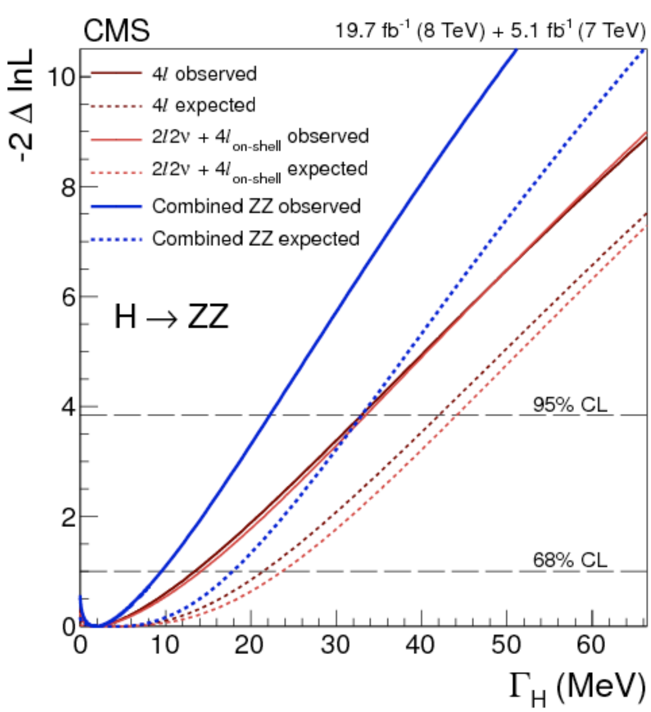

Γ_H < 22 MeV at 95% C.L.

Higgs Width at TLEP

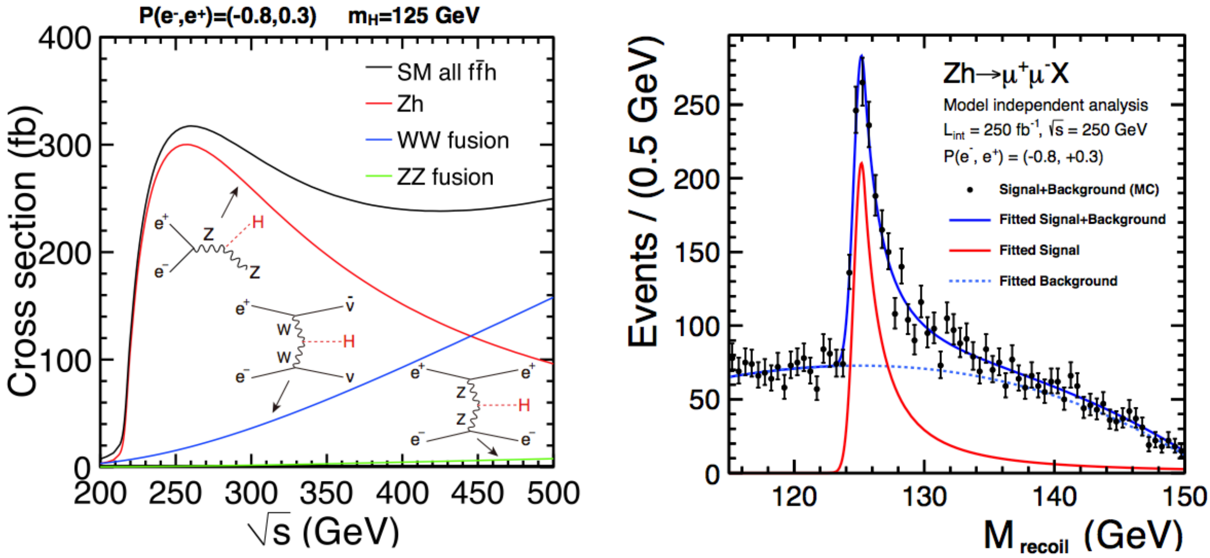

Fig. 11: Cross sections for the main Higgs production mechanisms in e^+e^- (left). Recoil-mass distribution in $e^+e^- \to Zh \to \mu\mu X$ (right) [8].

P

- Misura model independent della sezione d'urto ee→Zh→μμ X, indipendente dal decadimento dell'Higgs, attraverso il picco nella misura della massa del sistema che accompagna la coppia dei muoni e la conoscenza del quadri-impulso iniziale: P_{in} = (√s,0); $P_H = P_{in} - P_Z$

$$M_H^2 = (\sqrt{s} - E_Z)^2 - P_Z^2 \quad = \mathrm{M}_{\mathrm{recoil}}$$

$$g_{ZZH}^2 \propto \sigma = N/L\epsilon$$

- Dalla misura inclusiva (model indepndent) della sez. d'urto si ricava una misura assoluta dei BR identificando I differenti canali di decadimento e quindi anche una misura model independent di Γ_H:

$$\sigma(ZH) \cdot \mathrm{BR}(H \to ii)$$

$$\Gamma_H = \Gamma(H \to ZZ)/\mathrm{BR}(H \to ZZ) \propto \sigma(ZH)/\mathrm{BR}(H \to ZZ)$$

Determinazione di J^P

- Una volta osservata una risonanza con sezione d'urto e decadimenti approssimativamente simili a quelli del bosone di Higgs del Modello Standard (a "Higgs-boson like resonance" negli articoli post-scoperta) la conferma mancante era la verifica dello spin e della parita' della nuova particella
- Dai decadimenti osservati sappiamo che la particella e' un bosone e che non puo' avere spin 1 dal teorema di Landau-Yang, visto che decade in due bosoni identici massless. Dunque J=0,2 …
- Landau-Yang: ampiezza piu' generale dipende da polarizzazioni (e) e dal momento dei fotoni, con termini come:

$$M_1 = (\vec{e}_1 \wedge \vec{e}_2)\cdot \vec{e}_V$$

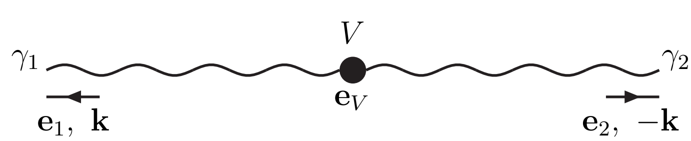

$$M_2 = (\vec{e}_1 \cdot \vec{e}_2)\cdot(\vec{e}_k \cdot \vec{k})$$

$$\text{N.B.:}\ \ \vec{e}_1 \cdot \vec{k} = 0\ ;\ \vec{e}_2 \cdot \vec{k} = 0\ \ \text{photon massless, transverse field}$$

- M_1 e M_2 non rispettano la simmetria di Bose-Einstein per per lo scambio 1←→2 di bosoni identici
- Inoltre la parita' del Higgs nello SM deve essere pari, mentre Higgs pseudo-scalari esistono per esempio nelle teorie supersimmetriche → occorre verificare questa proprieta'.

Determinazione di J

- Nel sistema di riferimento della particella scalare, l'angolo di decadimento e' isotropico nel caso di particella scalare altrimenti abbiamo una dipendenza non triviale dal tipo di stato iniziale e dallo spin, in generale un polinomio di secondo grado in $\cos^2\theta^*$

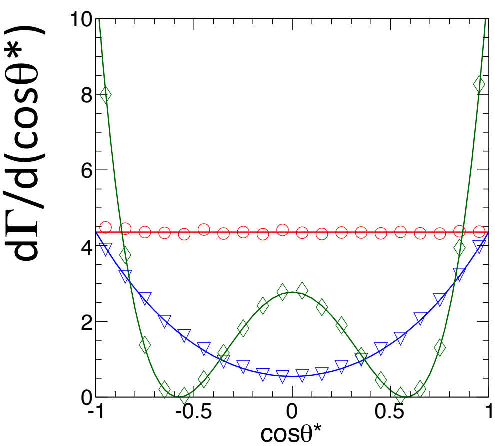

$$F^J_{i,j}(\theta^*) = \sum_{m=0,\pm1,\pm2} f_m\, d^J_{im}(\theta^*) d^J_{jm}(\theta^*)$$

Con m=+/-1 per annichilazioni qqbar 0,+/-2 per gluon-gluon, e dove le d sono le funzioni di Wigner e.g.

$$d^2_{2,2} = \left(\frac{1+\cos\theta}{2}\right)^2$$

Phys.Rev.D86:095031,2012; arxiv:1208.4018

Acceptance
Low energy gamma

$$|\cos\theta^*| = \frac{|\sinh(\Delta\eta^{\gamma\gamma})|}{\sqrt{1+(p_T^{\gamma\gamma}/m_{\gamma\gamma})^2}} \frac{2p_T^{\gamma 1} p_T^{\gamma 2}}{m^2_{\gamma\gamma}}$$

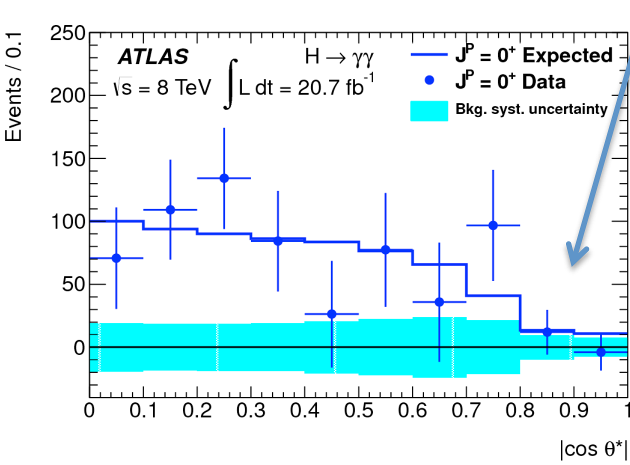

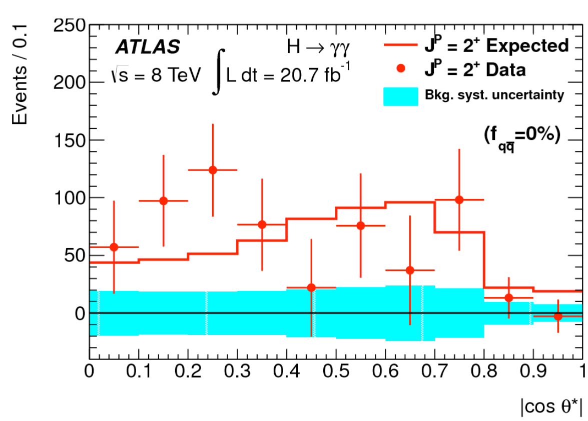

Determinazione di J

ATLAS-CONF-2015-008

Tested Hypothesis	$H \to \gamma\gamma$				
	$p^{ALT}_{exp,\mu=1}$	$p^{ALT}_{exp,\mu=\hat{\mu}}$	p^{SM}_{obs}	p^{ALT}_{obs}	Obs. $\mathrm{CL_s}$ (%)
2^+	0.13	$7.5 \cdot 10^{-2}$	0.13	0.34	39
$2^+(\kappa_q = 0;\ p_\mathrm{T} < 300)$	$4.3 \cdot 10^{-4}$	$< 3.1 \cdot 10^{-5}$	0.16	$2.9 \cdot 10^{-4}$	$3.5 \cdot 10^{-2}$
$2^+(\kappa_q = 0;\ p_\mathrm{T} < 125)$	$9.4 \cdot 10^{-2}$	$5.6 \cdot 10^{-2}$	0.23	0.20	26
$2^+(\kappa_q = 2\kappa_g;\ p_\mathrm{T} < 300)$	$9.1 \cdot 10^{-4}$	$< 3.1 \cdot 10^{-5}$	0.16	$8.6 \cdot 10^{-4}$	0.10
$2^+(\kappa_q = 2\kappa_g;\ p_\mathrm{T} < 125)$	0.27	0.24	0.20	0.54	68

Tested Hypothesis	$H \to WW^* \to e\nu\mu\nu$				
	$p^{ALT}_{exp,\mu=1}$	$p^{ALT}_{exp,\mu=\hat{\mu}}$	p^{SM}_{obs}	p^{ALT}_{obs}	Obs. $\mathrm{CL_s}$ (%)
0^+_h	0.31	0.29	0.91	$2.7 \cdot 10^{-2}$	29
0^-	$6.4 \cdot 10^{-2}$	$3.2 \cdot 10^{-2}$	0.65	$1.2 \cdot 10^{-2}$	3.5
2^+	$6.4 \cdot 10^{-2}$	$3.3 \cdot 10^{-2}$	0.25	0.12	16
$2^+(\kappa_q = 0;\ p_\mathrm{T} < 300)$	$1.5 \cdot 10^{-2}$	$4.0 \cdot 10^{-3}$	0.55	$3.0 \cdot 10^{-3}$	0.6
$2^+(\kappa_q = 0;\ p_\mathrm{T} < 125)$	$5.6 \cdot 10^{-2}$	$2.9 \cdot 10^{-2}$	0.42	$4.4 \cdot 10^{-2}$	7.5
$2^+(\kappa_q = 2\kappa_g;\ p_\mathrm{T} < 300)$	$1.5 \cdot 10^{-2}$	$4.0 \cdot 10^{-3}$	0.52	$3.0 \cdot 10^{-3}$	0.7
$2^+(\kappa_q = 2\kappa_g;\ p_\mathrm{T} < 125)$	$4.4 \cdot 10^{-2}$	$2.2 \cdot 10^{-2}$	0.69	$7.0 \cdot 10^{-3}$	2.2

Tested Hypothesis	$H \to ZZ^* \to 4\ell$				
	$p^{ALT}_{exp,\mu=1}$	$p^{ALT}_{exp,\mu=\hat{\mu}}$	p^{SM}_{obs}	p^{ALT}_{obs}	Obs. $\mathrm{CL_s}$ (%)
0^+_h	$3.2 \cdot 10^{-2}$	$5.2 \cdot 10^{-3}$	0.80	$3.6 \cdot 10^{-4}$	0.18
0^-	$8.0 \cdot 10^{-3}$	$3.6 \cdot 10^{-4}$	0.88	$1.2 \cdot 10^{-5}$	$1.0 \cdot 10^{-2}$
2^+	$3.3 \cdot 10^{-2}$	$5.7 \cdot 10^{-4}$	0.91	$3.6 \cdot 10^{-5}$	$4.0 \cdot 10^{-2}$
$2^+(\kappa_q = 0;\ p_\mathrm{T} < 300)$	$3.9 \cdot 10^{-2}$	$9.0 \cdot 10^{-3}$	0.95	$2.7 \cdot 10^{-5}$	$5.4 \cdot 10^{-2}$
$2^+(\kappa_q = 0;\ p_\mathrm{T} < 125)$	$4.6 \cdot 10^{-2}$	$1.1 \cdot 10^{-2}$	0.93	$3.0 \cdot 10^{-5}$	$4.3 \cdot 10^{-2}$
$2^+(\kappa_q = 2\kappa_g;\ p_\mathrm{T} < 300)$	$4.6 \cdot 10^{-2}$	$1.1 \cdot 10^{-2}$	0.66	$3.3 \cdot 10^{-3}$	0.97
$2^+(\kappa_q = 2\kappa_g;\ p_\mathrm{T} < 125)$	$5.0 \cdot 10^{-2}$	$1.3 \cdot 10^{-2}$	0.88	$3.2 \cdot 10^{-4}$	0.27

Combinazione γγ, WW e ZZ

Tested Hypothesis	$p^{ALT}_{exp,\mu=1}$	$p^{ALT}_{exp,\mu=\hat{\mu}}$	p^{SM}_{obs}	p^{ALT}_{obs}	Obs. CL_S (%)
0^+_h	$2.5 \cdot 10^{-2}$	$4.7 \cdot 10^{-3}$	0.85	$7.1 \cdot 10^{-5}$	$4.7 \cdot 10^{-2}$
0^-	$1.8 \cdot 10^{-3}$	$1.3 \cdot 10^{-4}$	0.88	$< 3.1 \cdot 10^{-5}$	$< 2.6 \cdot 10^{-2}$
2^+	$4.3 \cdot 10^{-3}$	$2.9 \cdot 10^{-4}$	0.61	$4.3 \cdot 10^{-5}$	$1.1 \cdot 10^{-2}$
$2^+(\kappa_q = 0;\ p_\mathrm{T} < 300)$	$< 3.1 \cdot 10^{-5}$	$< 3.1 \cdot 10^{-5}$	0.52	$< 3.1 \cdot 10^{-5}$	$< 6.5 \cdot 10^{-3}$
$2^+(\kappa_q = 0;\ p_\mathrm{T} < 125)$	$3.4 \cdot 10^{-3}$	$3.9 \cdot 10^{-4}$	0.71	$4.3 \cdot 10^{-5}$	$1.5 \cdot 10^{-2}$
$2^+(\kappa_q = 2\kappa_g;\ p_\mathrm{T} < 300)$	$< 3.1 \cdot 10^{-5}$	$< 3.1 \cdot 10^{-5}$	0.28	$< 3.1 \cdot 10^{-5}$	$< 4.3 \cdot 10^{-3}$
$2^+(\kappa_q = 2\kappa_g;\ p_\mathrm{T} < 125)$	$7.8 \cdot 10^{-3}$	$1.2 \cdot 10^{-3}$	0.80	$7.3 \cdot 10^{-5}$	$3.7 \cdot 10^{-2}$

Determinazione parita’

- Utilizziamo il potere analizzante delle distribuzioni angolari nei decadimenti H→ZZ*→4l
- Per uno scalare che decade in due vettori di spin 1, esistono 3 possibili stati del momento angolaro relativo L dei due bosoni Z, corrispondenti a L=0,1,2
- L=0,2 corrispoondono ad ampiezze a parita’ positiva ($P=(-1)^L$) (CP ugualmente pari, particelle identiche), L=1 ad ampiezze a parita’ negative
- Nel caso generale del decadimento di uno scalare in due particelle di spin 1, avremo 3 ampiezze indipendenti corrispondenti ai 3 stati possibili di momento angolare e caratterizzate da proprieta’ di trasformazione sotto CP diverse.

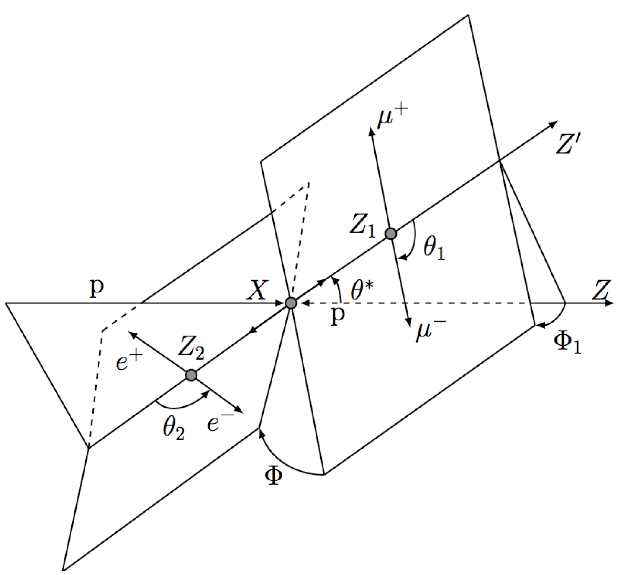

- Una base appropriata per le ampiezze e’ quella di elicita’, in cui sono classificate in base all’elicita’ dei due boasoni dello stato finale A_{00}, A_{++}, A_{--}. Gli angoli di decadimento dei leptoni nel frame di uno Z sono sensibili all’elicita’ dello Z
- Nel caso H→ZZ e’ usuale parametrizzare l’ampiezza come:

$$A(X \to Z_1 Z_2) = v^{-1}\left(\boxed{g_1 m_Z^2 \epsilon_1^* \epsilon_2^*} + \boxed{g_2 f^{*(1)}_{\mu\nu} f^{*(2),\mu\nu}} + g_3 f^{*(1),\mu\nu} \cancel{f^{*(2)}_{\mu\alpha} \frac{q_\nu q^\alpha}{\Lambda^2}} + \boxed{g_4 f^{*(1)}_{\mu\nu} \tilde{f}^{*(2),\mu\nu}}\right)$$

SM Higgs BSM scalar pseudoscalar

L=0,2 L=1

Determinazione parita'

phase space + propagator

$$\frac{d\Gamma_J(m_1,m_2,\Omega)}{dm_1 dm_2 d\Omega} \propto P(m_1,m_2)\cdot\sum_i K_i(m_1,m_2) f_i(\Omega)$$

J=0: three helicity combinations (A_{++}, A_{--}, A_{00})

$\Rightarrow K_i = |A_{++}|^2, \mathrm{Re}(A_{++}A_{00}^*), \mathrm{Im}(A_{++}A_{00}^*)$ ... (9 terms)

$$\mathbf{\Omega} = \{\cos\theta^*, \phi_1, \cos\theta_1, \cos\theta_2, \phi\}$$

arXiv:1208.4018

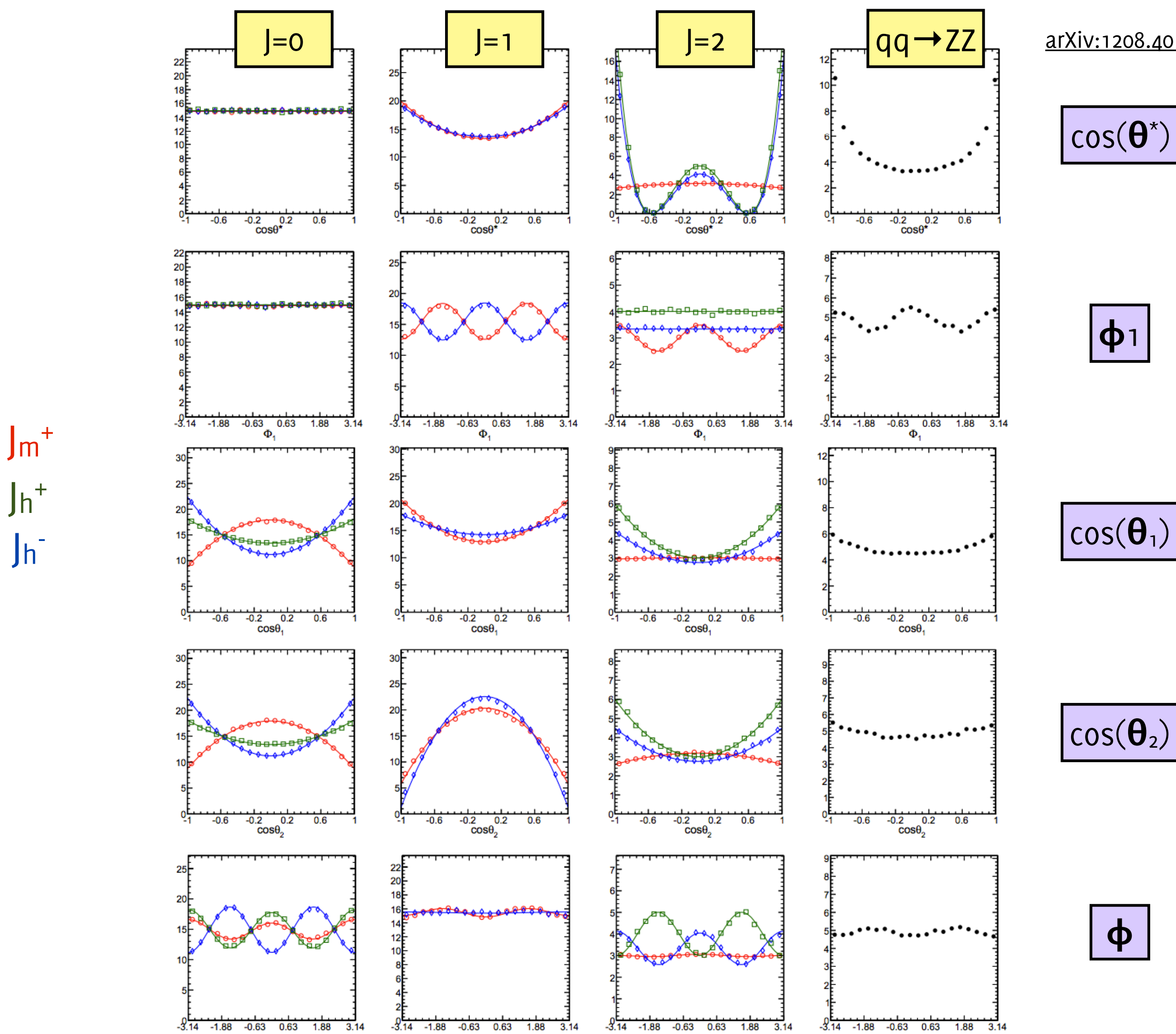

Determinazione parita’

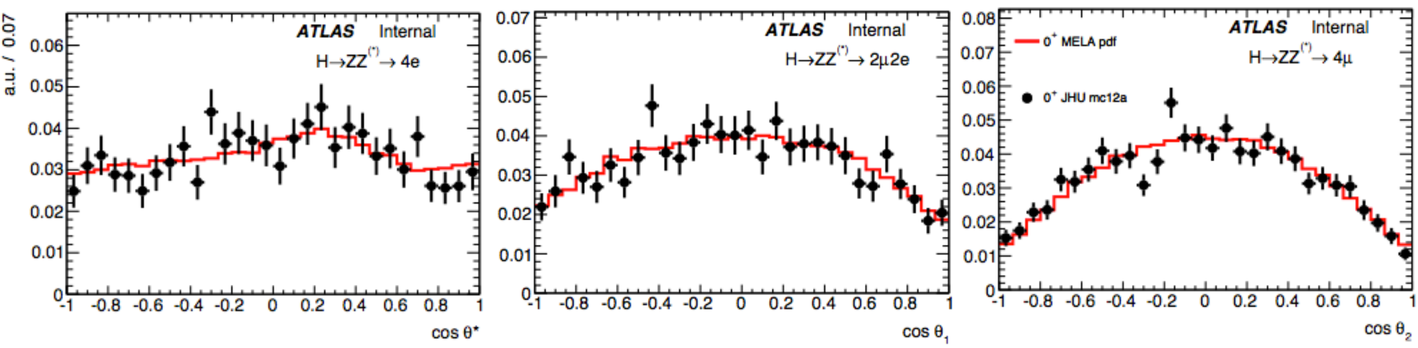

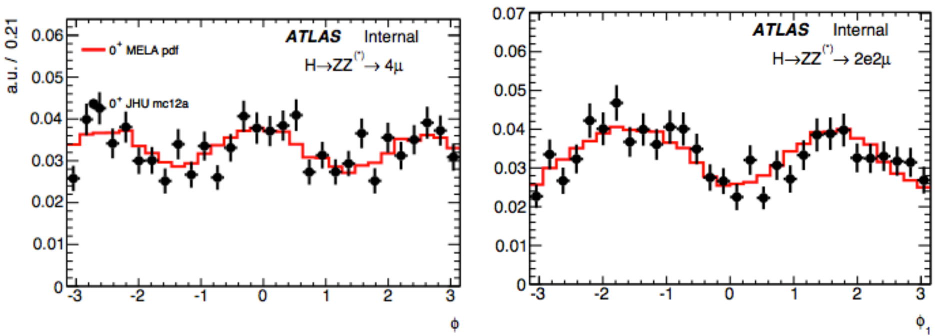

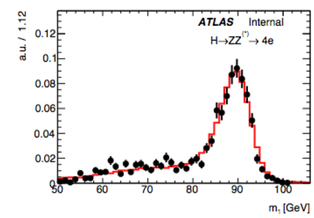

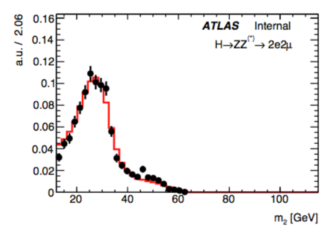

good description of full-sim MC for all tested models

this avoids loss in separation between hypotheses

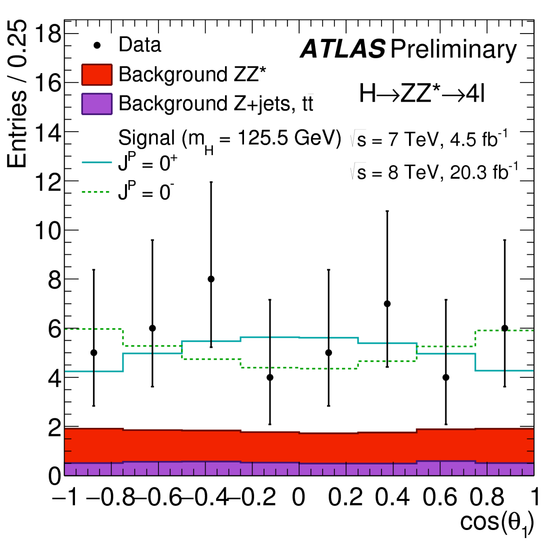

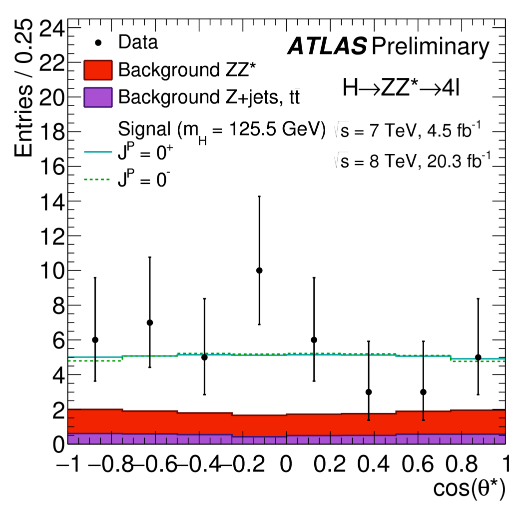

Determinazione parita'

ATLAS-CONF-2015-008

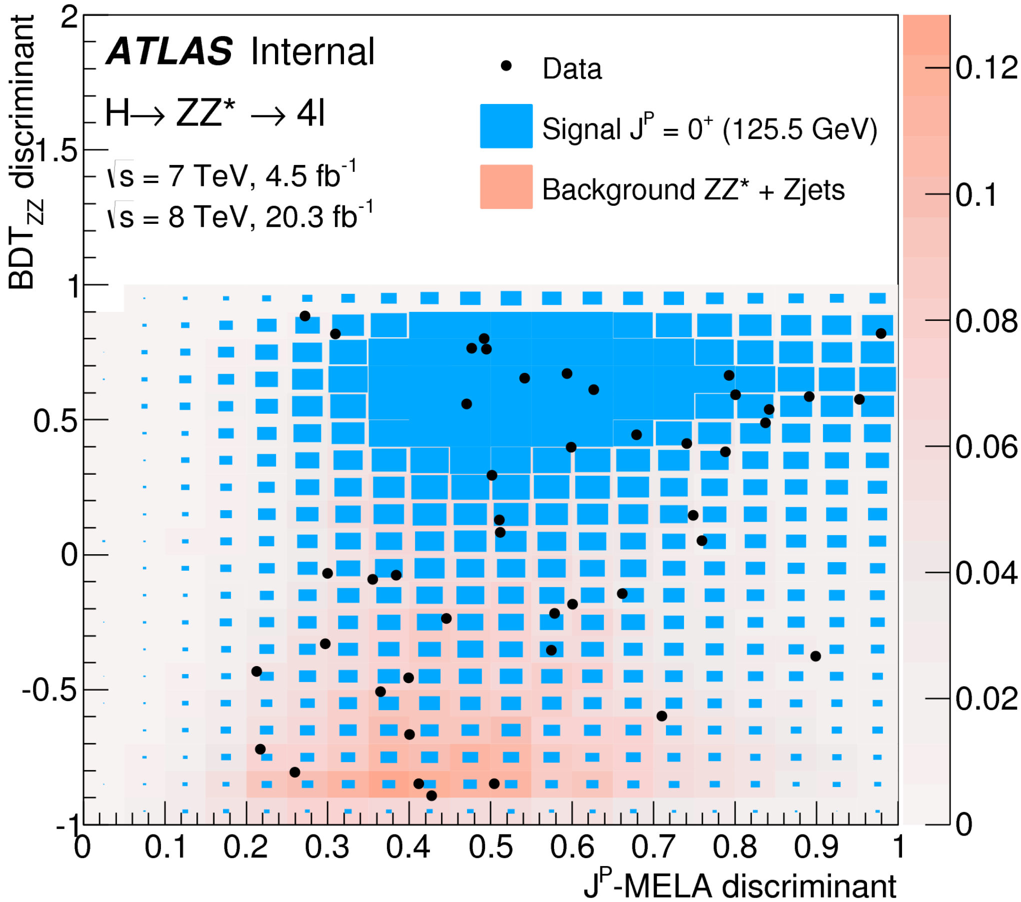

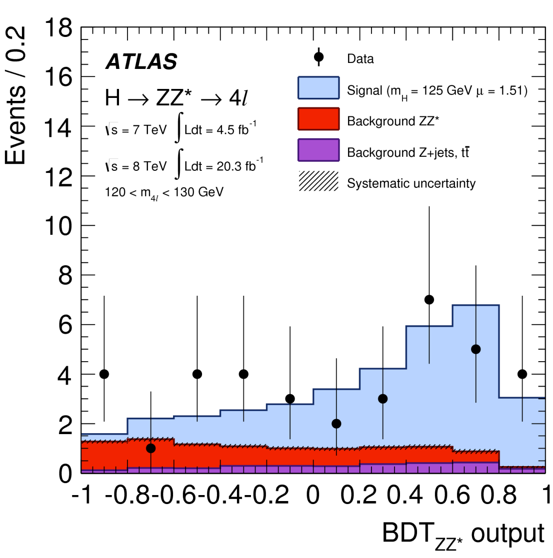

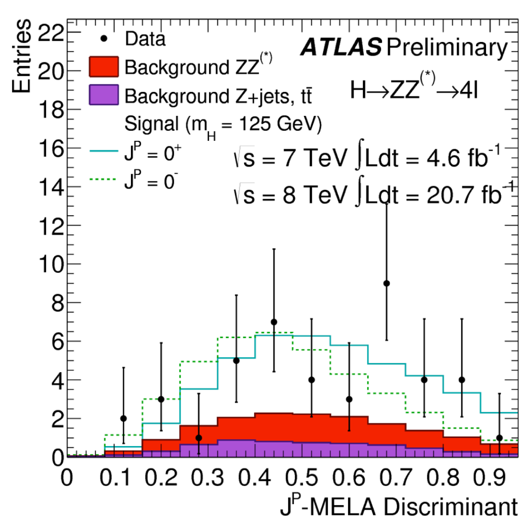

Determinazione di parita’

ATLAS-CONF-2015-008

Tested Hypothesis	$H \to \gamma\gamma$ $p^{ALT}_{exp,\mu=1}$	$p^{ALT}_{exp,\mu=\hat{\mu}}$	p^{SM}_{obs}	p^{ALT}_{obs}	Obs. CL_s (%)
2^+	0.13	$7.5 \cdot 10^{-2}$	0.13	0.34	39
$2^+(\kappa_q = 0;\ p_T < 300)$	$4.3 \cdot 10^{-4}$	$< 3.1 \cdot 10^{-5}$	0.16	$2.9 \cdot 10^{-4}$	$3.5 \cdot 10^{-2}$
$2^+(\kappa_q = 0;\ p_T < 125)$	$9.4 \cdot 10^{-2}$	$5.6 \cdot 10^{-2}$	0.23	0.20	26
$2^+(\kappa_q = 2\kappa_g;\ p_T < 300)$	$9.1 \cdot 10^{-4}$	$< 3.1 \cdot 10^{-5}$	0.16	$8.6 \cdot 10^{-4}$	0.10
$2^+(\kappa_q = 2\kappa_g;\ p_T < 125)$	0.27	0.24	0.20	0.54	68

Tested Hypothesis	$H \to WW^* \to e\nu\mu\nu$ $p^{ALT}_{exp,\mu=1}$	$p^{ALT}_{exp,\mu=\hat{\mu}}$	p^{SM}_{obs}	p^{ALT}_{obs}	Obs. CL_s (%)
0^+_h	0.31	0.29	0.91	$2.7 \cdot 10^{-2}$	29
0^-	$6.4 \cdot 10^{-2}$	$3.2 \cdot 10^{-2}$	0.65	$1.2 \cdot 10^{-2}$	3.5
2^+	$6.4 \cdot 10^{-2}$	$3.3 \cdot 10^{-2}$	0.25	0.12	16
$2^+(\kappa_q = 0;\ p_T < 300)$	$1.5 \cdot 10^{-2}$	$4.0 \cdot 10^{-3}$	0.55	$3.0 \cdot 10^{-3}$	0.6
$2^+(\kappa_q = 0;\ p_T < 125)$	$5.6 \cdot 10^{-2}$	$2.9 \cdot 10^{-2}$	0.42	$4.4 \cdot 10^{-2}$	7.5
$2^+(\kappa_q = 2\kappa_g;\ p_T < 300)$	$1.5 \cdot 10^{-2}$	$4.0 \cdot 10^{-3}$	0.52	$3.0 \cdot 10^{-3}$	0.7
$2^+(\kappa_q = 2\kappa_g;\ p_T < 125)$	$4.4 \cdot 10^{-2}$	$2.2 \cdot 10^{-2}$	0.69	$7.0 \cdot 10^{-3}$	2.2

Tested Hypothesis	$H \to ZZ^* \to 4\ell$ $p^{ALT}_{exp,\mu=1}$	$p^{ALT}_{exp,\mu=\hat{\mu}}$	p^{SM}_{obs}	p^{ALT}_{obs}	Obs. CL_s (%)
0^+_h	$3.2 \cdot 10^{-2}$	$5.2 \cdot 10^{-3}$	0.80	$3.6 \cdot 10^{-4}$	0.18
0^-	$8.0 \cdot 10^{-3}$	$3.6 \cdot 10^{-4}$	0.88	$1.2 \cdot 10^{-5}$	$1.0 \cdot 10^{-2}$
2^+	$3.3 \cdot 10^{-2}$	$5.7 \cdot 10^{-4}$	0.91	$3.6 \cdot 10^{-5}$	$4.0 \cdot 10^{-2}$
$2^+(\kappa_q = 0;\ p_T < 300)$	$3.9 \cdot 10^{-2}$	$9.0 \cdot 10^{-3}$	0.95	$2.7 \cdot 10^{-5}$	$5.4 \cdot 10^{-2}$
$2^+(\kappa_q = 0;\ p_T < 125)$	$4.6 \cdot 10^{-2}$	$1.1 \cdot 10^{-2}$	0.93	$3.0 \cdot 10^{-5}$	$4.3 \cdot 10^{-2}$
$2^+(\kappa_q = 2\kappa_g;\ p_T < 300)$	$4.6 \cdot 10^{-2}$	$1.1 \cdot 10^{-2}$	0.66	$3.3 \cdot 10^{-3}$	0.97
$2^+(\kappa_q = 2\kappa_g;\ p_T < 125)$	$5.0 \cdot 10^{-2}$	$1.3 \cdot 10^{-2}$	0.88	$3.2 \cdot 10^{-4}$	0.27

Combinazione γγ, WW e ZZ

Tested Hypothesis	$p^{ALT}_{exp,\mu=1}$	$p^{ALT}_{exp,\mu=\hat{\mu}}$	p^{SM}_{obs}	p^{ALT}_{obs}	Obs. CL_S (%)
0^+_h	$2.5 \cdot 10^{-2}$	$4.7 \cdot 10^{-3}$	0.85	$7.1 \cdot 10^{-5}$	$4.7 \cdot 10^{-2}$
0^-	$1.8 \cdot 10^{-3}$	$1.3 \cdot 10^{-4}$	0.88	$< 3.1 \cdot 10^{-5}$	$< 2.6 \cdot 10^{-2}$
2^+	$4.3 \cdot 10^{-3}$	$2.9 \cdot 10^{-4}$	0.61	$4.3 \cdot 10^{-5}$	$1.1 \cdot 10^{-2}$
$2^+(\kappa_q = 0;\ p_T < 300)$	$< 3.1 \cdot 10^{-5}$	$< 3.1 \cdot 10^{-5}$	0.52	$< 3.1 \cdot 10^{-5}$	$< 6.5 \cdot 10^{-3}$
$2^+(\kappa_q = 0;\ p_T < 125)$	$3.4 \cdot 10^{-3}$	$3.9 \cdot 10^{-4}$	0.71	$4.3 \cdot 10^{-5}$	$1.5 \cdot 10^{-2}$
$2^+(\kappa_q = 2\kappa_g;\ p_T < 300)$	$< 3.1 \cdot 10^{-5}$	$< 3.1 \cdot 10^{-5}$	0.28	$< 3.1 \cdot 10^{-5}$	$< 4.3 \cdot 10^{-3}$
$2^+(\kappa_q = 2\kappa_g;\ p_T < 125)$	$7.8 \cdot 10^{-3}$	$1.2 \cdot 10^{-3}$	0.80	$7.3 \cdot 10^{-5}$	$3.7 \cdot 10^{-2}$

Determinazione limiti sui parametri della lagrangiana efficace

ATLAS/HIGG-2013-17

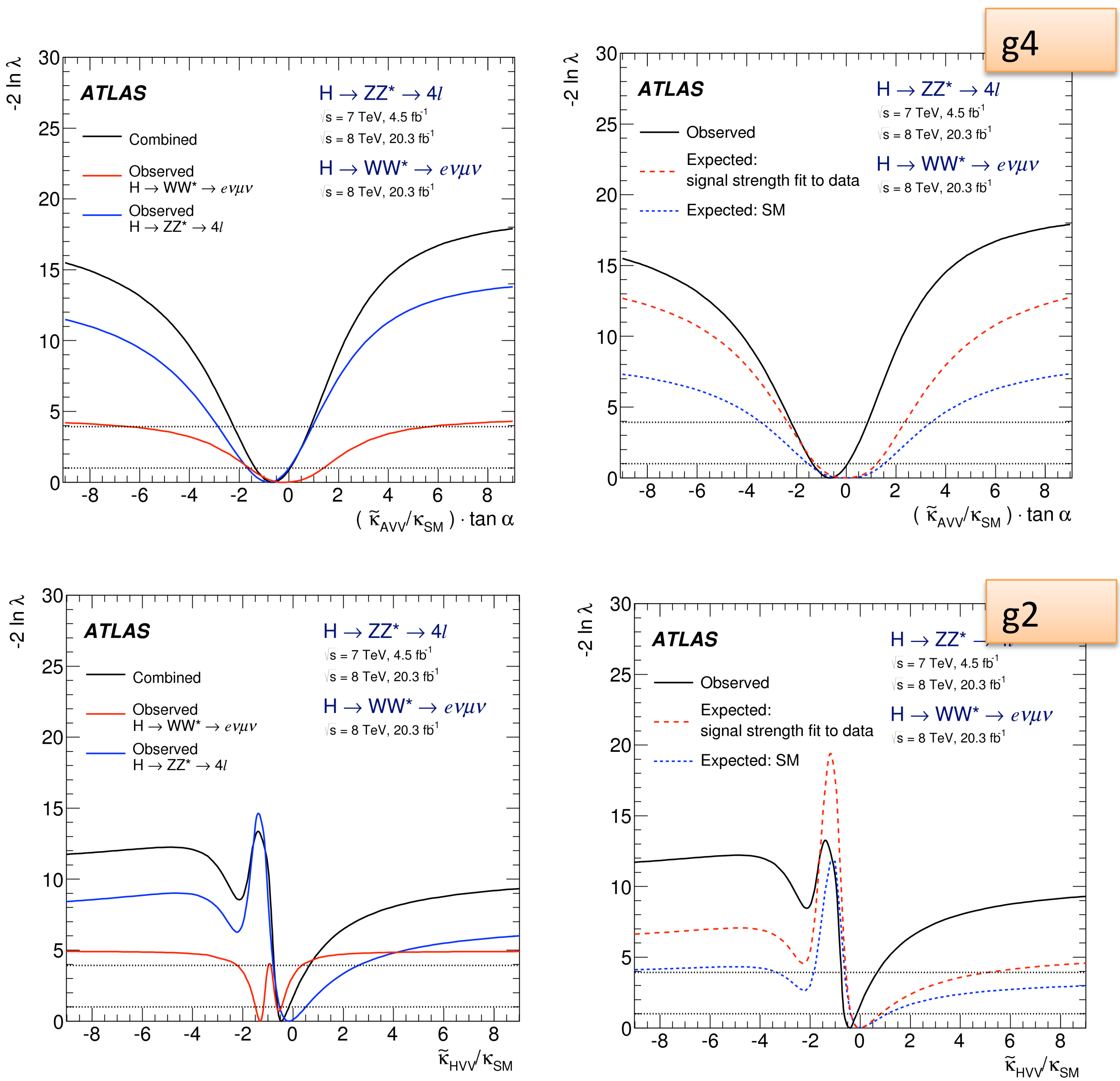

ULTERIORI CANALI DI DECADIMENTO DEL BOSONE DI HIGGS

H→WW*(Latest/ATLAS)

[ATLAS-HIGG-2013-13]

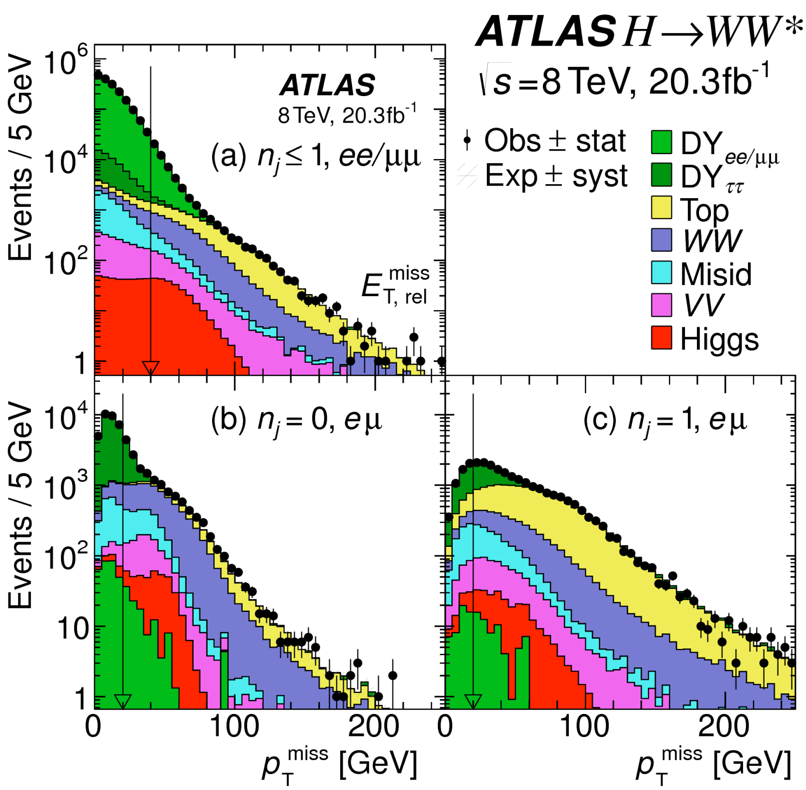

- Stati finali con due leptoni e due neutrini, background molto difficili da controllare, nelle configurazioni di interesse per selezionare il segnale
- Variabile fondamentale per sopprimere il fondo Drell-Yan, la missing transverse energy

Correlazioni di spin

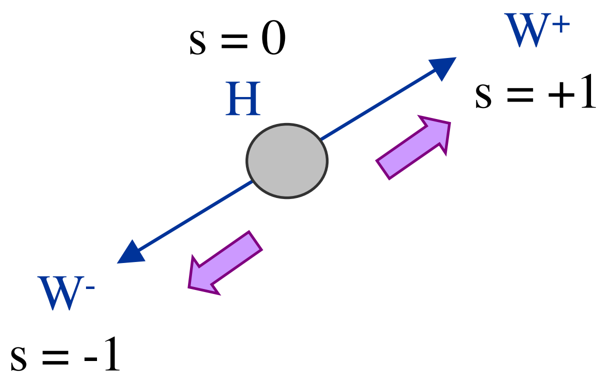

I leptoni carichi a causa della loro elicità opposta tendono ad avere la stessa direzione :

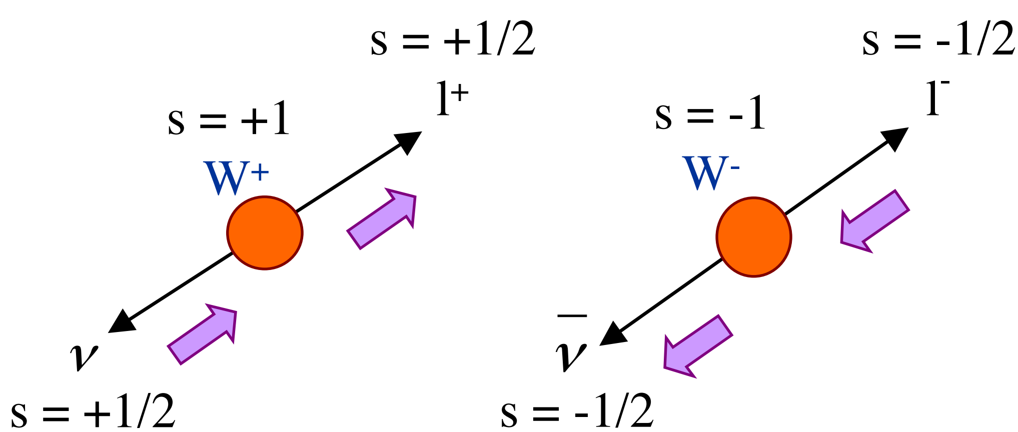

Uso del piccolo angolo di apertura tra i leptoni per distinguerli da quelli del fondo

H→WW*(Latest/ATLAS)

ATLAS-HIGG-2013-13

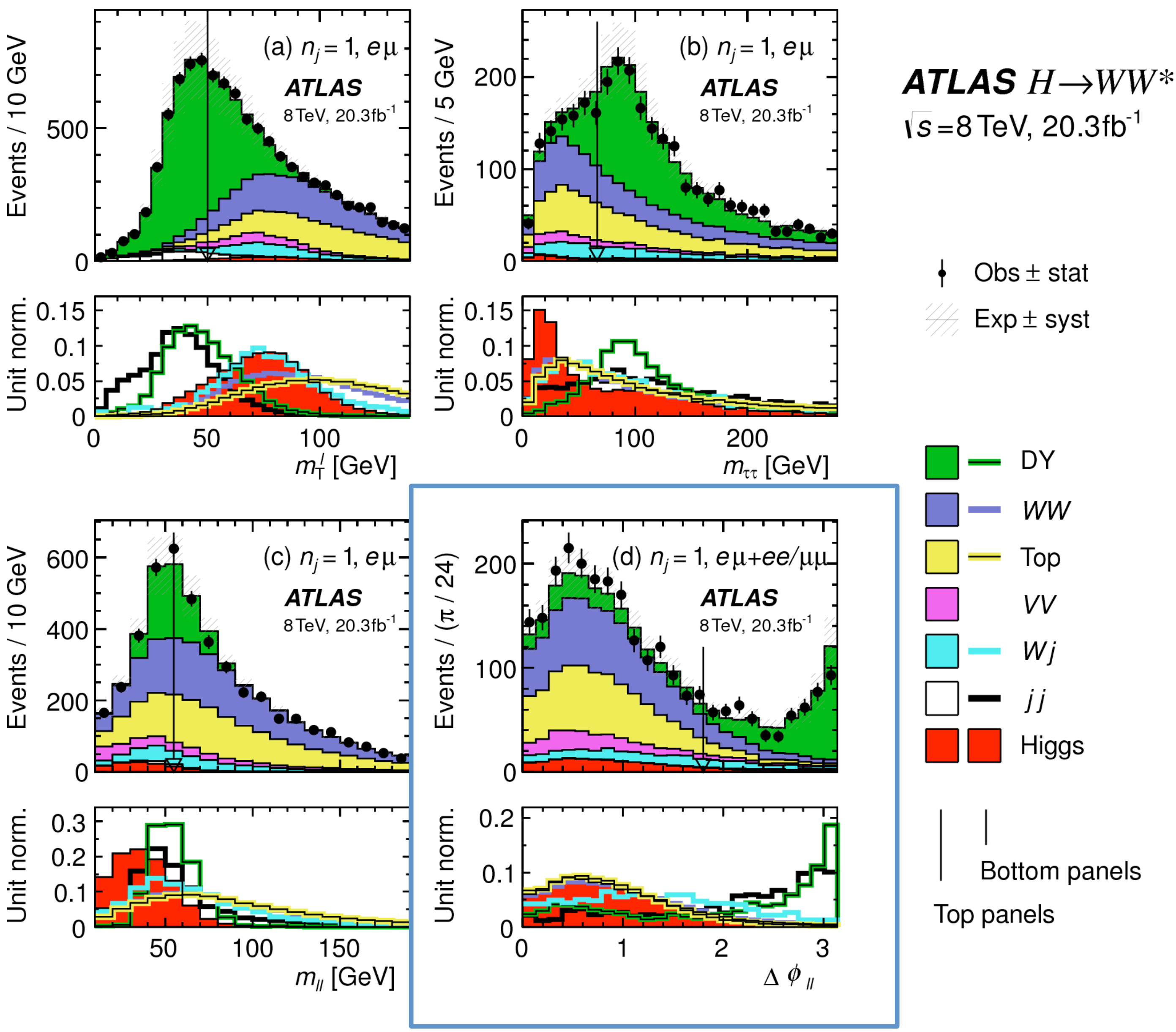

$\Delta\phi_{ll}$ variable sensibile allo spin del Higgs

H→WW*(Latest/ATLAS)

[ATLAS-HIGG-2013-13]()

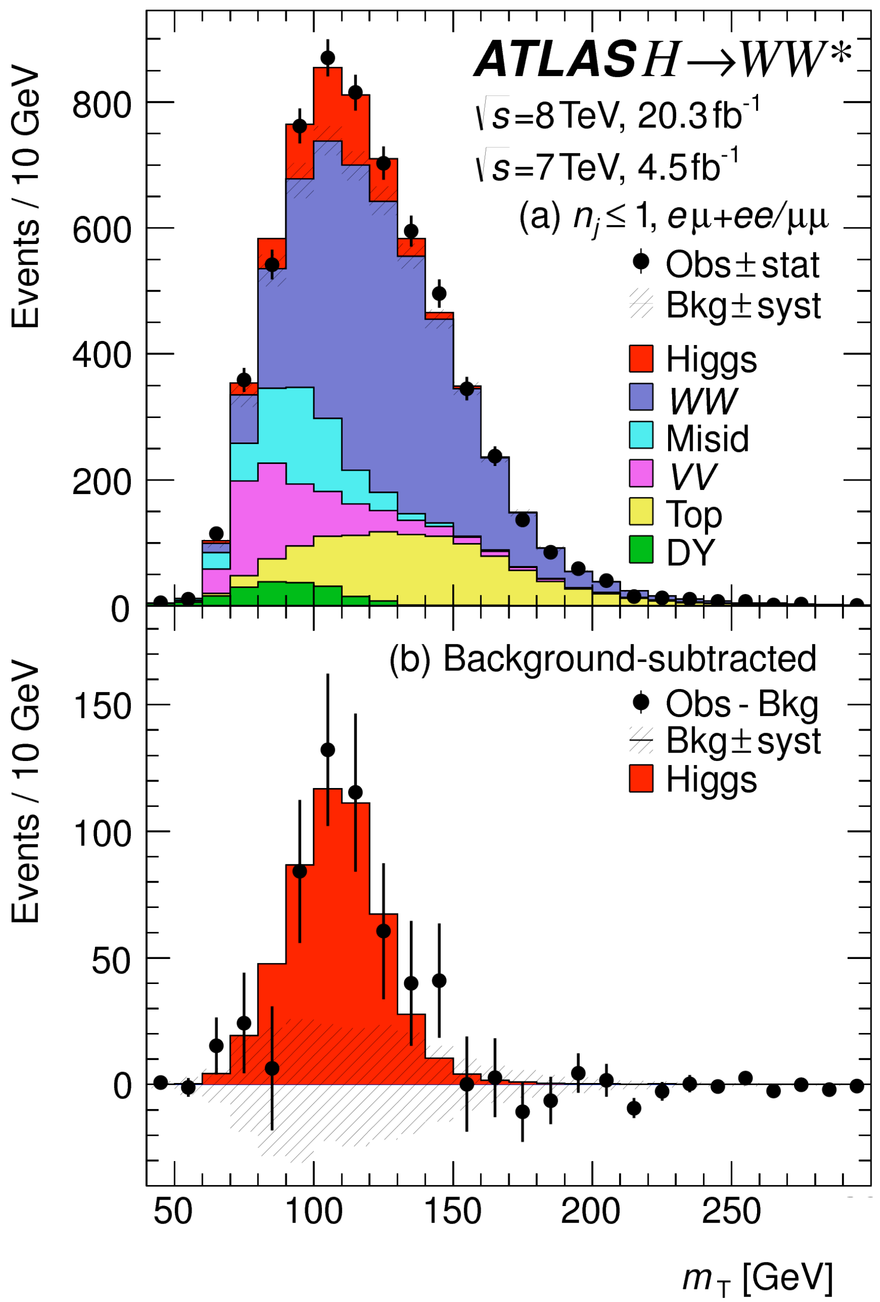

H→WW*(Latest/ATLAS)

ATLAS-HIGG-2013-13

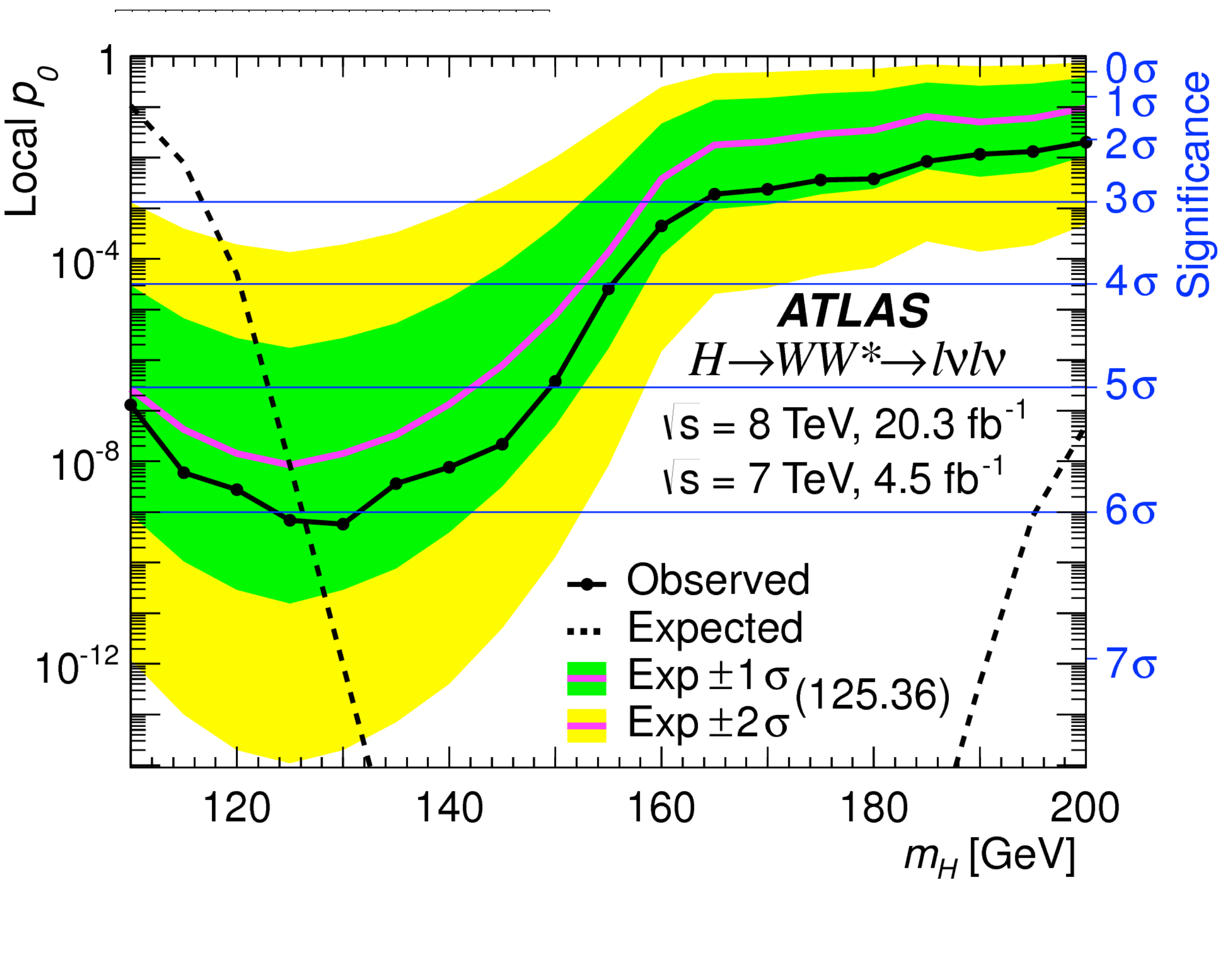

H→WW*(Latest/ATLAS)

ATLAS-HIGG-2013-13

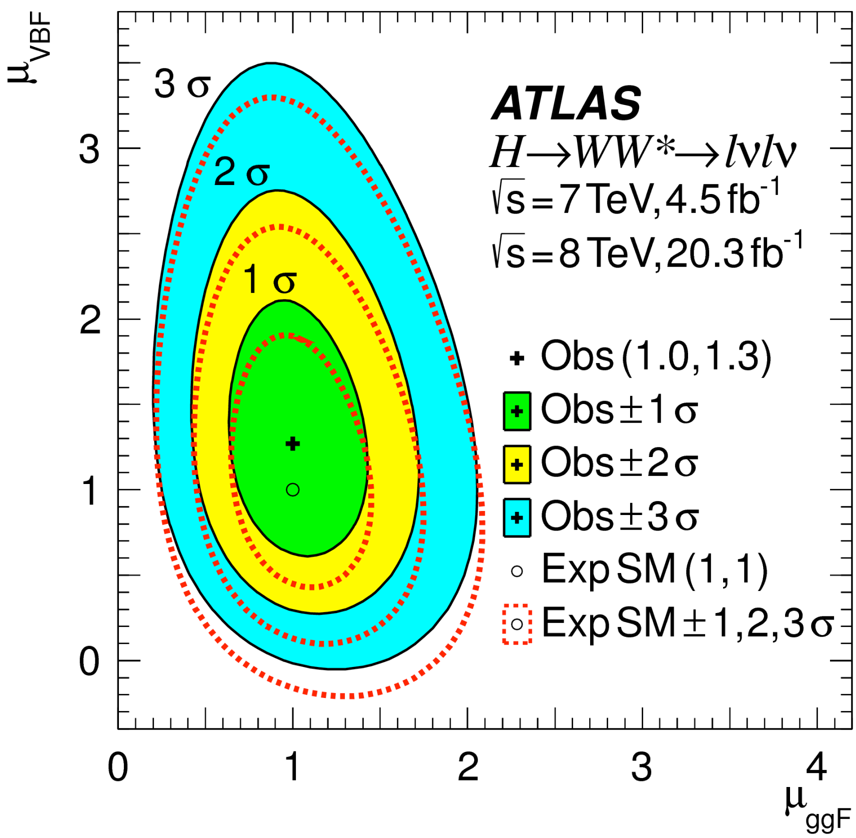

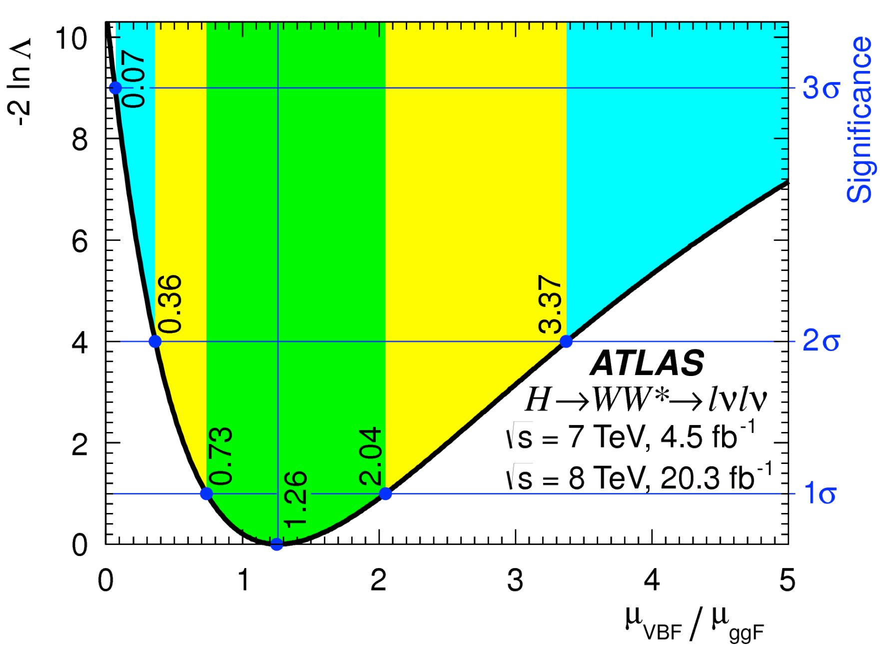

H→bb

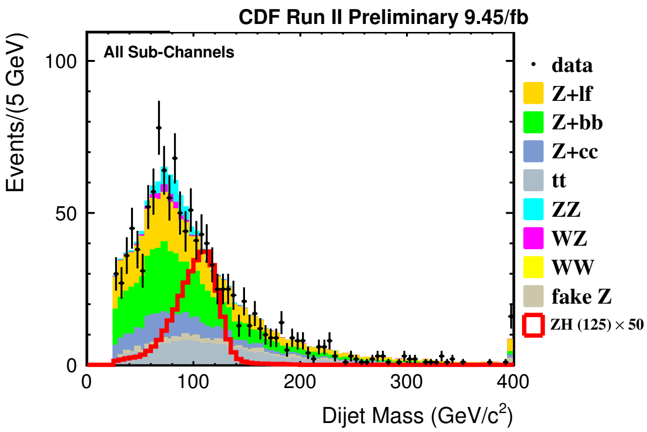

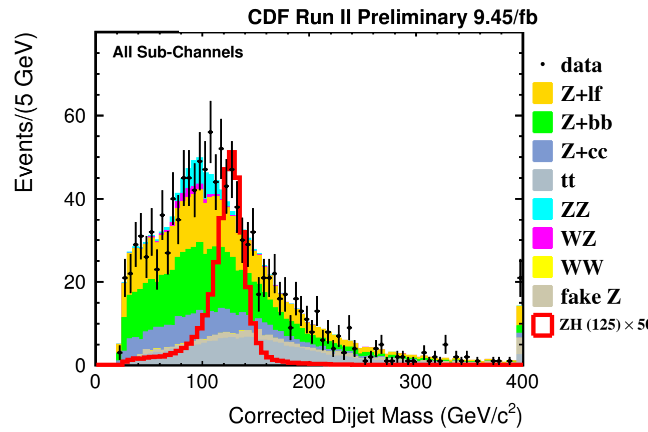

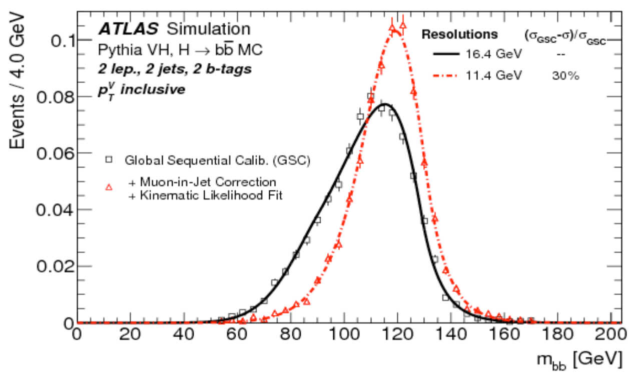

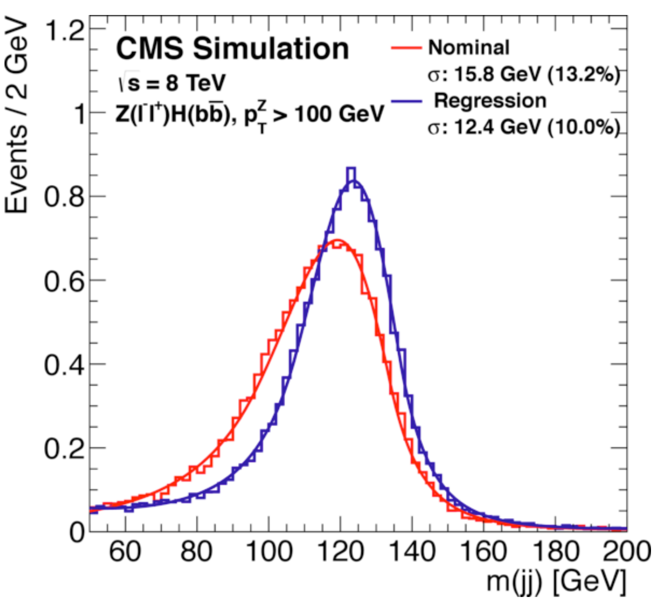

- Cruciale aumentare la risoluzione in massa invariante del sistema bb per aumentare significativita'. Si raggiungono valori di σ/M fino a 10% utilizzando tutta l'informazione dell'evento in eventi del tipo ZH→llbb
- Da confrontare con risoluzioni di ~2% H→γγ
- Al Tevatron e' il canale piu' sensibile per mH=125 GeV, al contrario che a LHC perche' la sezione d'urto del fondo cresce molto piu' che per il segnale tra p-antip a 1.96 TeV e pp a 8 TeV

H→bb

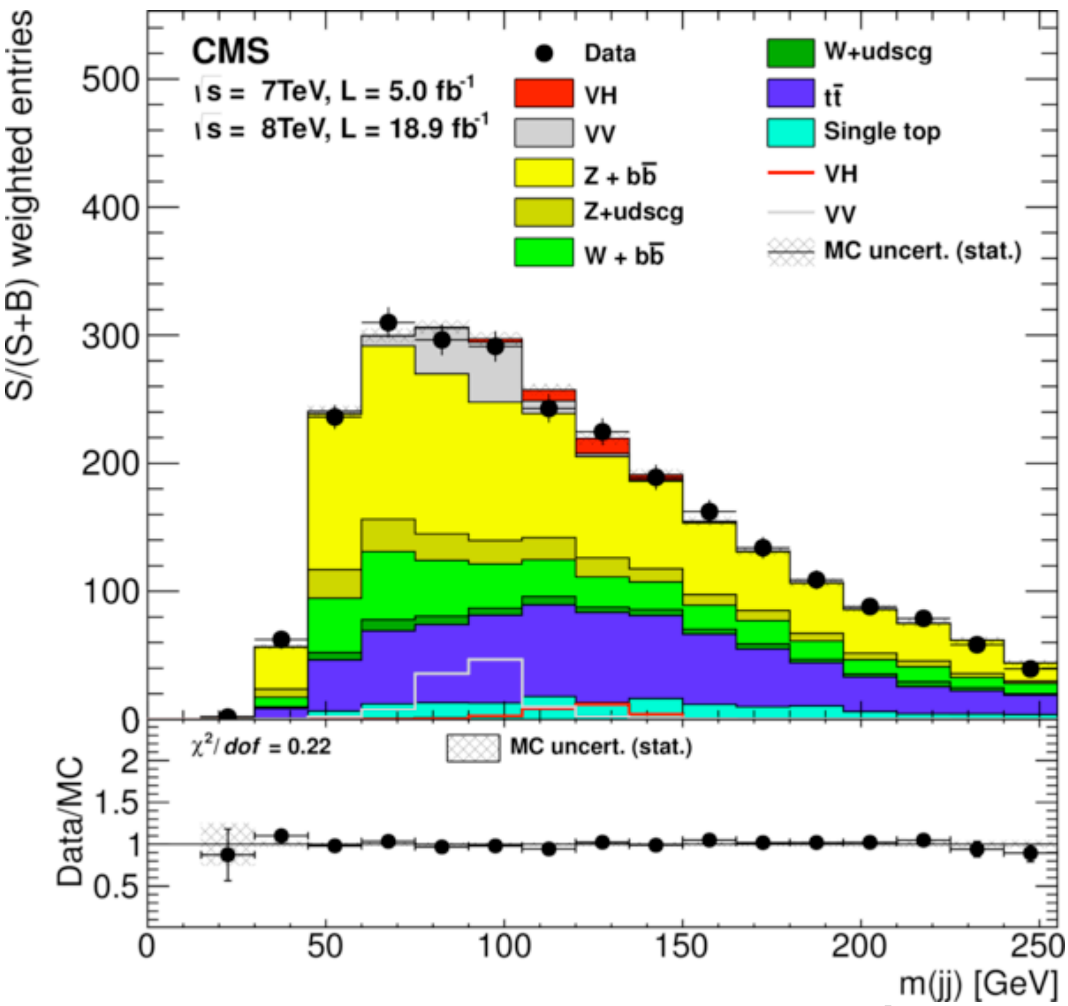

- Analisi suddivisa in molti sottocanali: WH→lnubb, ZH→llbb, ZH→nunu bb, regioni cinematiche e diverse categorie di b-tagging e dei disciminanti basati sulle caratteristiche degli eventi
- Il plot qui mostrato e' solo illustrativo e rappresenta la distribuzione finale di massa invariante pesata per la significativita' aspettata in ciascuna categoria
- Da un'idea del rapporto S/B e della difficolta' di questa ricerca

H→bb

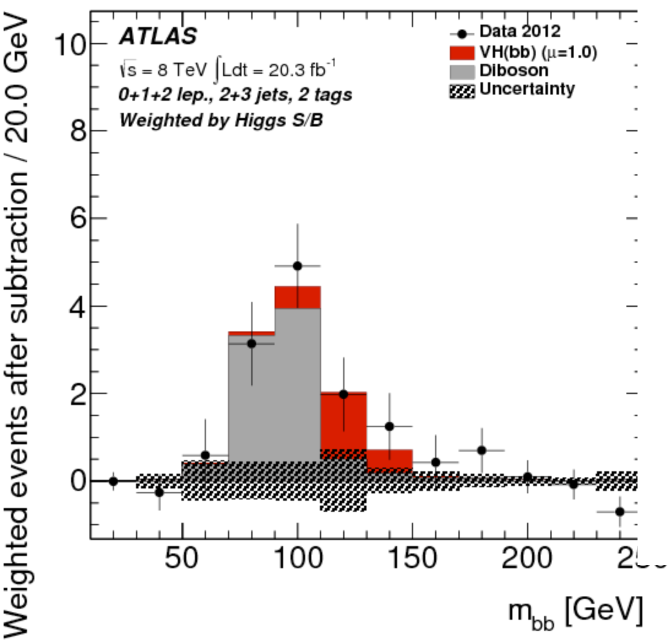
ATLAS
√s = 8 TeV ∫Ldt = 20.3 fb⁻¹
0+1+2 lep., 2+3 jets, 2 tags
Weighted by Higgs S/B
Data 2012
VH(bb) (μ=1.0)
Diboson
Uncertainty
Weighted events after subtraction / 20.0 GeV
m_bb [GeV]

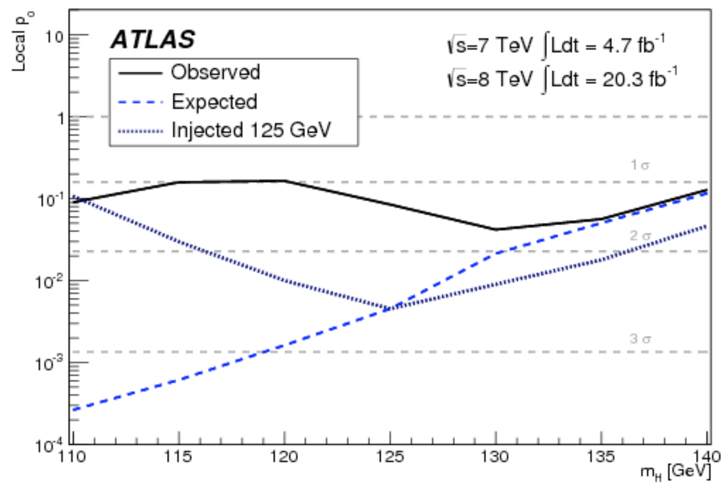
ATLAS
√s=7 TeV ∫Ldt = 4.7 fb⁻¹
√s=8 TeV ∫Ldt = 20.3 fb⁻¹
Observed
Expected
Injected 125 GeV
Local p₀
1σ
2σ
3σ
m_H [GeV]

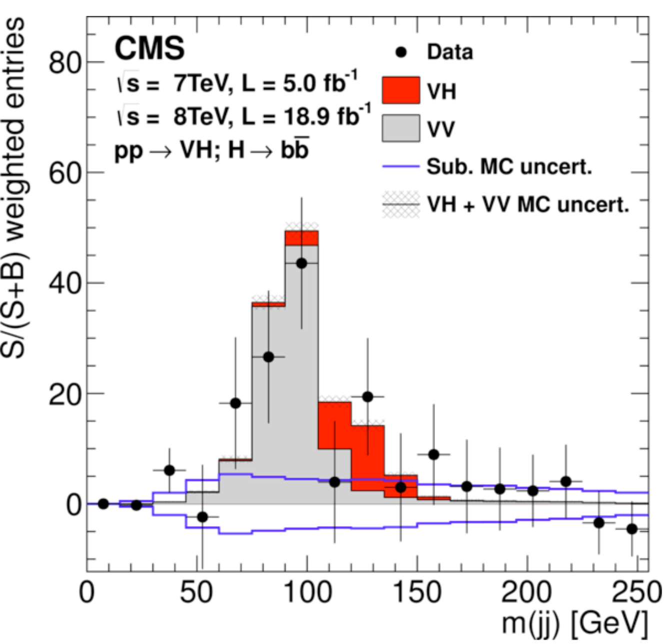
CMS
√s = 7TeV, L = 5.0 fb⁻¹
√s = 8TeV, L = 18.9 fb⁻¹
pp → VH; H → bb̄
Data
VH
VV
Sub. MC uncert.
VH + VV MC uncert.
S/(S+B) weighted entries
m(jj) [GeV]

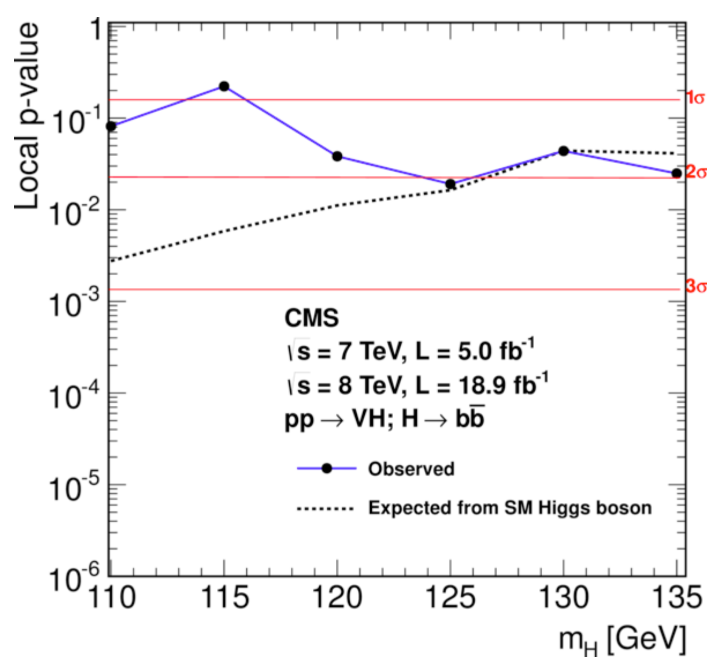
Local p-value
1σ
2σ
3σ
CMS
√s = 7 TeV, L = 5.0 fb⁻¹
√s = 8 TeV, L = 18.9 fb⁻¹
pp → VH; H → bb̄
Observed
Expected from SM Higgs boson
m_H [GeV]

H→bb Tevatron combination

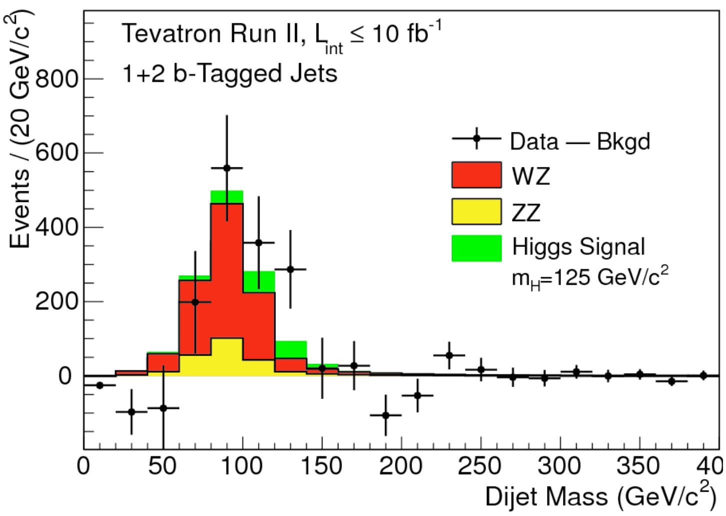

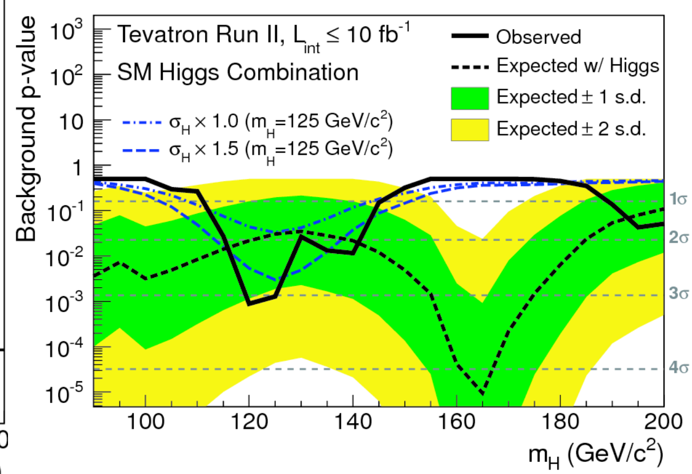

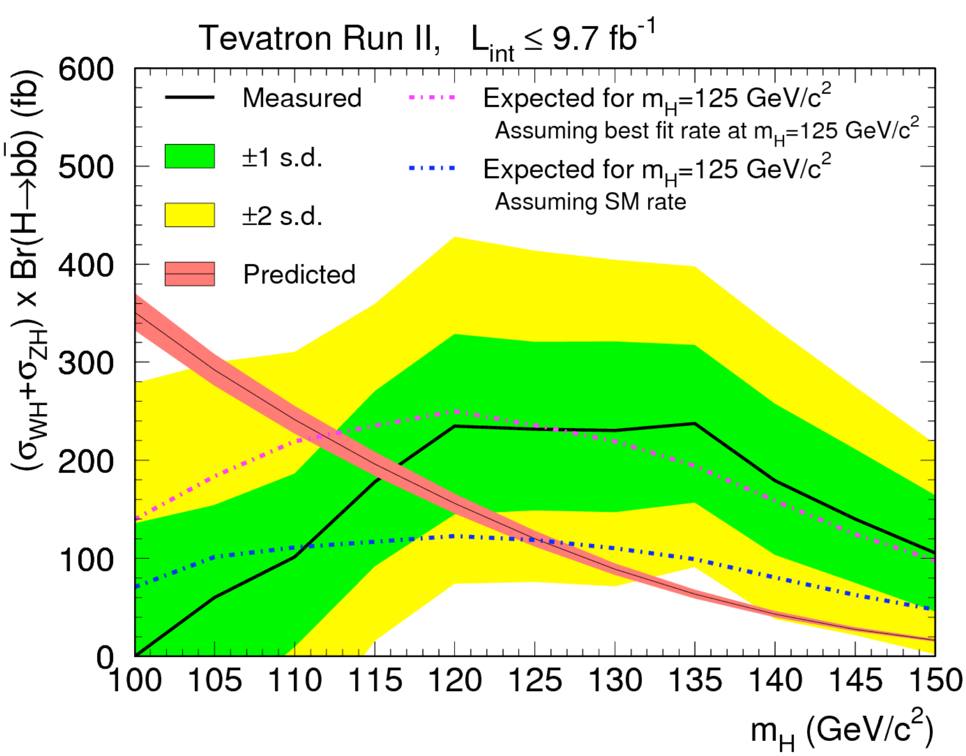

H→ττ

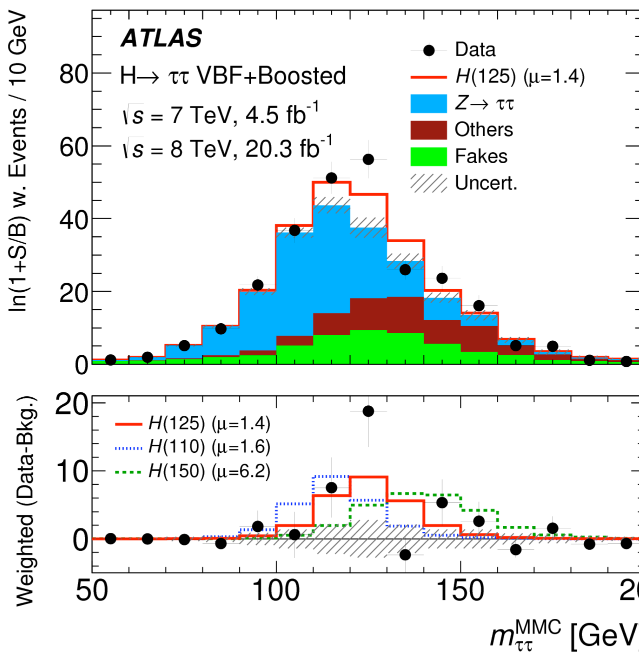

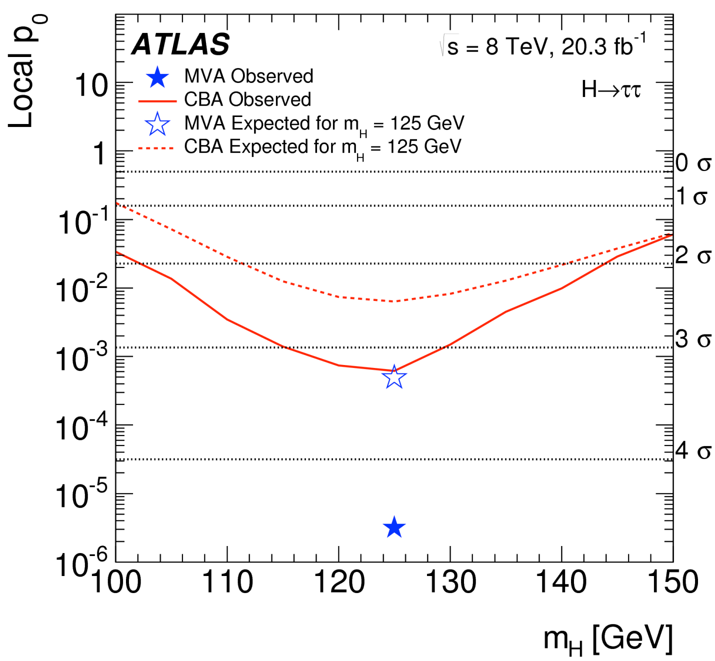

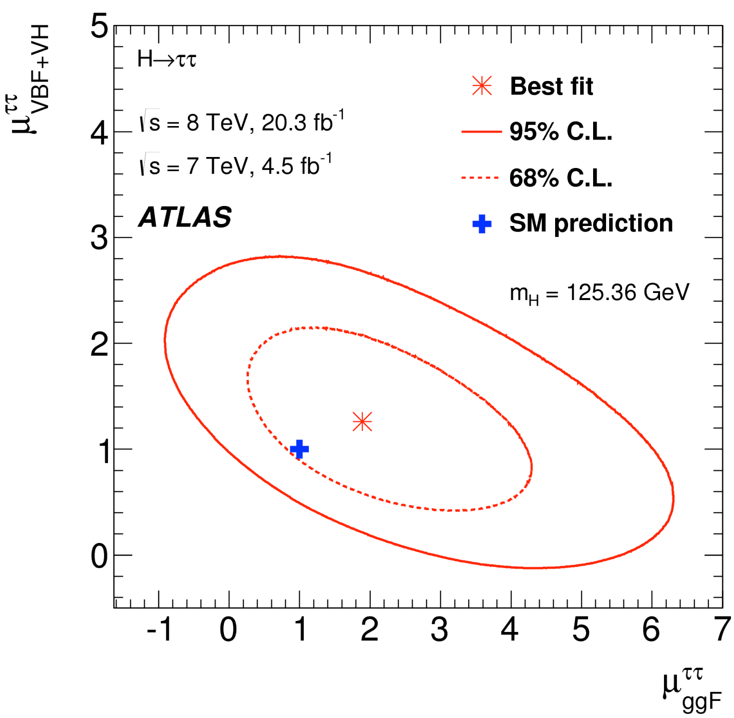

- Unico canale realisticamente osservabile con Higgs che decade in leptoni
- Evidenza a >3σ ottenuta in ATLAS

Higgs coupling in SM

- Given Higgs Mass no free parameter in the SM !

$$V(|\varphi|) = \mu^2 |\varphi|^2 + \lambda |\varphi|^4$$

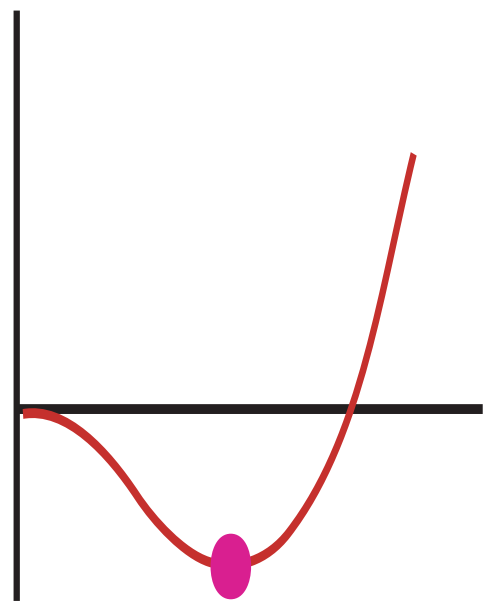

$$m_h = \sqrt{2|\mu^2|} = \sqrt{\lambda/2}v$$

With $$m_W^2 = \frac{g^2}{4}v^2 \qquad m_Z^2 = \frac{g^2 + g'^2}{4}v^2$$

$$m_W / m_Z = \cos\theta_w$$

Then Higgs – Boson and Higgs – Fermion (Yukawa) interaction perfectly determined given particle masses

EWK Lagrangian

$$\mathcal{L}_{EW} = \mathcal{L}_K + \mathcal{L}_N + \mathcal{L}_C + \mathcal{L}_H + \mathcal{L}_{HV} + \mathcal{L}_{WWV} + \mathcal{L}_{WWVV} + \mathcal{L}_Y$$

$$\mathcal{L}_K = \sum_f \bar{f}(i\partial\!\!\!/ - m_f)f - \frac{1}{4}A_{\mu\nu}A^{\mu\nu} - \frac{1}{2}W^+_{\mu\nu}W^{-\mu\nu} + m_W^2 W^+_\mu W^{-\mu} - \frac{1}{4}Z_{\mu\nu}Z^{\mu\nu} + \frac{1}{2}m_Z^2 Z_\mu Z^\mu + \frac{1}{2}(\partial^\mu H)(\partial_\mu H) - \frac{1}{2}m_H^2 H^2$$

$$\mathcal{L}_N = eJ_\mu^{em}A^\mu + \frac{g}{\cos\theta_W}(J_\mu^3 - \sin^2\theta_W J_\mu^{em})Z^\mu$$

$$\mathcal{L}_C = -\frac{g}{\sqrt{2}}\left[\bar{u}_i\gamma^\mu\frac{1-\gamma^5}{2}M_{ij}^{CKM}d_j + \bar{\nu}_i\gamma^\mu\frac{1-\gamma^5}{2}e_i\right]W_\mu^+ + h.c.$$

$$\mathcal{L}_H = -\frac{gm_H^2}{4m_W}H^3 - \frac{g^2m_H^2}{32m_W^2}H^4 \qquad \mathcal{L}_Y = -\sum_f \frac{gm_f}{2m_W}\bar{f}fH$$

$$\mathcal{L}_{HV} = \left(gm_W H + \frac{g^2}{4}H^2\right)\left(W_\mu^+W^{-\mu} + \frac{1}{2\cos^2\theta_W}Z_\mu Z^\mu\right)$$

$$\mathcal{L}_{WWV} = -ig[(W^+_{\mu\nu}W^{-\mu} - W^{+\mu}W^-_{\mu\nu})(A^\nu\sin\theta_W - Z^\nu\cos\theta_W) + W^-_\nu W^+_\mu(A^{\mu\nu}\sin\theta_W - Z^{\mu\nu}\cos\theta_W)]$$

$$\mathcal{L}_{WWVV} = -\frac{g^2}{4}\left\{[2W_\mu^+W^{-\mu} + (A_\mu\sin\theta_W - Z_\mu\cos\theta_W)^2]^2 - [W_\mu^+W_\nu^- + W_\nu^+W_\mu^- + (A_\mu\sin\theta_W - Z_\mu\cos\theta_W)(A_\nu\sin\theta_W - Z_\nu\cos\theta_W)]^2\right\}$$

Precision measurement of the Higgs couplings will be possibly one of the most important driver of the field in the next decade(s) (provided no surprises behind the corner)

Higgs Coupling/tree level decays

$$\mathcal{L}_H = -\frac{gm_H^2}{4m_W}H^3 - \frac{g^2m_H^2}{32m_W^2}H^4 \qquad \mathcal{L}_Y = -\sum_f \frac{gm_f}{2m_W}\bar{f}fH$$

$$\mathcal{L}_{HV} = \left(gm_W H + \frac{g^2}{4}H^2\right)\left(W_\mu^+W^{-\mu} + \frac{1}{2\cos^2\theta_W}Z_\mu Z^\mu\right)$$

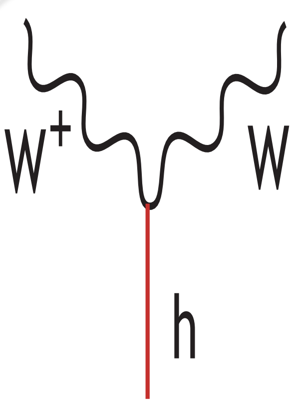

= g M_W
= 2 $M_W{}^2$/v

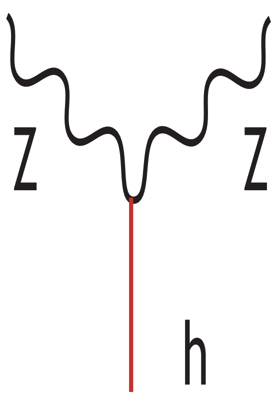

= g M_W /2cos$(\theta_w)^2$
= $M_z{}^2$/v

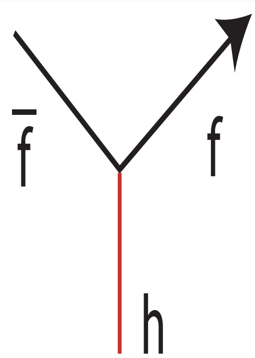

= -g m/2M_W
= -m/v

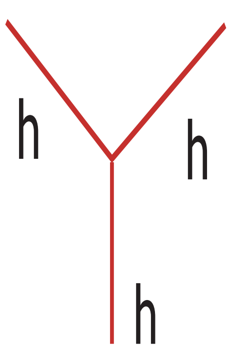

= -3 $m_H{}^2$/v

That’s not for now, wait for >10 yr

Higgs coupling/important loops !

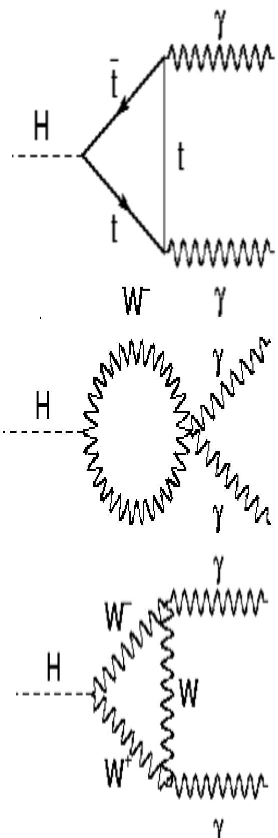

Gamma Gamma decay drives the signal significance, proceeds through fermion and boson loops: W and top most important, negative interference:

W and Top amplitude weights in the H→γγ partial width:

$$\sim \kappa_\gamma^2 = |1.28\,\kappa_W - 0.28\,\kappa_t|^2$$

Decay

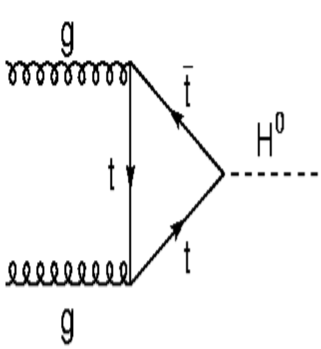

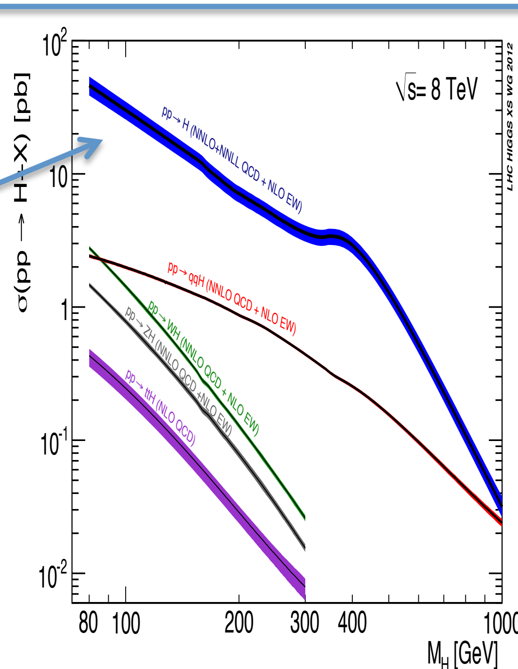

Gluon fusion provides dominant Higgs boson production mechanism Top loop dominant (-10% interference from bottom loop).

Production

SIGNAL STRENGTH MEASUREMENTS

Grand Summary

CMS-HIG-14-009

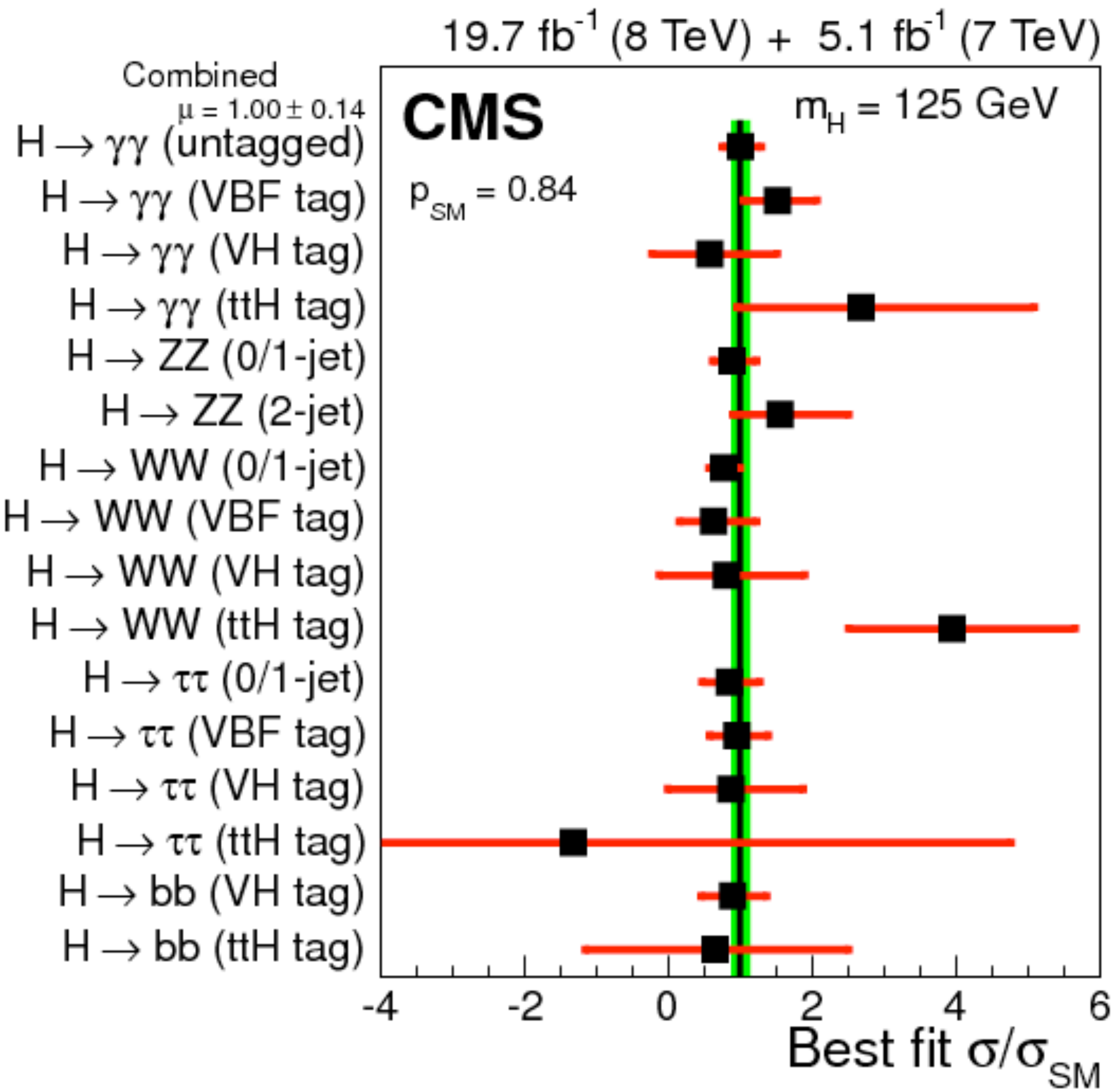

Grand Summary

CMS-HIG-14-009

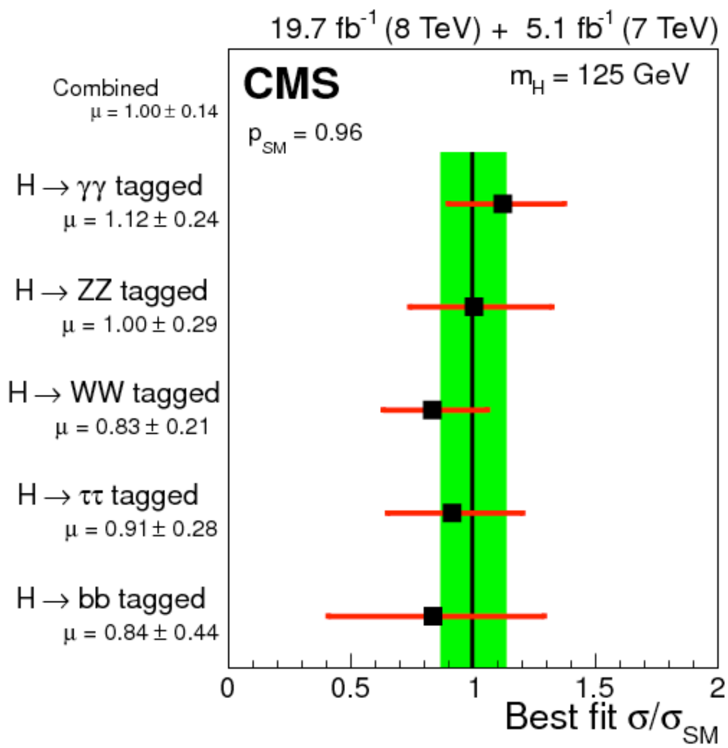

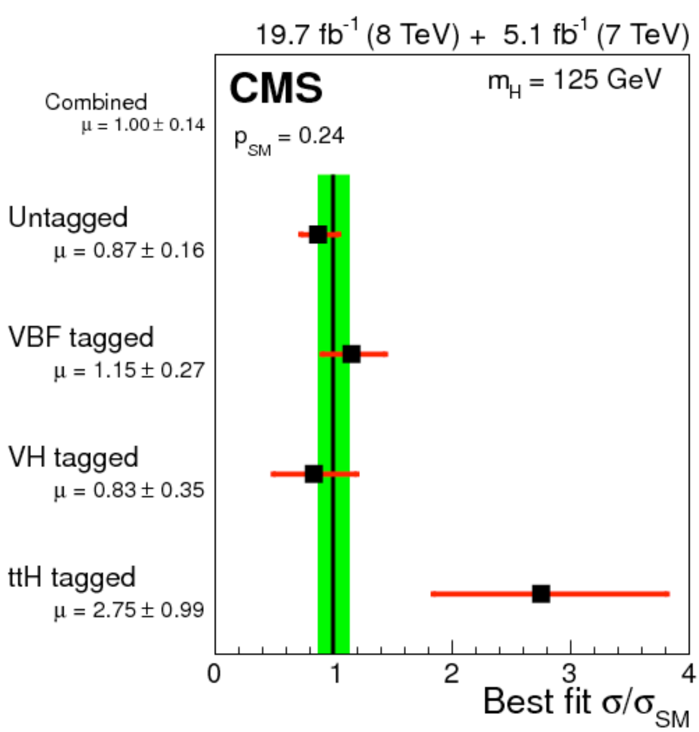

Grand Summary

[CMS-HIG-14-009]

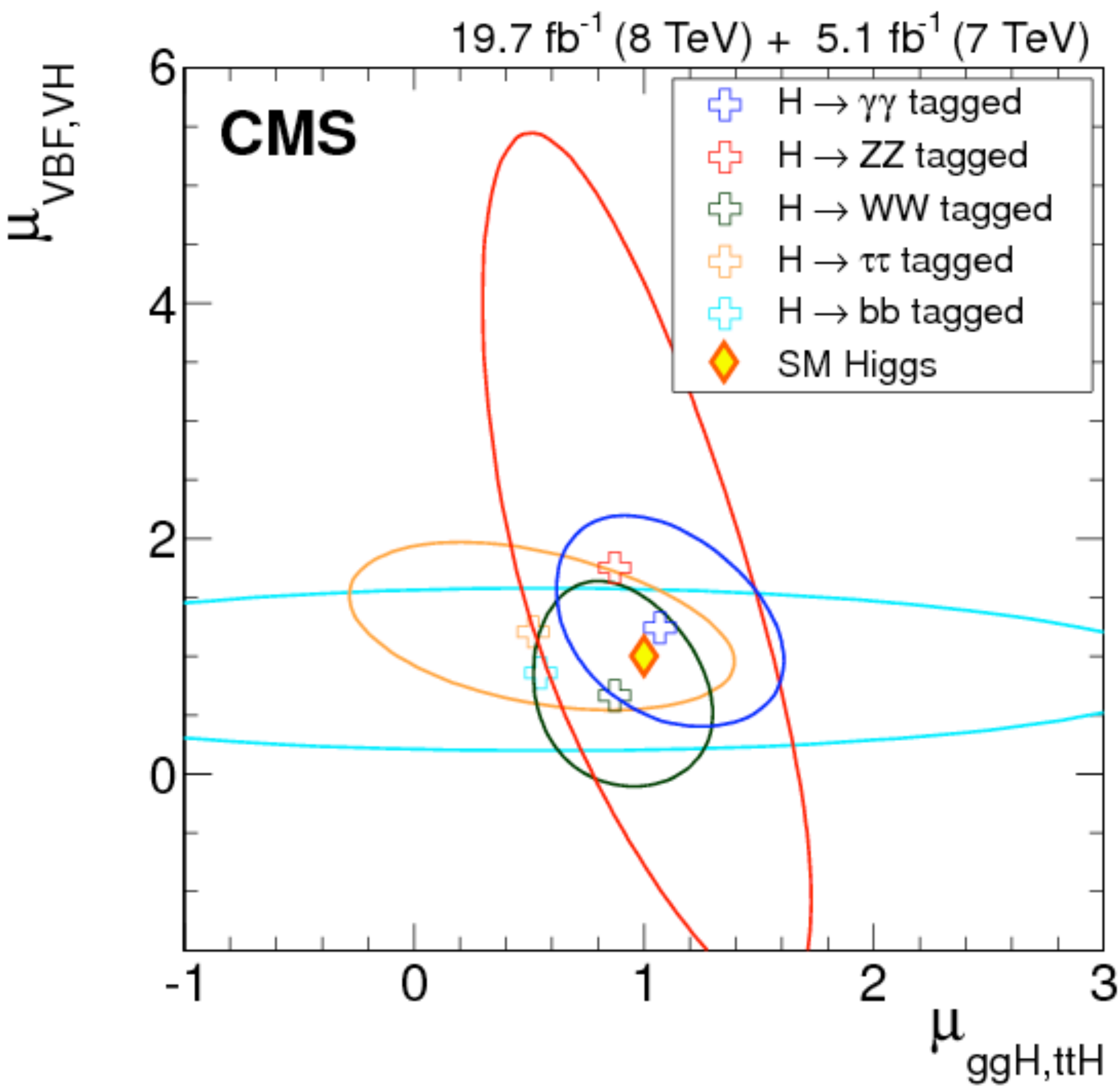

Grand Summary

[CMS-HIG-14-009]

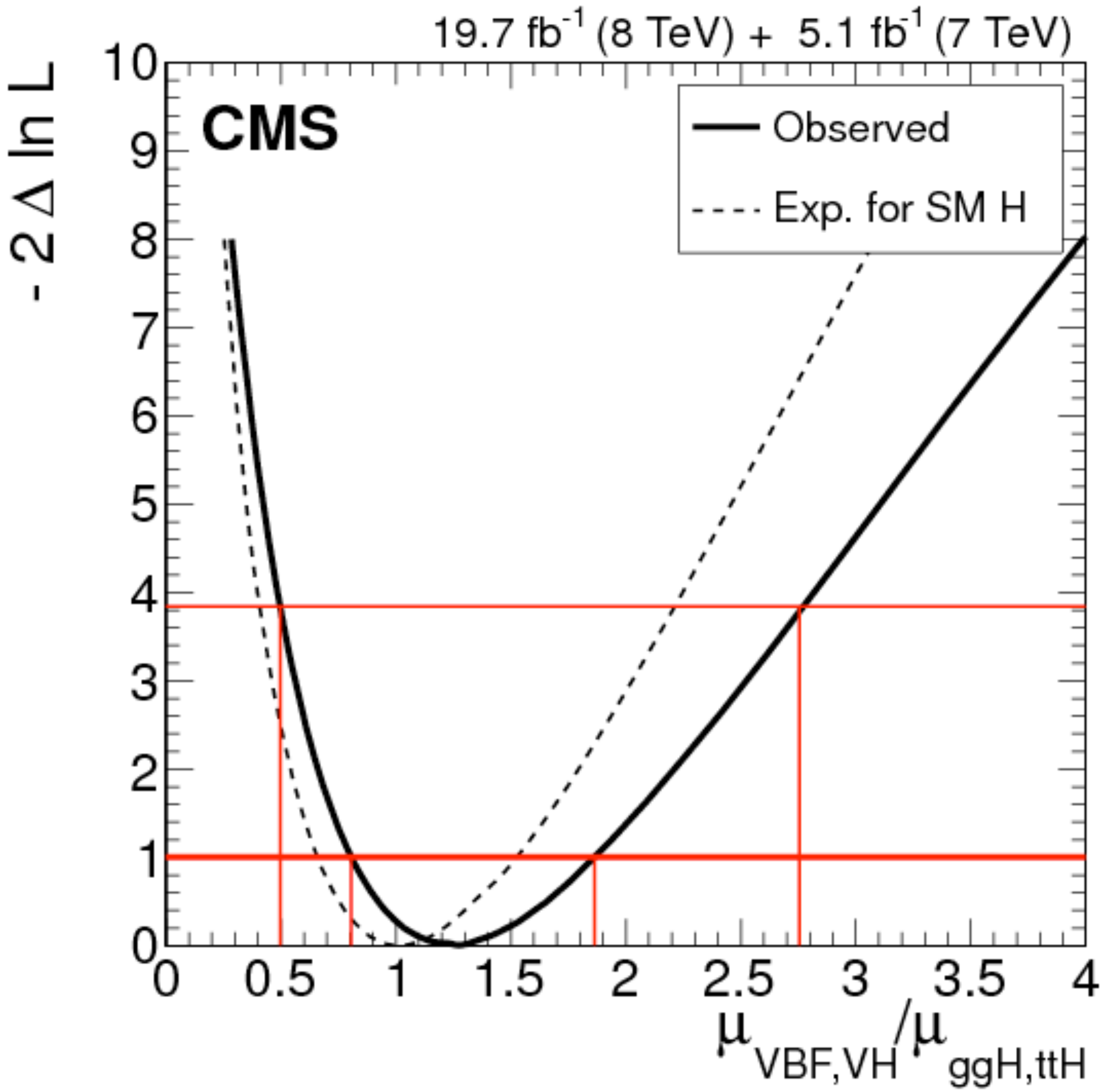

Verifica della sensibilita' dei dati ad un contributo >0 del processo VBF (rapporto di sezioni d'urto normalizzate alla teoria SM

General Strategy

based on recommendation in arXiv:1209.0040

- Assumptions
  - Single resonance
  - No modification to kinematics of Higgs events: acceptance is the same as in SM
    - Lorentz structure of amplitude as in the SM
  - Zero width approximation: igrnore effect of interference with SM amplitudes etc.

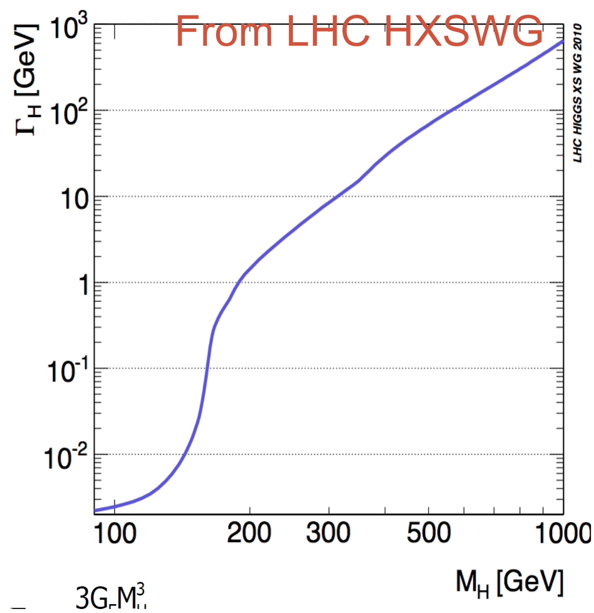

- Cross sections can then be written as:

$$\sigma \times BR(ii \rightarrow \mathrm{H} \rightarrow ff) = \frac{\sigma_{ii} \cdot \Gamma_{ff}}{\Gamma_{\mathrm{H}}}$$

- Parameterize deviation from SM through scaling factor for couplings such that :

$$\boxed{\Gamma_{ff} = \kappa_f^2 \Gamma_{ff}^{SM} \;\; ; \; \Gamma_H = \kappa_H^2 \Gamma_H^{SM} \; ; \;\; \sigma_i = \kappa_i^2 \sigma_i^{SM}}$$

- Taking into account dependency from various sub-components in loop process scale factors e.g.:

$$\boxed{\kappa_{\gamma\gamma}^2 = \kappa_{\gamma\gamma}^2(\kappa_t;\kappa_w;m_H) \;\; ; \;\; \kappa_{ggH}^2 = \kappa_{ggH}^2(\kappa_b;\kappa_t;m_H)}$$

- SM prediction incudes state-of-the-art higher order corrections. Accuracy breaks for k!=1, but important NLO QCD corrections factorize

General Strategy/ Benchmark Fits

- Total width cannot be directly measured at LHC
  - Assume no invisible/undetected decays are possible such that:

$$\boxed{\Gamma_H = \kappa_H^2 \Gamma_H^{SM} = \kappa_H^2(\kappa_i, m_H)\Gamma_H^{SM} \quad i = l, t, b, \tau, g, W, Z\ldots}$$

  - Measure ratio of coupling scale factors k_i, including one ratio to the total Higgs width

- Current dataset do not allow yet the precise determination of all the coupling scale factors → Atlas & CMS performed several simplified fits (blue one shown in the following):
  - **κ_V vs. κ_F:** universal scale for boson and for fermions
  - **κ_W vs κ_Z:** W vs. Z boson (custodial symmety)
  - **κ_u vs. κ_d:** fermion type, up vs. down (all up/down type fermions receive universal corrections)
  - **κ_q vs. κ_l:** quarks vs. leptons
  - **κ_g vs. κ_γ:** model independent test for BSM contribution to 1-loop coupling
  - **BR_{inv}:** test invisible or undetected decays in total width assuming BSM effect only in loops and SM tree level couplings

Grand Summary

[CMS-HIG-14-009]

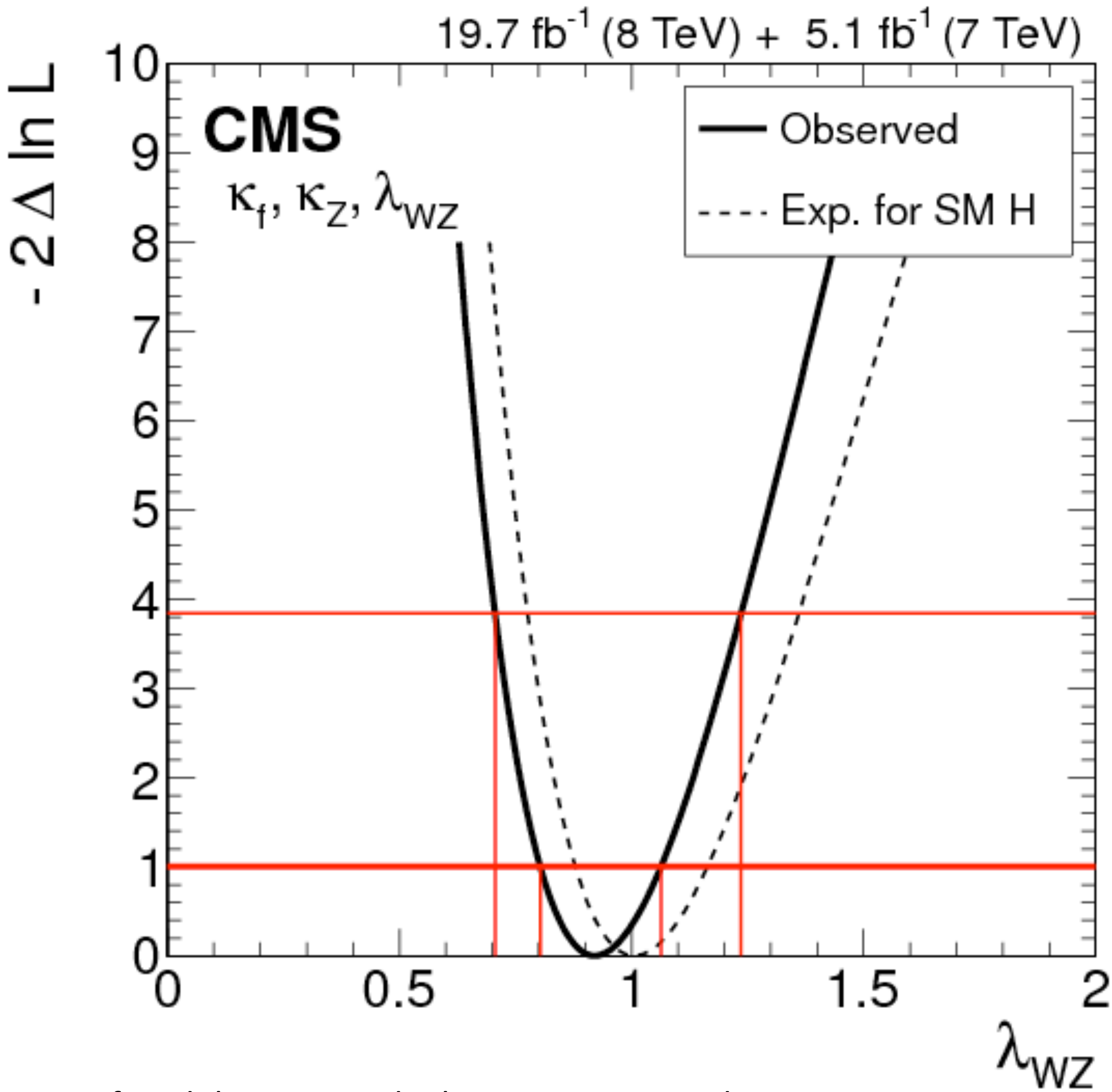

Verifica del rapporto degli accoppiamenti di W e Z

Grand Summary

[CMS-HIG-14-009]

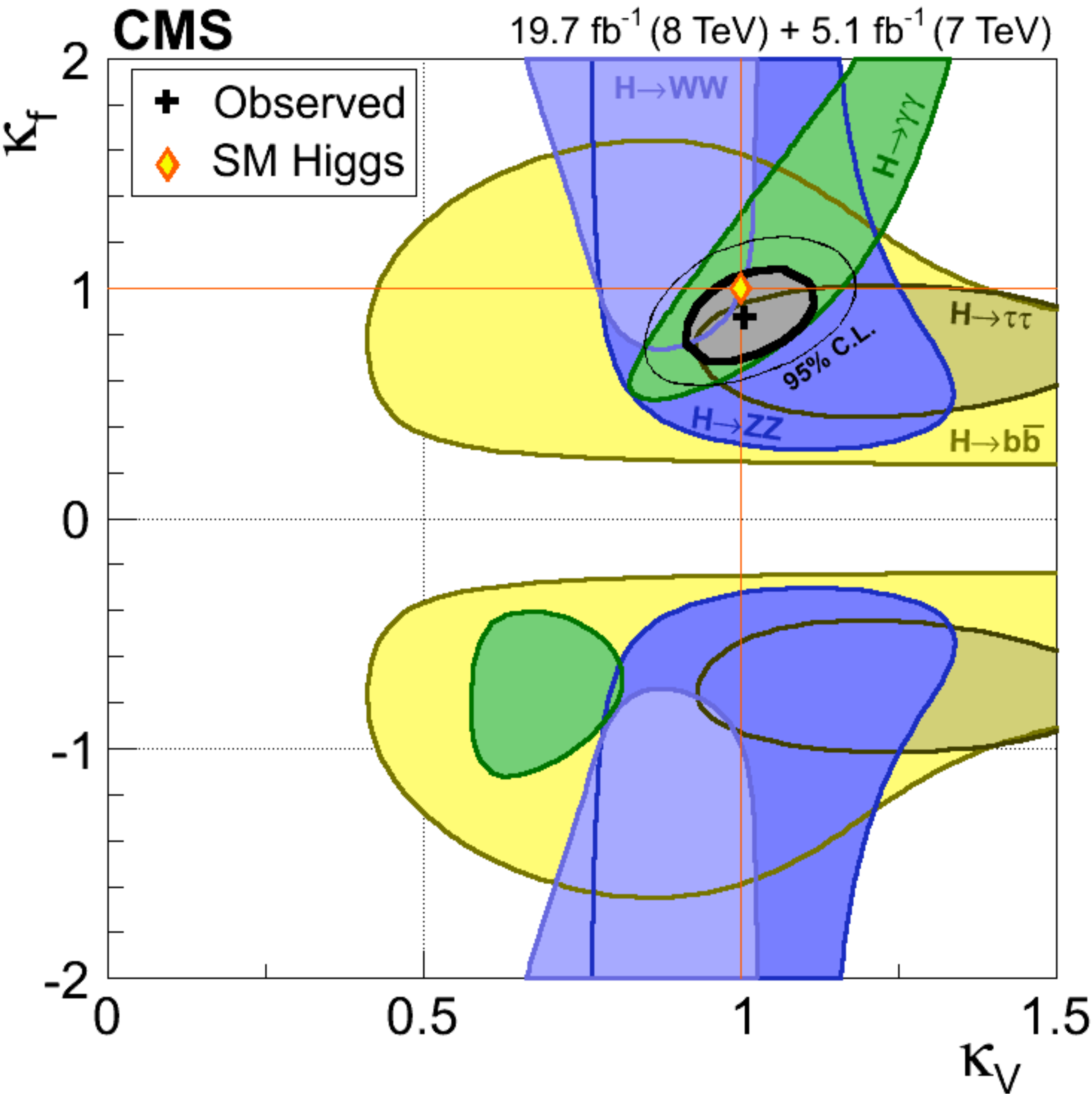

Verifica del rapporto degli accoppiamenti di W e Z

BSM Higgs: composite Higgs

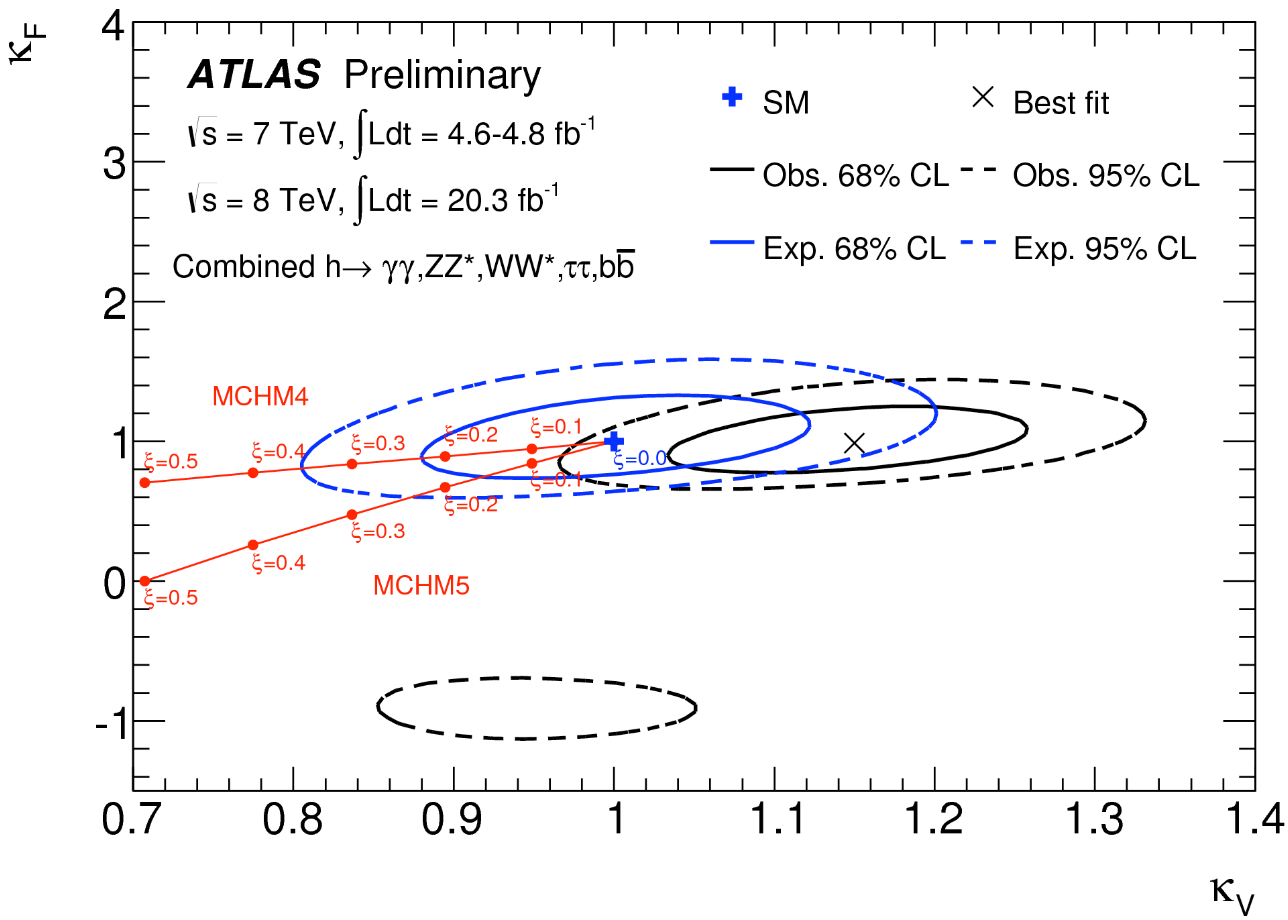

Coupling to Vector Boson and to fermions deviations can be interpreted in different Beyond the Standard Model classes. As an exmple the Higgs as a composite object (MCHM4) would produce a reduction of both the k_V and k_F couplings as:

$$\kappa = \kappa_V = \kappa_F = \sqrt{1-\xi}, \qquad \xi = v^2/f^2$$

Where f is the compositeness scale: ξ<0.2 → f > 550 GeV

Up vs down type fermions

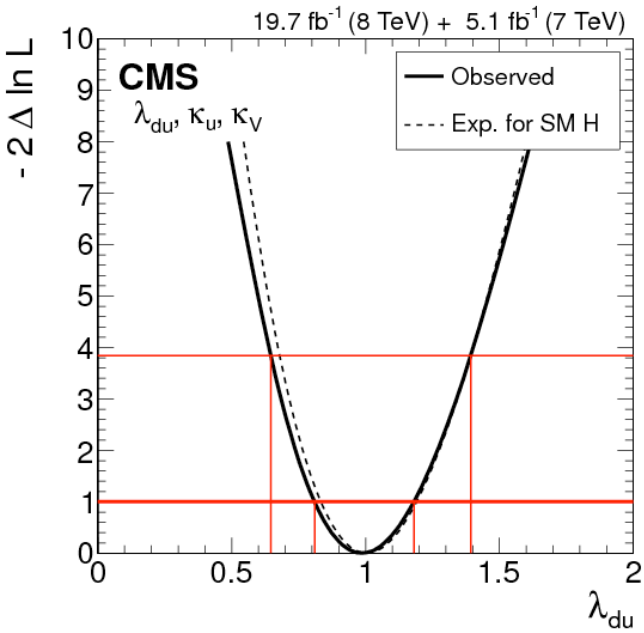

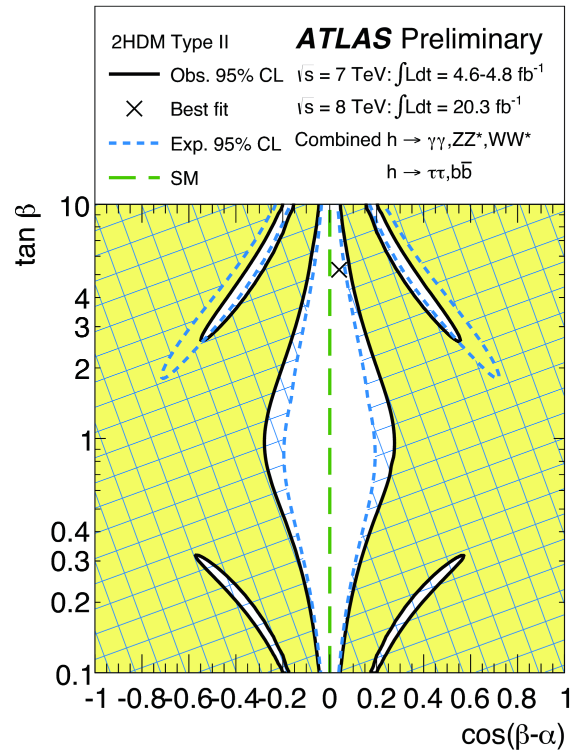

- Up type fermions (top) vs down type fermions (bottom + tau) comparison → no anomaly within 40% @ 95% CL
- Important input for BSM Higgs models, where up and down type fermions couple to different Higgs doubles. As an example in a model with 2 Higgs doubles as in SUSY, coupling to bottom and tau fermions are proportional to $\tan\beta = v_2/v_1$: the ratio of the vacuum expectation values of the two Higgs doublet fields.
- Low and high $\tan\beta$ region are excluded by the approximate coincidence of the measured Higgs rate to the SM predictions
- Regions of low $\cos(\beta-\alpha)$ correspond to a low mixing angle between the two Higgs doublets, implying the W/Z boson coupling are very similar to the SM ones

Grand Summary

[CMS-HIG-14-009]

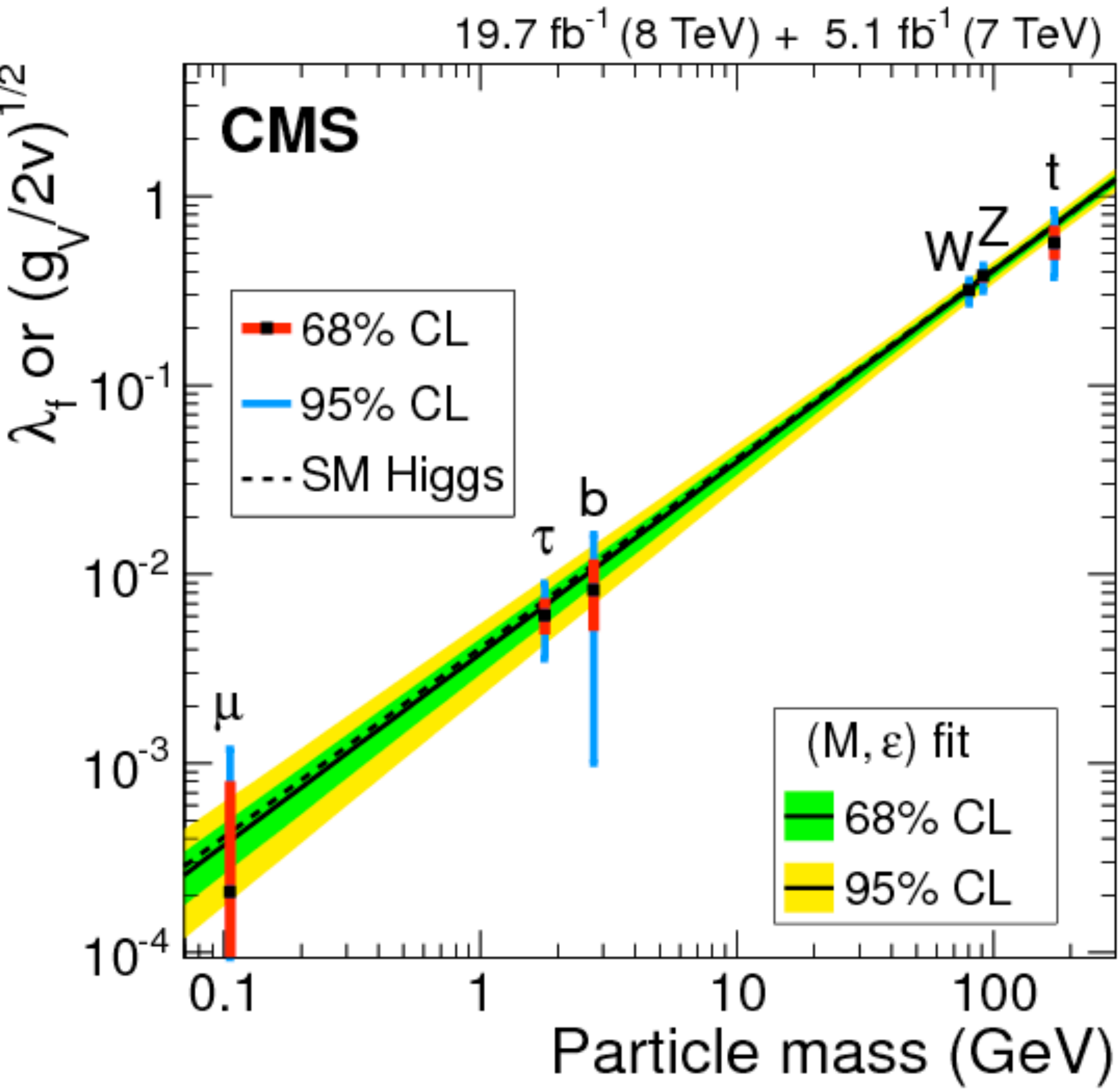

Indirect bound on H→invisible

[CMS-HIG-14-009]

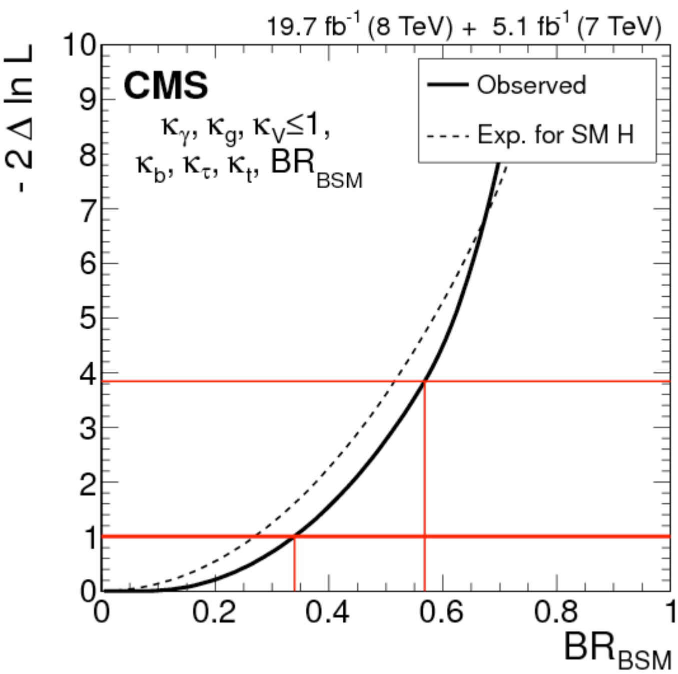

κ_γ can vary freely ($H \to \gamma\gamma$);

κ_g can vary freely ($gg \to H$);

k_V constrained to be negative

(reasonable in most BSM models)

$BR_{inv} < 0.57$(expexted 0.53) @ 95% C.L.

- Relaxing assumption on total width: allow undetectable and/or invisible decays
- Assume BSM effects only in 1-loop couplings
- Likelihood scan for effective scale factors for gluon and photon widths and total Higgs width, assuming no deviation in tree level contribution to Higgs width a bound on invisible width can be obtained from :

$$\Gamma_H = \frac{\kappa_H^2(\kappa_i)}{(1 - BR_{inv.,undet.})}\Gamma_H^{SM}$$

Grand Summary Combined
[ATLAS-CONF-2015-044/ CMS-PAS-HIG-15-002]

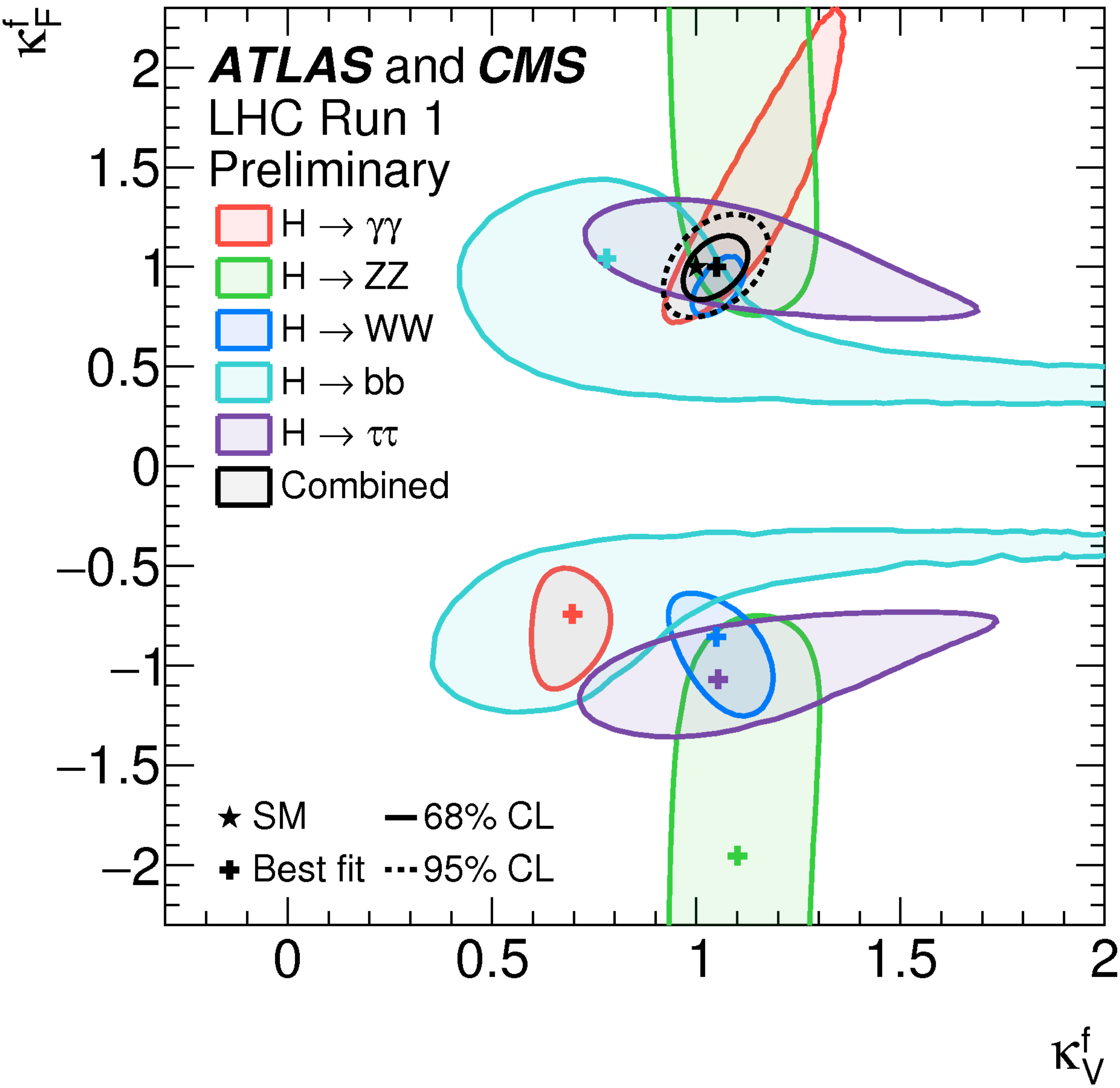

Verifica del rapporto degli accoppiamenti di W e Z

Grand Summary Combined
[ATLAS-CONF-2015-044/ CMS-PAS-HIG-15-002]

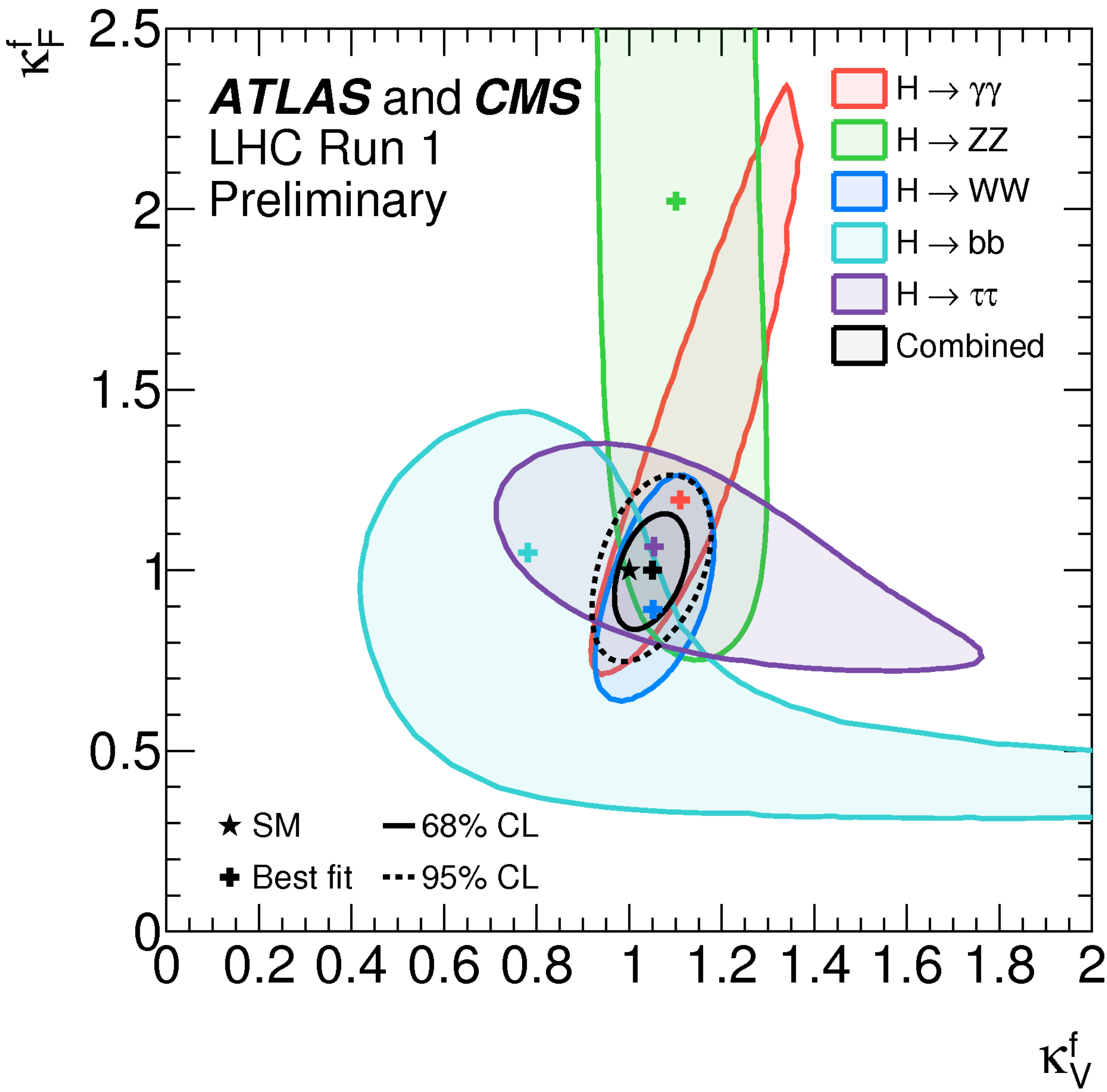

Verifica del rapporto degli accoppiamenti di W e Z

Grand Summary Combined
ATLAS-CONF-2015-044/ CMS-PAS-HIG-15-002

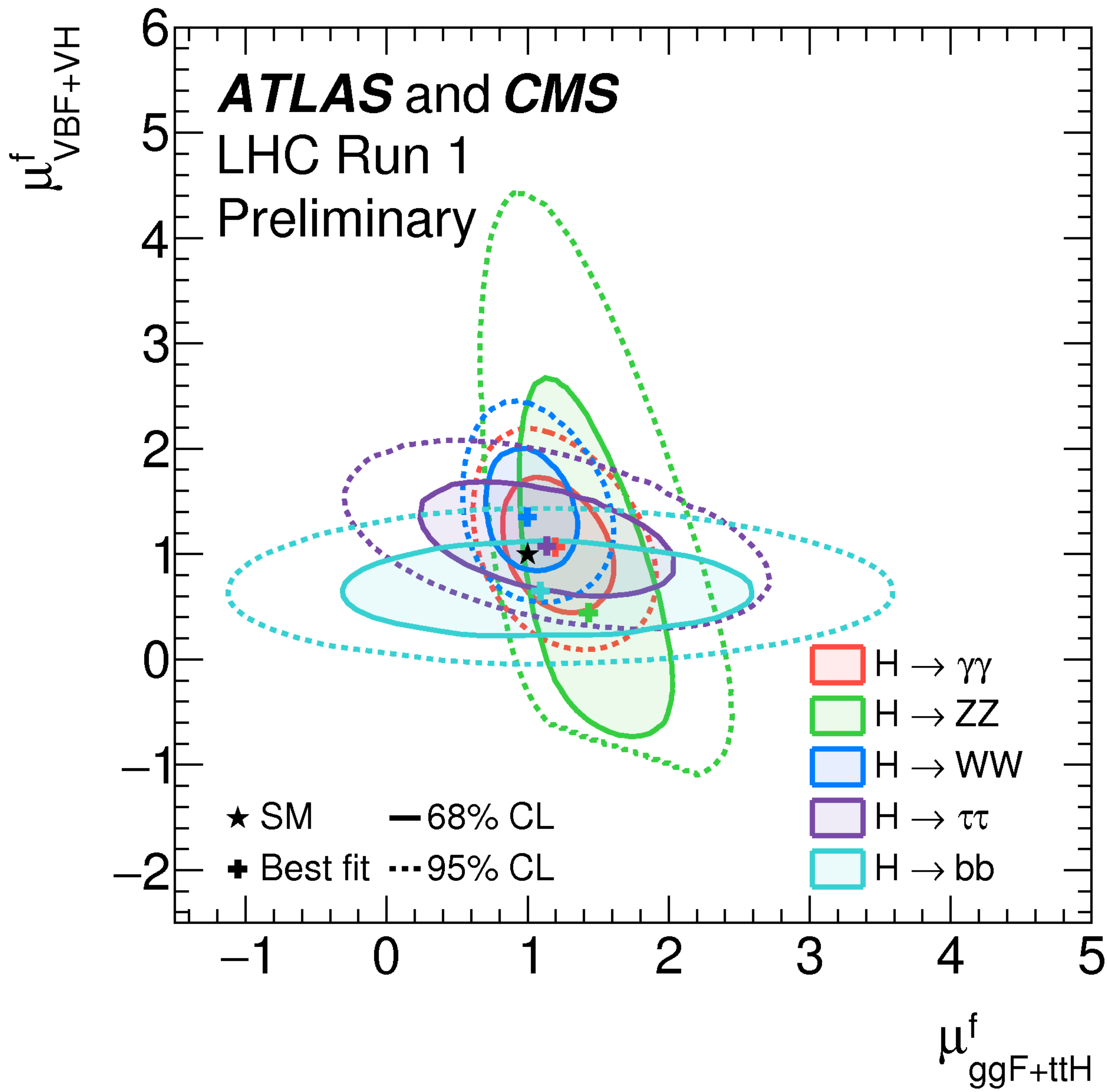

Verifica del rapporto degli accoppiamenti di W e Z vs top

Grand Summary Combined

ATLAS-CONF-2015-044/ CMS-PAS-HIG-15-002

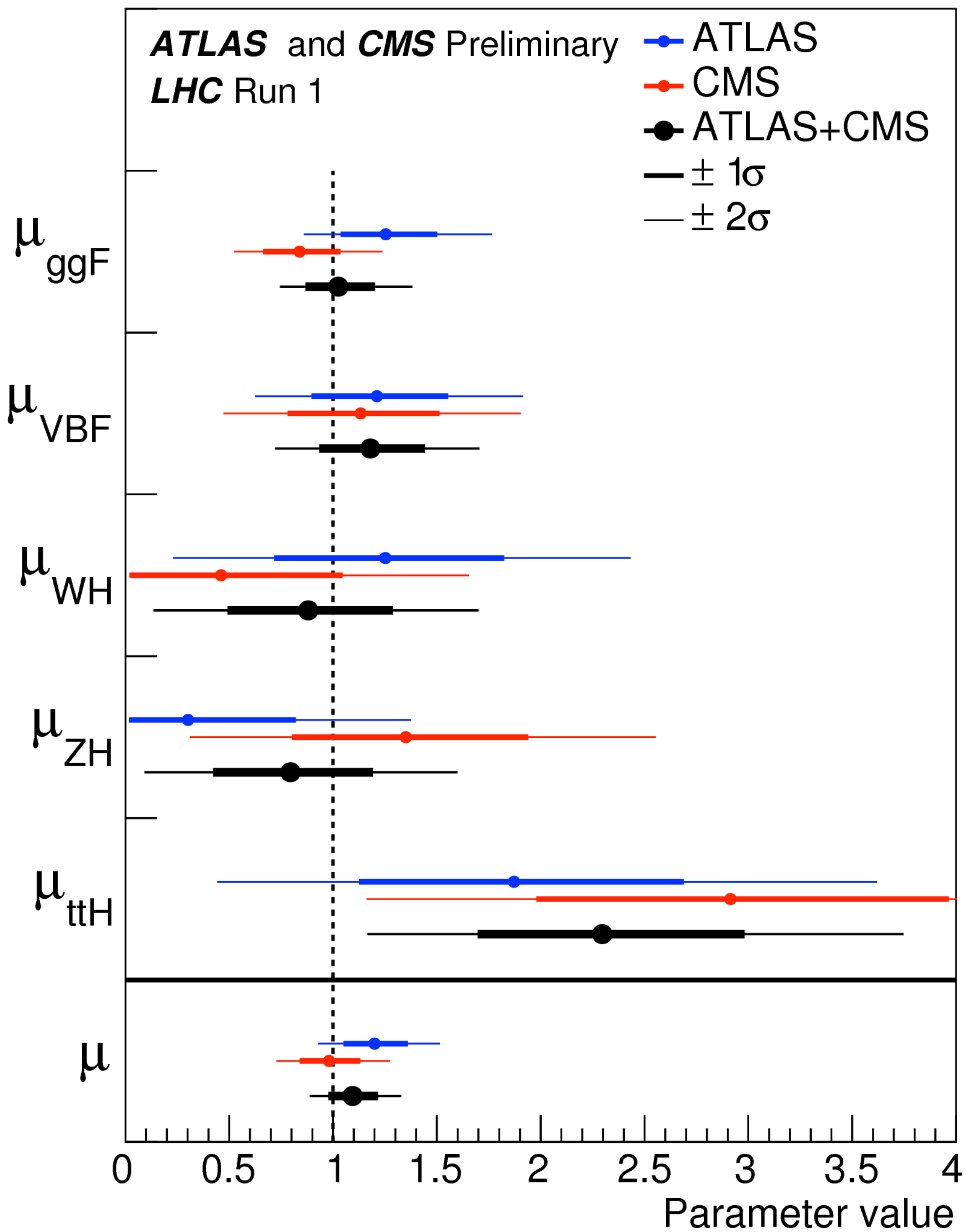

Verifica del rapporto dei modi di produzione

Grand Summary Combined
ATLAS-CONF-2015-044/ CMS-PAS-HIG-15-002

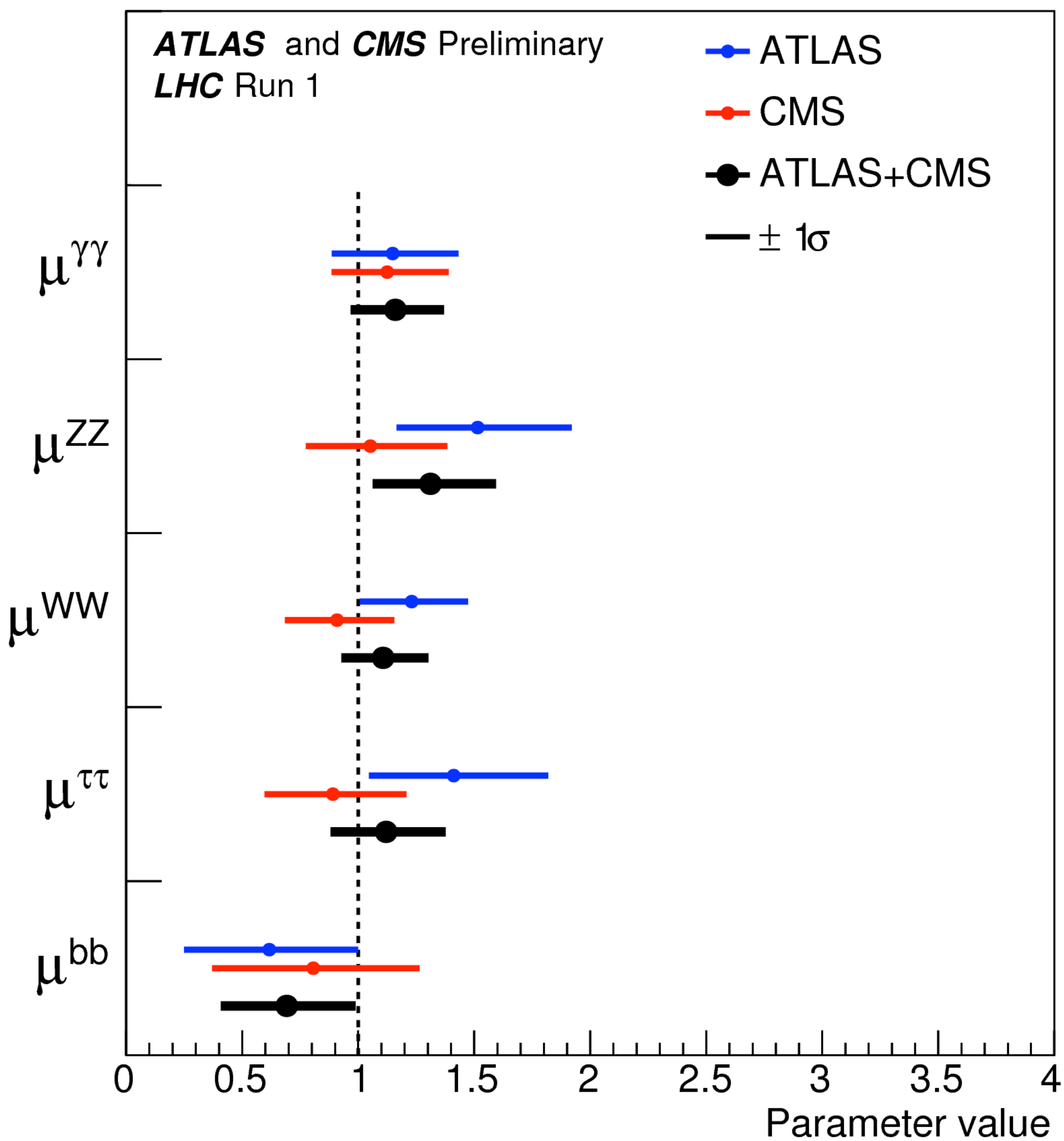

Verifica del rapporto degli accoppiamenti di H

Grand Summary Combined
[ATLAS-CONF-2015-044/ CMS-PAS-HIG-15-002]

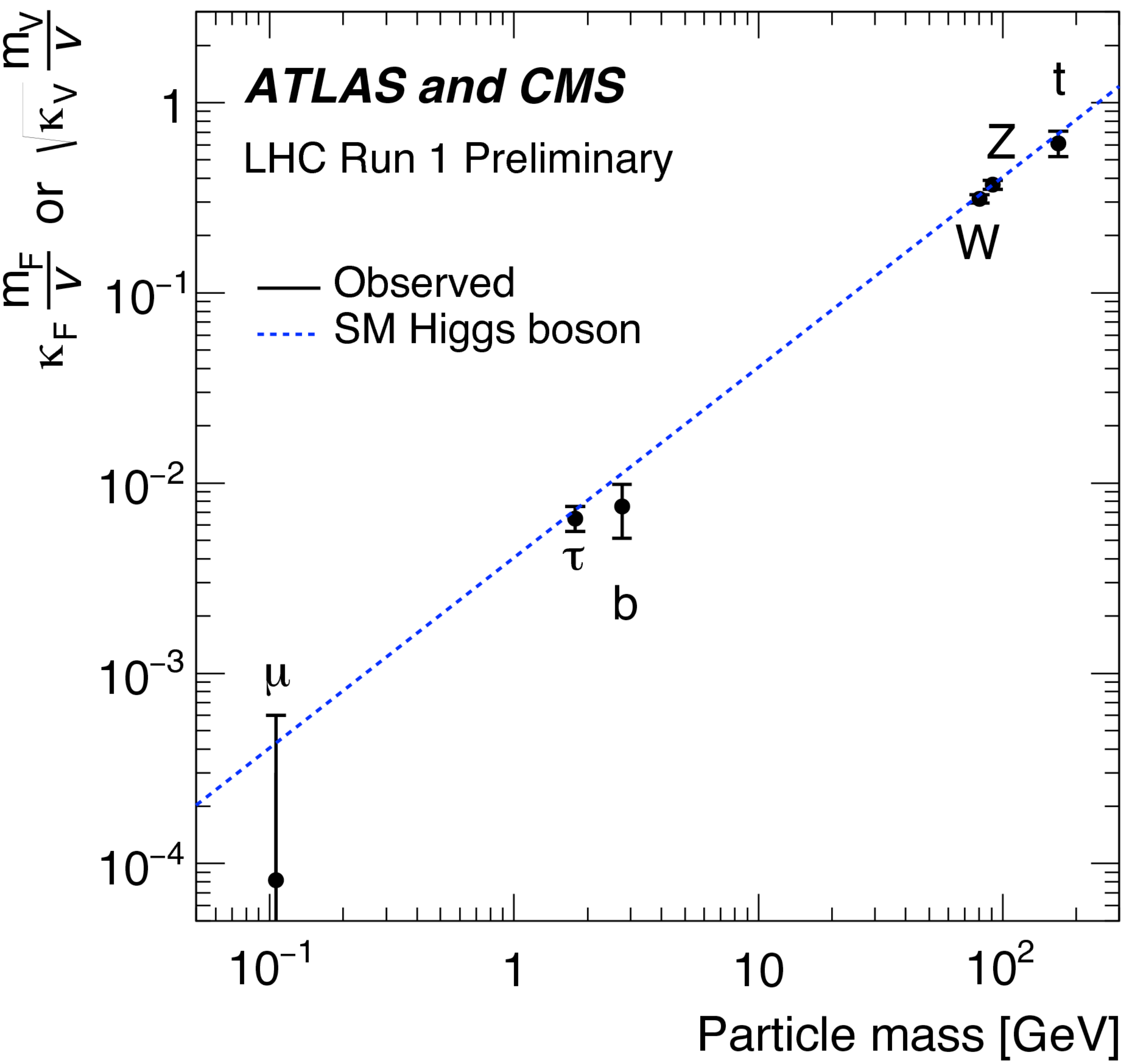

Verifica del rapporto degli accoppiamenti di H

Perspective – HL-LHC

ATLAS-PHYS-PUB-2012-004

- Show case the potentia for HL-LHC
  - Precision of a few percent seems reachable
- Ex. k_V vs k_F fi with (without) theory uncertainty

	300 fb^{-1}	3000 fb^{-1}
κ_V	3.0% (5.6%)	1.9% (4.5%)
κ_F	8.9% (10%)	3.6% (5.9%)

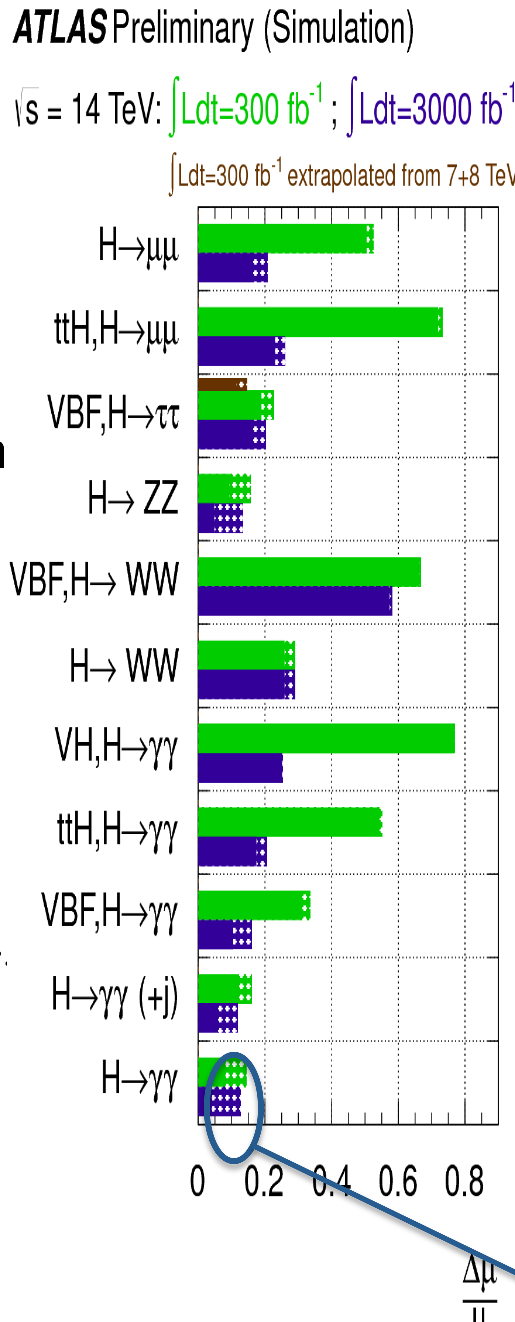

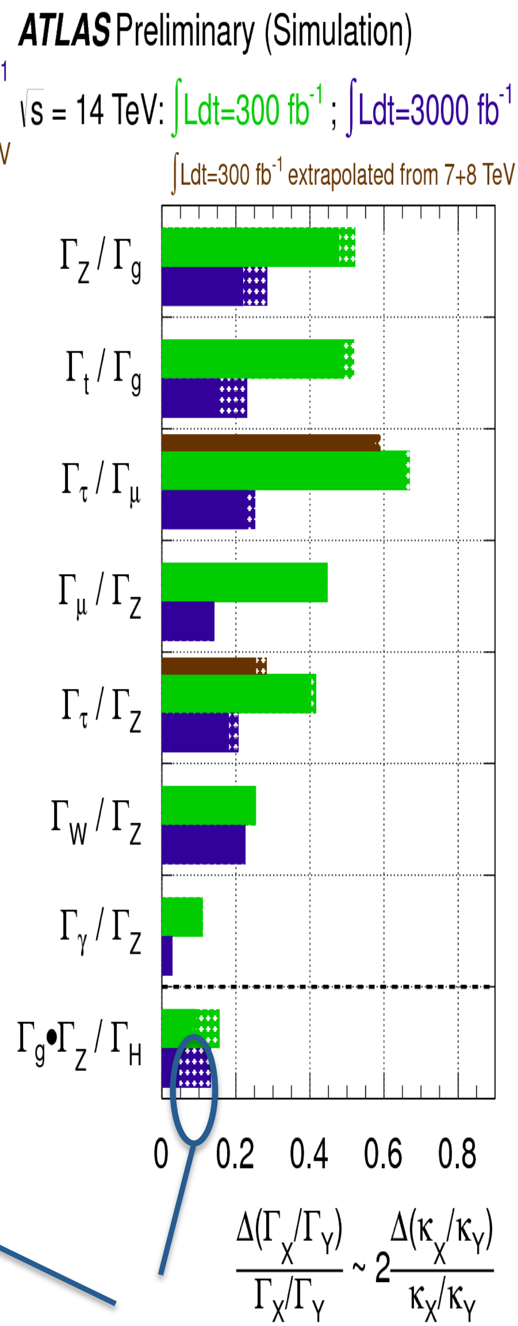

Current th uncertainty

Bibliografia

- Higgs discovery:
  - A Massive Particle Consistent with the Standard Model Higgs Boson observed with the ATLAS Detector at the Large Hadron Collider **Science 338 (2012) 1576-1582**: http://inspirehep.net/record/1223730
  - Observation of a new particle in the search for the Standard Model Higgs boson with the ATLAS detector at the LHC **Phys.Lett. B716 (2012) 1-29: http://inspirehep.net/record/1124337**
  - Observation of a new boson at a mass of 125 GeV with the CMS experiment at the LHC **Phys.Lett. B716 (2012) 30-61:** http://inspirehep.net/record/1124338
- CMS coupling fits: https://cds.cern.ch/record/1979247
- ATLAS BSM fits https://cds.cern.ch/record/1670531